Use of Human Blood-Derived Endothelial Progenitor Cells to Improve the Performance of Vascular Grafts

by

John David Stroncek

Department of Biomedical Engineering
Duke University

Date:_____
Approved:

_____
William M. Reichert, Supervisor

_____
Bruce Klitzman

_____
Jeffrey Lawson

_____
Thomas Povsic

_____
George Truskey

Dissertation submitted in partial fulfillment of
the requirements for the degree of Doctor of Philosophy in the Department of
Biomedical Engineering in the Graduate School
of Duke University

2011

ABSTRACT

Use of Human Blood-Derived Endothelial Progenitor Cells to Improve the Performance of Vascular Grafts

by

John David Stroncek

Department of Biomedical Engineering
Duke University

Date:_____
Approved:

_____
William M. Reichert, Supervisor

_____
Bruce Klitzman

_____
Jeffrey Lawson

_____
Thomas Povsic

_____
George Truskey

An abstract of a dissertation submitted in partial fulfillment of the requirements for the degree of Doctor of Philosophy in the Department of Biomedical Engineering in the Graduate School of Duke University

2011

Copyright by
John David Stroncek
2011

Abstract

Synthetic small diameter vascular grafts fail clinically due to thrombosis and intimal hyperplasia. The attachment of endothelial cells (ECs) onto the inner lumen of synthetic small diameter vascular grafts can improve graft patency; however, significant challenges remain that prevent wide clinical adoption. These issues include difficulties in the autologous sourcing of ECs, the lack of attachment, growth and retention of the layer of ECs to the graft lumen, and the maintenance of an anti-thrombotic and anti-inflammatory profile by the layer of ECs.

This dissertation describes the isolation, characterization, and use of endothelial progenitor cells (EPCs) to improve the performance of small diameter vascular grafts. First, EPC isolation efficiency and expression of critical EC markers was compared between young healthy volunteers and patients with documented coronary artery disease (CAD). EPCs were isolated and expanded from patients with CAD and had a similar phenotype to EPCs isolated from healthy donors, and a control population of human aortic ECs. Second, we assessed the ability to enhance the anti-thrombotic activity of patient derived EPCs through the over expression of thrombomodulin (TM). *In vitro* testing showed TM-transfected EPCs had significantly increased production of key anti-thrombotic molecules, reduced platelet adhesion, and extended clotting times over untransfected EPCs. Finally, native and TM-transfected EPCs were seeded onto

small diameter vascular grafts and tested for their ability to improve graft performance. EPCs sodded onto the lumen of small diameter ePTFE vascular grafts had strong adhesion and remained adherent during graft clamping and exposure to flow. TM-transfected EPCs improved graft anti-thrombotic performance significantly over bare grafts and grafts seeded with native EPCs. Based on these promising *in vitro* results, grafts were implanted bilaterally into the femoral arteries of athymic rats. Bare grafts and grafts with air removed clotted and had only 25% patency at 7 days. In contrast, graft sodded with native EPCs or TM-transfected EPCs had 87% and 89% respective patency rates. High patency rates continued with 28 day implant testing with EPC sodded grafts (88% Native; 75% TM). There were no significant differences in patency rates at 7 or 28 days between native and TM-transfected grafts. These *in vivo* data suggest patient blood-derived EPCs can be used to improve the performance of small diameter vascular grafts.

Dedication

To my parents and grandparents. I am forever grateful for all your love and support.

Contents

Abstract iv

List of Tables xiii

List of Figures xiv

Acknowledgements xix

1. Specific Aims 1

1.1 Significance 1

1.2 Hypotheses 2

1.3 Specific Aims 2

2. Background 5

2.1 Cardiovascular Disease and Surgical Treatment 5

2.2 Tissue Response to Synthetic Vascular Grafts 5

2.3 Strategies to Minimize Vascular Graft Failure 7

2.3.1 Endothelial Cell Attachment and Coverage 7

2.3.1.1 Direct Seeding of ECs 7

2.3.1.2 Recruitment of Blood-Derived ECs 9

2.3.2 Immobilization of Bioactive Molecules on Vascular Grafts 12

2.3.2.1 Thrombin Inhibitors 12

2.3.2.2. Nitric Oxide 13

2.3.2.3 Vascular Endothelial Growth Factor 13

2.3.3 Effect of Graft Compliance 14

2.3.3.1 Polyurethanes 14

2.3.3.2 Decellularized Vessels 15

2.3.3.3 Tissue Engineered Grafts 16

2.4 Use of Clinically Relevant ECs: Endothelial Progenitor Cells 18

2.5 Genetic Modification of ECs 20

2.6 Thrombomodulin 22

Chapter 3. Comparison of Endothelial Cell Phenotypic Markers of Late Outgrowth EPCs Isolated from Coronary Artery Disease Patients and Healthy Volunteers 25

3.1 Synopsis 25

3.2 Introduction 26

3.3 Methods and Materials 29

3.3.1 Donor Subjects 29

3.3.2 Cell Isolation and Culture 30

3.3.3 Doubling Time 31

3.3.4 Flow Cytometry 31

3.3.5 Substrate for Measuring Cell Spreading and Adhesion 31

3.3.6 Cell Spreading 32

3.3.7 Strength of Adhesion 32

3.3.8 Surface Expression of $\alpha_5\beta_1$ and $\alpha_v\beta_3$ Integrins 33

3.3.9 In Vitro Vasculogenesis Assay 34

3.3.10 Effect of Shear Stress on Cell Morphology and Nitric Oxide Expression 35

3.3.11 Quantitative real-time RT-PCR 36

3.3.12 Nitric Oxide Assay 37

3.3.13 Statistical Analysis 37

3.4 Results 38

3.4.1 Characteristics of Study Subjects and EPC Proliferation Potential 38

3.4.2 Frequency of Isolation 39

3.4.3 Culture Phenotype 43

3.4.4 Cell Attachment to Teflon-AF™ 45

3.4.4.1 Cell Spreading 45

3.4.4.2 Cell retention 46

3.4.5 Integrin Expression 47

3.4.6 *In vitro* Vasculogenesis Assay 47

3.4.7 Effect of Shear Stress on Cell Morphology and Nitric Oxide Expression 49

3.5 Discussion 51

3.6 Conclusions 58

Chapter 4. *In Vitro* Functional Testing of Endothelial Progenitor Cells that Overexpress Thrombomodulin 59

4.1 Synopsis 59

4.2 Introduction 60

4.3 Methods and Materials 63

4.3.1 EPC Isolation and Cell Culture 63

4.3.2 Virus Production 64

4.3.3 Adenoviral Transfection Optimization 65

4.3.4 Long-term Thrombomodulin Expression 66

4.3.5 Effect of Shear Stress on Cell Adhesion and Morphology 67

4.3.6 Assessment of TM Function 69

4.3.7 Statistics 71

4.4 Results 72

4.4.1 EPC Isolation and Transfection Optimization 72

4.4.3 Time Course of TM Expression 75

4.4.4 Orientation of EPCs Subject to Flow 76

4.4.5 APC Activity 78

4.4.6 Leukocyte Adhesion 78

4.4.7 Platelet Adhesion 81

4.4.7 Clotting times 82

4.5 Discussion 83

4.6 Conclusion 88

Chapter 5. *In Vivo* Testing of Small Diameter Vascular Grafts Lined with Endothelial Progenitor Cells that Overexpress Thrombomodulin 89

5.1 Synopsis 89

5.2 Introduction 90

5.3 Methods and Materials 92

5.3.1 EPC Isolation and Cell Culture 92

5.3.2 Adenovirus Virus and Transfection Conditions 93

5.3.3 Vascular Graft Conditions 93

5.3.4 Vascular Graft Endothelialization 93
5.3.5 EPC Adhesion Assessment 95
5.3.6 APC Production 96
5.3.7 *In Vivo* Testing 96
5.3.7.1 Animal Selection 96
5.3.7.2 Femoral Artery Interposition Grafting 96
5.3.7.3 Explant 97
5.3.8 Histology 98
5.3.9 Computational Model 99
5.3.10 Statistics 100
5.4 Results 100
5.4.1 Vascular Graft Sodding 100
5.4.2 EPC Adhesion on ePTFE Grafts 101
5.4.3 APC Production 103
5.4.4 *In Vivo* Testing 104
5.4.5 Computational Modeling 113
5.5 Discussion 116
5.6 Conclusion 121
Chapter 6. Overview and Future Studies 122
6.1 Overview 122
6.2 An Ideal Small Diameter Vascular Graft 125
6.2 Future Work 128

6.2.1 Retrospective Evaluation of Experimental Design 128

6.2.2 Vector System Used for Gene Therapy 129

6.2.3 Vascular Graft Scaffold 130

6.2.4 EPCs Isolation Efficiency 130

6.2.5 Induced Pluripotent Stem Cells (iPSCs) 132

Appendix A 134

Appendix B 157

References 165

Biography 193

List of Tables

Table 1. Baseline donor characteristics of young healthy donors versus patients with coronary artery disease (CAD).....39

Table 2. Characteristics of donor population with coronary artery disease.....41

Table 3. Isolation frequency of late-outgrowth endothelial progenitor cells (EPCs). 42

Table 4. Number of Mononuclear cells in collected peripheral blood samples. 43

Table 5. EPC angle of orientation pre and post exposure to 48 hour laminar flow (*p<0.0001 vs static condition).....77

Table 6: Patency rates of grafts implanted 7 or 28 days (*p<0.05 versus Bare Graft and Denucleated Graft).....105

Table 7: Differential gene expression from gene array across different conditions. 143

List of Figures

Figure 1. Representative growth and expansion of late outgrowth EPCs isolated from peripheral blood of CAD patients and healthy donors. Cultures had either high proliferation potential, low proliferation potential, or no colonies (A). Late outgrowth EPCs colonies appeared 2-3 weeks after plating peripheral blood mononuclear cells (C). Upon passaging, some cultures from CAD and healthy donors showed exponential growth. Cells typical EC cobblestone morphology while growing to confluence and were defined as high proliferation potential (A,B). In four healthy donors, cultures were unable to be expanded to over 10^7 cells and the cultures were defined as low proliferation potential (A). Cells from low proliferation cultures had a larger area and more irregular shape (D). Low proliferation cultures stained positive for β-galactosidase, a marker of cell senescence (E). Scale bar 100 μm (B,D,E), 200 μm (C). ... 40

Figure 2. Immunotypic analysis of expanded late-outgrowth EPCs from patients with CAD (CAD EPCs), late-outgrowth EPCs from healthy donors (EPCs), and control human aortic ECs (HAECs) (black lines: fluorescent signals of isotypic controls, bold green lines: fluorescence signals of specific antigens). CAD EPCs, EPCs, and HAECs were positive for endothelial markers CD31 and CD105. CAD EPCs, EPCs, and HAECs showed no positive fraction for stem cell marker CD133 or hematopoietic markers CD45 and CD14. Shown are representative data from three independent experiments using different CAD EPCs and healthy EPCs with similar results. 44

Figure 3. Cell spreading and adhesion on fibronectin-coated Teflon-AF. Late outgrowth EPCs from healthy donors spread at a higher rate than EPCs from CAD patients and HAECs (A). EPCs from healthy donors had a significantly larger area at 4 hours and 24 hours (*$p<0.05$ EPC vs HAEC, # $p<0.05$ EPC vs. CAD EPC). ECs were seeded onto Teflon-AF coated with fibronectin for 20 minutes. All three cell types had over 95% adhesion after exposure up to 187 dynes/cm^2 (B). 46

Figure 4. Late outgrowth EPCs from CAD patients and healthy donors expressed significantly higher levels of $\alpha_5\beta_1$ compared to HAECs. $\alpha_v\beta_3$ was expressed at significantly higher levels in CAD EPC (* $p<0.05$ versus HAEC, # $p<0.05$ versus EPC)... 47

Figure 5. *In vitro* vasculogenesis assay. Representative image of late outgrowth EPCs from CAD patient seeded onto Matrigel™ and viewed after 4 hours by phase contrast microscopy (A). Tubes were more defined after 24 hours (B). There were no significant differences in total vessel length versus cell type when measured at 4, 6, and 24 hours (C). Scale bar 200 μm (A), 100 μm (B). 48

Figure 6. Effect of shear stress on cell morphology. Representative immunoflourescent images of late outgrowth EPCs from patient with CAD under static conditions stained for f-actin (A) and CD31 (B). Cultures were exposed to laminar shear stress (15 dynes/cm^2) for 48 hours. Late outgrowth EPCs tended to elongate and align parallel to the direction of flow (C,D). Scale bar 100 μm. 49

Figure 7. Effect of shear stress on flow responsive genes and nitric oxide expression. KLF2 and eNOS gene expression by patients with CAD and healthy donors were significantly lower than HAECs (A,B). Upon exposure to 48 hr laminar shear, KLF-2 and eNOS mRNA levels increased for all cell types, though expression was significantly reduced for healthy donors compared to HAECs (A,B) (* $p<0.05$ versus HAECs, # $p<0.05$ versus CAD EPCs). Late outgrowth EPCs from CAD patients, healthy individuals, and HAECs all increased their production of nitric oxide during exposure to flow (C). No significant differences were observed in NO release between the three cell groups. 51

Figure 8: Optimization of adenoviral transfection of EPCs. EPCs were assessed for transfection efficiency after AdTM by flow cytometry for CD141-PE. Representative image of native EPCs (black line) and EPCs transfected 4 hours with 100 MOI (green bold line) (A). The percentage of EPC expressing CD141 higher than native EPCs increased with viral concentration (white bars: 4 hour transfection time; gray bars: 24 hour transfection time) (B). Surface expression of CD141 was increased with greater vector concentrations (C). Four days after transfecting EPCs with AdTM, EPC numbers were decreased versus native EPCs (all cultures initially had 1.9×10^5 cells at transfection) (D). 73

Figure 9. Long-term thrombomodulin expression measured through TM mRNA expression (A) and TM surface expression (B) in native and AdTM-transfected EPCs (*$p<0.05$ versus native EPCs). 76

Figure 10. Transfected EPCs maintain firm adhesion and reorient in the direction of flow. Before the exposure to flow, AdTM EPCs had a random orientation and stained for PECAM (green), F-actin (red), and nuclei (blue). After 48 hours of laminar flow, AdTM-transfected EPCs remained adherent and aligned with the direction of flow (white arrow) (B) (scale bar 100 μm). 77

Figure 11. APC production rate of bare wells, EPCs, EPCs + AdCV, and EPCs + AdTM (*$p<0.05$ versus bare well, #$p<0.05$ versus native EPCs and EPCs + AdCV). 78

Figure 12. Dynamic neutrophil adhesion to confluent layers of EPCs. Unstimulated EPCs had low levels of neutrophil adhesion. IL-1β prestimulation resulted in increased

neutrophil adhesion (*p<0.0001 versus no stimulation) and TM-transfected EPCs had significantly fewer neutrophils compared to native EPCs (#p<0.05 versus native EPCs).79

Figure 13. Surface expression of ICAM-1, VCAM-1, and E-Selectin on native or transfected EPCs assessed by flow cytometry. EPCs were either unstimulated (Media) or stimulated (Media + IL-1β) for four hours prior to running the assay. 80

Figure 14. Platelet area coverage was determined after 30 minute incubation with platelet rich plasma. Representative phase contrast and fluorescent images showing EPCs and CD41-labeled platelets (green). Collagen I coated wells had highest coverage (A), followed by EPCs (B), EPCs+AdCV (C), and EPCs+AdTM (D). 81

Figure 15. Percent platelet area coverage was determined after 30 minute incubation with platelet rich plasma (* p<0.0001 versus collagen coated well, #p<0.05 versus native EPCs or EPCs+AdCV). 82

Figure 16. The clotting time of activated whole blood was measured on TCPS, and confluent layers of EPCs, EPCs+AdCV, and EPCs+AdTM (* p<0.05 versus bare well, #p<0.05 versus native EPCs and EPCs+AdCV)..... 83

Figure 17: EPC sodding of 1 mm inner diameter ePTFE vascular grafts. Transfection with AdCV one day prior to sodding allowed the visualization of transfected EPCs grossly (A) and though bright field microscopy at 100x magnification (B) (scale bar 500 μm). SEM images show the lumen structure of a bare graft (C) and a graft sodded with EPCs (D) (scale bars 50 μm)..... 101

Figure 18: EPC graft coverage after 30 minutes of vascular clamping and exposure to short term flow at 100 dynes/cm^2 (n =4)..... 102

Figure 19: APC production rate of Bare, EPC, EPC + AdCV, and EPC+ AdTM sodded grafts (* p<0.05 versus bare grafts, #*p*<0.05 versus grafts with native EPC and EPC+AdCV) (n=4). 103

Figure 20: Surgical procedure for implanting 1 mm ID grafts into the femoral arteries of athymic rats (A). 7 mm long grafts were sutured interpositionally (B). Vascular clamps were removed allowing grafts to fill with blood (C). 104

Figure 21: Representative H&E vascular graft wall images of bare (A), denucleated (B), EPC sodded (C), EPC + AdCV sodded (D), and EPC + AdTM sodded (E) graft after 7 days *in vivo* (graft lumen: "L" and scale bar: 100 μm). 106

Figure 22: Representative midgraft H&E ePTFE vascular graft cross sections after 7 days *in vivo*. Location of the serial graft cross-sections (A). Bare (B) and denucleated (C) grafts had extensive thrombus. Grafts sodded with native EPCs (D), AdCV EPCs (E), and AdTM (F) had little thrombus present (scale bar 500 μm). 107

Figure 23: Analysis of graft cross-sectional thrombosis after 7 days (n=7 for EPC, n=5 for EPC+AdCV, n=6 for EPC+AdTM). 107

Figure 24: Representative of serial cross-sections of single EPC-sodded implant from the proximal to distal end. 108

Figure 25: Analysis of graft cross sectional neointimal hyperplasia split by section. 109

Figure 26: Representative H&E and Masson's Trichrome staining of distal ePTFE vascular graft cross sections after 28 days *in vivo*. All EPC sodded graft conditions had regions of neointimal hyperplasia near the proximal and distal anastomosis. Scale bar 40x images: 250 μm; 100x images: 500 μm. 110

Figure 27: Diagram showing the location of the distal graft-to-femoral artery anastomosis (A). Representative H&E and Masson's trichrome staining of distal anastomosis after 28 days (B). 111

Figure 28: Representative images of von Willebrand Factor (vWF) staining. ECs lining the control femoral artery stained positively for vWF (A) (scale bar 200 μm). EPC Sodded grafts showed confluent EC coverage luminal coverage at 28 days (B) (scale bar 500 μm). EPC sodded graft having neointimal hyperplasia also stained positive for vWF (C,D). Arrows point to positive both within graft and along region of hyperplasia (scale bars were 200 μm (C) and 100 μm (D)). 112

Figure 29: Staining of ePTFE grafts for human MHC-I (green) and cell nuclei (blue). Bare grafts had cell nuclei lining the outer walls of the graft and within the clot but showed no human MHC-I staining (A). Grafts sodded with native EPCs showed positive MHC-I staining near the graft lumen 7 days after implantation and nuclei were observed on the lumen and within the graft wall (B). After 28 days, sodded human EPCs remained on the graft original ePTFE lumen but not on the region of hyperplasia (C,D). 113

Figure 30: Computational model geometry and mesh showing the entire construct (A) and at higher detail at the proximal graft anastomosis (B). 114

Figure 31: Fluid flow lines over one pulse from 0.27 to 0.40 seconds. Lines are colored by fluid velocity. 115

Figure 32: Shear stress over one pulse from 0.27 to 0.40 seconds. Color bar ranges from 150 to 0 dynes/cm^2. 116

Figure 33: Venn diagram representation of gene overlap under different experimental conditions. The left hand diagram shows that while a large number of genes (575 for CAD and 740 for healthy) are differentially regulated in response to flow condition, 225 of those genes are shared between the two cell types. In contrast, while much fewer genes are differentially regulated between cell types for flow vs static culturing, only 18 genes are always differentially regulated in these two groups. 144

Figure 34: Functional analysis of differentially expressed genes. 146

Figure 35: Gene expression patterns of EPCs isolated from healthy donors (designated "EPC") and EPCs isolated from patients with CAD (designated "CAD EPC"). Global gene expression patterns were sorted by hierarchical clustering. Red markers represent increased expression for a particular gene and green markers indicate reduced expression. Color intensity indicates the level of such regulation. While expression of individual genes vary, static and flow conditions induce a clear difference in expression patterns in both EPC and CAD EPC conditions while the difference between the EPC and CAD EPC groups is substantially less clear. 147

Figure 36: Response of cell adhesion genes to shear stress. 149

Figure 37: RNA expression levels determined by real time RT-PCR. 152

Figure 38: Levels of nitric oxide products in media after flow experiments 153

Acknowledgements

Thank you to Monty Reichert for all the support and giving me the opportunity to take this project and run with it. I would also like to thank each of my committee members for their valuable contributions to this work. Thank you to my undergraduate student researchers: Brian Grant, Beza Abebe, Enping Hong, Yujing Xue, and Nabila Haque. Thanks to my Reichert lab mates and fellow Duke graduate students for making this an interesting, unpredictable, and overall enjoyable experience. Finally, I would like to thank my parents and extended family for their unwavering encouragement.

1. Specific Aims

1.1 Significance

Cardiovascular disease remains the number one cause of death in the United States (1). Bypass surgery, the use of autologous vessels to re-route blood flow around an obstructed vessel, is a leading treatment option for coronary artery and peripheral vascular disease. Each year, however, over 100,000 patients lack the healthy autologous venous or arterial vessels necessary for this critical procedure (2). While synthetic grafts are suitable for large diameter vessels (>6 mm), small diameter synthetic grafts remain incapable of being used clinically due to unacceptable patency rates caused by luminal surface thrombosis and intimal hyperplasia.

Several studies have shown that the presence of a functional endothelium improves the patency of synthetic small diameter grafts. However, endothelialized synthetic grafts have not received widespread adoption due to three major factors: (1) difficulties in the autologous sourcing of endothelial cells (ECs), (2) lack of attachment, growth and retention of the layer of ECs to the graft lumen, and (3) the maintenance of an anti-thrombotic and anti-inflammatory profile by the layer of ECs.

1.2 Hypotheses

This project attempted to utilize clinically relevant autologous sources of ECs and test three hypotheses. The first hypothesis was that autologous late outgrowth endothelial progenitor cells (EPCs) could be obtained noninvasively and expanded from peripheral blood of patients with coronary artery disease (CAD) and function similarly to those isolated from healthy individuals. Expression of the appropriate EC phenotype for endothelialization of small diameter synthetic vascular grafts was assessed. The second hypothesis was that transfection of EPCs with the gene for human thrombomodulin would improve the anti-thrombotic and anti-inflammatory response of EPCs isolated from CAD patients. Third, small diameter vascular grafts sodded with EPCs transfected with thrombomodulin would have improved *in vivo* performance in terms of reduced thrombosis and intimal hyperplasia compared to unsodded grafts and grafts sodded with untransfected EPCs.

1.3 Specific Aims

Specific Aim 1: Isolate and characterize late outgrowth EPCs derived from peripheral blood of patients with coronary artery disease

This aim examined the isolation and expansion of late outgrowth EPC samples of peripheral blood drawn from patients with significant coronary artery disease (CAD)

and healthy young volunteers. In cases where late outgrowth EPCs were successfully isolated, the cells were analyzed *in vitro* for their expression of EC markers, proliferation potential, ability to endothelialize synthetic materials, and produce key active molecules such as nitric oxide. The phenotype of late outgrowth EPCs were compared to a control population of human aortic ECs. These experiments were designed to determine the suitability of using late outgrowth EPCs from patients with CAD for the endothelialization of synthetic vascular grafts.

Specific Aim 2: Optimize the transfection of EPCs and assess the functional state of the thrombomodulin

Late outgrowth EPCs isolated from patients with CAD were transfected to over-express thrombomodulin. Thrombomodulin is a key anti-thrombotic molecule expressed on the surface of ECs that also has anti-inflammatory properties. The optimal transfection protocol for EPCs from CAD patients was determined with an adenoviral vector. Transfected cells were assessed for expression of TM over time, ability to produce activated protein C, reduction in clotting times, and resistance to neutrophil adhesion. Neutrophil interactions with the endothelium were quantified by dynamic adhesion experiments and inflammatory molecule expression by EPCs.

Specific Aim 3: Patency testing of native and TM-transfected endothelialized ePTFE vascular grafts in athymic nude rats.

Endothelialization of ePTFE vascular grafts was accomplished using a cell sodding method. EPC graft overage was assessed through experiments attempting to mimic the surgical conditions that grafts would be exposed to during *in vivo* testing. Grafts were tested in vitro for their ability to produce activated protein C. Sodded grafts were tested in vivo through a femoral artery interpositional model in athymic rats. Graft conditions will included: bare grafts, denucleated grafts, EPC sodded, EPC sodded and transfected with TM, EPC sodded and transfected with an adenoviral control (β-galactosidase). Grafts were explanted after 7 and 28 days and assessed for patency, EC coverage, and intimal hyperplasia.

2. Background

2.1 Cardiovascular Disease and Surgical Treatment

Coronary artery disease (CAD) affects approximately 14 million people in the United States and was responsible for more than 400,000 deaths in 2007 (3). Surgical treatments for CAD and peripheral vascular disease include angioplasty, stent placement, and artery bypass surgery. Stent placement is a first option treatment and is used in 70% of angioplasty procedures to limit proliferative restenosis. Coronary bypass of arterial blockage using autologous vein grafts remains a surgical mainstay although the grafts occlude over time, with patency rates of 85% after the first year and 60% at 10 years (4). When these bypasses undergo stenosis they must be replaced; however, 100,000 patients per year needing surgery are unable to undergo the procedure due to their lack of a healthy autologous mammary artery or saphenous vein (2). Accordingly, the development of an engineered small-diameter vascular graft has been an area of intense interest.

2.2 Tissue Response to Synthetic Vascular Grafts

Synthetic grafts made out of expanded polytetrafluoroethylene (ePTFE) and woven or knitted polyethylene terephthalate fiber (Dacron) have been the most widely used materials to date for large diameter vessel applications that have high blood flow

rates. The host's biological response to either implanted graft materials are similar (reviewed by Davids et al. (5)). Minutes after implantation non-specific protein adsorption occurs as serum proteins, albumin, fibrinogen, and antibodies attach to the graft. Within days, a fibrillar layer of fibrin covers the graft surface and platelets become interspersed. The thickness of the fibrin layer increases and may not reach a steady state until after a year and a half in humans (6, 7). Neutrophils and monocytes interrogate and attach to the fibrin layer, secreting cytokines and growth factors leading to EC and smooth muscle cell (SMC) ingrowth. In grafts with high porosity (pore diameter >45 μm), ECs and SMCs are able to migrate from the adventitia inward towards the lumen (transmural ingrowth). EC ingrowth occurs after 3-4 weeks in dogs whereas in human is may take over 3-6 months, if at all (8). ECs and SMCs are also capable of undergoing transanastomotic growth whereby the cells grow into the graft from the host's adjacent vessel at the anastomosis. EC migration and growth from the host to the synthetic graft is limited in humans however. For example, 1 cm transanastomotic endothelialization can occur after 4-8 weeks in dogs (9), while taking 56 weeks to achieve an equivalent distance in humans (10).

The lack of a confluent endothelium on vascular grafts becomes a critical problem in small diameter applications as the lower flow rate results in thrombus formation on the surface of the graft (11, 12). In addition to the immediate risk of thrombus that causes occlusion, adherent platelets and leukocytes release wide array of

molecules including: ET-1, thromboxane A_2, serotonin, platelet derived growth factor, platelet factor VI, fibrinogen, fibronectin, thrombospondin, vWF, β thromboglobulin, and reactive oxygen species. Not only can these molecules initiate a thrombotic response but can also trigger SMC migration and proliferation, leading to intimal hyperplasia near the graft anastomosis (13, 14). Thrombus formation occurs within the first week while intimal hyperplasia progresses over weeks to months (15). Due to the risks of thrombosis and intimal hyperplasia, the use of synthetic vascular grafts are currently limited to large diameter applications having high flow rates.

2.3 Strategies to Minimize Vascular Graft Failure

Researchers have focused on three key methods to improve the performance of small diameter synthetic vascular grafts: 1) creating a biological coating lined with endothelium capable of resisting platelet and leukocyte adhesion, 2) attaching or releasing bioactive molecules from the graft to mimic the endothelium, and 3) improving the mechanical properties of the graft so that they mimic those of a native elastic artery (16).

2.3.1 Endothelial Cell Attachment and Coverage

2.3.1.1 Direct Seeding of ECs

ECs makeup the inner lining of all natural blood vessels and perform several crucial functions: act as a structural barrier between the circulation and the surrounding

tissue, control vascular hemodynamics and vascular tone, modulate platelet adhesion and clotting, and express receptors that mediate the interaction of circulating leukocytes with the vessel wall (17). Given the key role the endothelium plays in vascular health, researchers have investigated seeding synthetic grafts with autologous cells as early as 1978 (18). Initial seeding studies used a single-stage technique whereby cells were isolated from the patient's saphenous vein, seeded onto the graft, and implanted into the patient -- all in the same day. These initial clinical studies had mediocre results due to the lack of complete EC coverage on the graft before implantation (19, 20). Fluid shear stress caused by blood flow recently harvested ECs, with up to 70% of the cells detached from the lumen within 35-40 minutes (21). Autologous ECs are generally obtained from tissue using methods involving high proteases such as collagenase and trypsin. These isolation conditions cleave critical cell adhesion integrins, reducing the ability for cells to strongly adhere to the graft surface (22). Our groups have shown that EC adhesion can be improved through the use of the "dual-ligand" system (23, 24) or mild trypsinization conditions (22).

The majority of the successful clinical vascular graft endothelialization studies have since focused on two-stage seeding, where ECs are extracted from the patient and cultured for 2-3 weeks to expand the cells before they are seeded onto the graft lumen Kannan et al (25). The endothelialized graft itself may also be cultured *in vitro* before it is implanted back into the patient. *In vitro* culture allows cells to form the mature

adhesions to the graft necessary to prevent cellular loss upon establishment of blood flow and typically results in greater EC graft coverage (26). While the two stage process precludes the use of the technique in emergency procedures, the clinical patency rates of the grafts are increased. Synthetic coronary artery bypass grafts engineered using ePTFE grafts seeded with ECs from the saphenous vein have 91% patency after 2.5 years (27). For peripheral bypass, ePTFE grafts seeded with vein or microvascular ECs have significantly increased patency over bare grafts and similar patency rates to autologous veins (28, 29). Small diameter grafts that are unseeded, in contrast, undergo stenosis are less significantly effective than autologous artery or vein grafts. For example, for coronary artery bypass, bare grafts had one year patency of 60% versus 86% for saphenous vein grafts (30). For below the knee infrapopliteal bypass, bare grafts had three year patency of 55% versus 73% for arm veins (31). Finally, for hemodialysis access, bare grafts have a 41% higher risk of failure than vein grafts (32).

2.3.1.2 Recruitment of Blood-Derived ECs

Another approach to obtain EC coverage on synthetic vascular grafts involves *in vivo* endothelialization via the recruitment of autologous ECs found in circulating blood. For decades, researchers have described finding discrete islands of ECs on the lumen of unseeded synthetic grafts that had been exposed to flowing blood (33). These observations have since been built upon as Asahara et al. (34) reported that peripheral

blood contains populations of circulating cells that could differentiate into cells with EC characteristics and defined these cells as endothelial progenitor cells (EPCs). Researchers hypothesized that bare graft lumens could be endothelialized *in vivo* with autologous endothelium by coating the graft with both soluble and bound attracting agents that recruit EPCs directly from the blood stream (reviewed by Avci-Adali et al. (35)).

Multiple methods have been developed to recruit and retain EPCs on the surface of synthetic grafts. The first approach involves immobilizing molecules onto a vascular material that attempt to specifically capture circulating ECs within the blood. Coating stents with cyclic Arg-Gly-Asp peptides (cRGD), important ligands for cell adhesion integrins ($\alpha_5\beta_1$, $\alpha_v\beta_3$, $\alpha_v\beta_1$ and $\alpha_v\beta_5$), increased the recruitment of ECs from circulation and reduced intimal hyperplasia area and percent area stenosis after 12 weeks versus bare metal stents (36). Another method exploits the cell surface antigen CD34, a cell surface marker that is believed to be expressed by late outgrowth EPCs as well as other cells derived from the bone marrow. Researchers have covalently attached anti-CD34 antibodies to ePTFE grafts with pig studies showing anti-CD34 grafts having rapid endothelialization after 3 days (95% EC coverage for anti-CD34) versus 5% for bare grafts (37). However, hyperplasia was not reduced. One explanation is that CD34+ is also expressed by lymphoid progenitor cells (immature B-cells, T-cells, natural killer cells, dendritic cells, monocytes, or granulocytes) and hematopoietic cells (immature

erythrocytes, platelets, basophils, or mast cells) (reviewed by Civin et al. (38)). CD34+ cells remain relatively rare in peripheral blood, making up less than 0.1% all cells in the blood versus 1.5% in the bone marrow. Once captured, CD34+ cells are also capable of differentiating into SMCs and myofibroblasts, both of which are known to contribute to intimal hyperplasia (35). In a different approach, researchers have used short single-stranded nucleic acid sequences called aptamers in the attempt to specifically recruit ECs (39). These sequences can be engineered to bind with high affinity to a wide range of target molecules including circulating EPCs, although it was unclear whether the aptamers bound specifically to early or late outgrowth EPCs (39).

The second strategy attempts to increase the concentration of CD34+ cells in the blood so that there is a greater opportunity for progenitor cells to adhere to and endothelialize the synthetic vessel. Cytokines such as granulocyte colony stimulating factor (G-CSF) are known to mobilize cells within the bone marrow and enhance neovascularization of ischemic tissue. Administration of G-CSF after implantation of bare synthetic grafts enhanced endothelialization by 60% in dogs (40). In a second study, synthetic grafts pre-seeded with ECs exposed to G-CSF treatment had better endothelialization and significantly reduced intimal hyperplasia compared to seeded control grafts (41).

2.3.2 Immobilization of Bioactive Molecules on Vascular Grafts

Small diameter vascular grafts are inherently thrombogenic due to their lack of endothelium. There are a wide variety of molecules available that can inhibit clot formation, platelet adhesion, and increase tissue vascularization when administered systemically. These molecules may improve synthetic graft patency; however, they have side effects with systemic administration so researchers have focused on ways to mobilize these molecules on the graft surface to restrict their localization.

2.3.2.1 Thrombin Inhibitors

Researchers have attempted to mimic the antithrombic activity of ECs through the attachment of molecules that inhibit thrombin. Heparin, which binds and increases the activity of anti-thrombin to prevent clotting, was first added to a biomaterial surface in 1963 (42). More recent clinical studies of heparin-bonded Dacron grafts showed disappointing results at 5 years versus uncoated ePTFE grafts (43). However, new attachment methods have been used to mobilize heparin on the graft more effectively. Preclinical studies with aortoiliac bypass in baboons show reduced platelet deposition and decreased intimal hyperplasia at both proximal and distal anastomosis with these grafts (44). Two year clinical patency rates for above and below the knee bypasses were similar to uncoated grafts (45, 46). While heparin coated grafts may reduce some aspects of the thrombotic and inflammatory response, their clinical benefit has not been proven.

Direct thrombin inhibitors such as recombinant hirudin (47, 48) and thrombomodulin (49) have also been conjugated to grafts but there have been no clinical studies to date.

2.3.2.2. Nitric Oxide

Nitric oxide (NO) releasing materials prevent the adhesive platelet receptor-ligand interactions that promote thrombus formation and growth. NO is also responsible for causing vessel dilation and suppressing SMC proliferation which is critical in preventing intimal hyperplasia. NO-releasing polyurethanes had decreased thrombus formation when used as arteriovenous grafts over 21 days (50). Interestingly, studies have not supported the use of NO to prevent hyperplasia in stents (51, 52) potentially due to short term release at insufficient concentrations. Newer NO-releasing materials are able to release NO over a more sustained period by converting endogenous nitrites and nitrosothiols to NO (53).

2.3.2.3 Vascular Endothelial Growth Factor

Vascular endothelial growth factor (VEGF) is important for stimulating endothelial cell proliferation and migration. Because endothelialization from the native blood vessel across the anastomosis and into the synthetic vascular graft is limited in humans, researchers have attempted to immobilize VEGF on synthetic grafts to improve the rate of graft endothelialization (54). In animal studies, coating grafts with a

laminin/collagen mixture containing VEGF increased endothelialization rates (55, 56) but also increased SMC density within the neointima (56). VEGF gene transfer at the host-synthetic graft interface has also had mixed results (57).

2.3.3 Effect of Graft Compliance

The influence of mechanical properties on vascular graft performance is controversial. While maintaining ample burst strength for the application is critical, the effect of vascular compliance and elasticity is debated. Natural blood vessels are distensible while many synthetic grafts are stiffer and unable to undergo deformation during exposure to pulsatile blood flow. It has been hypothesized that this compliance mismatch between the native vessel and the prosthetic graft is responsible for graft failure (58, 59). However, the effect of graft compliance on shear stresses is modest in end-to-end anastomoses (60) and there has been no direct demonstration that graft failure is due directly to compliance mismatch. Therefore, while graft compliance similar to native arteries is desirable, it is still unclear if it is critical.

2.3.3.1 Polyurethanes

Porous polyurethane (PU) have been pursued as an alternative to Dacron/ePTFE due to PU's compliance being more similar to that of natural arteries (25). PU graft tensile strength and tensile modulus is tunable by changing material hard and soft

segments. Microfibrous weaves of polyurethanes and polyurea-urethanes have been used to produce composite grafts that have been endothelialized for implantation animal studies (61, 62). However, first generation PU-based grafts have been slow to gain acceptance due to *in vivo* degradation which can result in graft occlusion (63) as well as the release of toxic byproducts (25). A biodegradable poly (ester urethane)urea and another phospholipid polymer having anti-thrombotic properties have been combined to make a compliant, biodegradable biomaterial, with improved anti-thrombotic performance over standard poly(ester urethane)urea material (64).

2.3.3.2 Decellularized Vessels

Decellularized grafts have emerged as a promising vascular prosthesis that more effectively mimics the mechanical structure a natural blood vessels while providing the added benefit of an off-the-shelf alternative to tissue engineered grafts. Creating a decellularized vessel involves removing the host's cells from donor artery or intestinal submucosa while preserving the structure of the biological scaffold to maintain the graft's mechanical properties (65, 66). Compliance, burst strength, and suture retention strength of decellularized vessels have been reported to be equivalent to their native counterparts (67, 68). These materials have been reported as intrinsically thrombogenic, thus EC seeding may be necessary to promote normal vessel function (69). In addition,

although all host cells are removed from decellularized vessels, grafts are still capable of inducing chronic inflammatory responses leading to graft degradation (70).

2.3.3.3 Tissue Engineered Grafts

The engineering of a completely biological blood vessel that contains a viable endothelium and layers of smooth muscle to provide sufficient mechanical strength remains the holy grail of vascular graft research. Although tissue engineered approaches are encouraging, most current grafts are limited as the mechanical strength of vessels derived from human cells is not sufficient (71-73). Other challenges include the ability to isolate sufficient numbers of autologous cells — specifically ECs and SMCs from patients with advanced cardiovascular disease (72) — as well as the 24 week culturing time needed for some vascular tissue engineering methods before a graft is ready for implantation (73).

Recent promising studies by Dahl et al. showed SMCs obtained from cadavers could be used to create a tissue engineered blood vessel (74). SMCs were harvested from human aortas and seeded onto degradable PGA tubular scaffolds and placed in a bioreactor. At the end of 7-10 weeks of culture, the graft was placed in a detergent to decellularize the graft and remove all antigenic material, allowing it to be used in any patient. Mechanical testing revealed the tissue engineered grafts had similar burst strength and suture retention as human internal mammary artery. Testing 6 mm inner

diameter grafts in a baboon arteriovenus shunt model, seven out of eight grafts were patent at time points ranging from one to six months. Note that for the duration of the protocol baboons were given anti platelet and anti-clotting medication. In additional *in vivo* testing of 3-4mm diameter grafts in dogs, three out of four tissue engineered grafts that had been seeded with autologous ECs were patent at time points ranging from one to 12 months (74).

Tissue engineered vessels with biodegradable scaffolds have been used clinically in 42 patients for low-pressure applications where the pulmonary outflow tract was reconstructed in pediatric patients (75). A separate group has recently performed safety studies using completely biological tissue engineered grafts (i.e. no material scaffold) for hemodialysis access and reported five out of eight grafts were patent 6 months post-implantation (76). The mechanical properties of these grafts, which have media composed of dermal fibroblasts from patients with advanced vascular disease, have similar burst pressures to native mammary arteries (77). Despite this, two of the three graft failures were due to dilation of the vessel which the authors suggested was due to high blood flow and the host's inflammatory response to the graft (76).

2.4 Use of Clinically Relevant ECs: Endothelial Progenitor Cells

Protocols involving EC transplantation have not gained wide clinical utility in part because the technical challenges involved with harvesting sufficient numbers of autologous ECs. The two most common sources of autologous ECs are cells harvested by trypsin and collagenase digestion from excised jugular or saphenous vein (78), and microvascular ECs isolated from liposuctioned fat (79) – both of which require significant interventional surgical procedures. Cell contamination, while often not a problem with EC isolation from excised vessels, is a concern with adipose-derived cells that are often heterogeneous and contaminated with other cell types (e.g. macrophages and fibroblasts) that are responsible for intimal hyperplasia and inflammation (80). Autologous ECs isolated from peripheral blood would be an essentially non-interventional source for endothelialization therapies.

Asahara et al. (34) were first to report that peripheral blood contains a population of bone marrow derived circulating cells that could differentiate into cells with some EC characteristics *ex vivo*, although the cells also displayed monocytic cell markers. These cells have been collectively termed endothelial progenitor cells (EPCs). Recent reports describe isolation of distinctly different EPC subpopulations from blood mononuclear cells (MNCs) dependent on the method of *ex vivo* culture (81-86). "Early outgrowth" EPCs (also known as Colony Forming Unit ECs) form spindle-shaped clusters of cells after only a few days following plating on fibronectin in angiogenic growth factor

enriched media. Early outgrowth EPCs express multiple EC markers and secrete high levels of angiogenic cytokines (87); however, these cells have limited proliferation potential, express markers typical of macrophages, and show the ability to ingest bacteria indicating hematopoietic origin (88). In contrast, "late outgrowth" EPCs (also called endothelial colony forming cells or endothelial outgrowth cells) are a much rarer subpopulation isolated from MNCs (89). Late outgrowth EPCs are highly proliferative cells that express EC markers (83), exhibit no hematopoietic or monocytic character (90), and are capable of forming capillaries (89) and endothelializing denuded vessels when injected *in vivo* (91). Late outgrowth EPCs have been described as "true" EPCs because they are capable of generating ECs that express typical endothelial surface markers and exhibit typical EC function (92). It still needs to be clarified whether these cells are derived from the bone marrow or dislodged from the vessel wall (81, 93).

Late outgrowth EPCs have recently been pursued as an alternative cell source for endothelialization strategies (94-99). However, if late outgrowth EPCs are to be used as an autologous source of ECs for vascular conduits, they will likely be procured from patients with extensive vascular disease. To date there has been little work in demonstrating whether autologous late outgrowth EPCs can be isolated and expanded in sufficient numbers from patients with significant coronary artery disease (CAD)(100, 101). It is also unclear if late outgrowth EPCs isolated from CAD patients exhibit

differences in proliferation, adhesion, and anti-thrombotic potential compared to healthy individuals. This dissertation seeks to address this gap in the field.

2.5 Genetic Modification of ECs

Effective EC seeding of the luminal surface of a vascular graft requires that a fully confluent monolayer of cells remain adherent or that the system is compensated for less than confluent ECs coverage. Gene therapy is an appealing therapeutic approach for cardiovascular disease because it has the potential to offset the lack of confluent coverage during graft seeding or cell loss due to flow and provide the sustained expression of proteins over a defined and predictable duration.

A variety of delivery systems have been tested for vascular gene therapy including naked plasmid DNA, DNA encapsulated within liposomes, recombinant retrovirus, adeno-associated virus, hepesvirus, and adenovirus vectors (reviewed by Chandiwal et al. (102)). Adenoviral vectors are the most commonly used for cardiovascular studies as they are able to transfect non dividing cells effectively and yield high transgene expression levels for a short time period (1 to 2 weeks *in vivo*) (102) (103). Long term *in vivo* gene augmentation is problematic as repeated gene delivery is prevented by the host immune response generated against the virus. Adeno-associated and lentiviral systems are limited by low transduction efficiency of vascular cells but are promising due to their long term expression with decreased immune response (103).

The feasibility of seeding genetically transfected ECs on synthetic vascular grafts was first demonstrated two decades ago with sustained expression of the genetic product β-galactosidase through a retroviral vector (104). Subsequent results using grafts seeded with retrovirally transfected cells have been mixed. Some studies have shown no changes in EC phenotype following transfection while others have even shown reduced EC retention and cell proliferation (105-108). Note that in certain cases the reduced adhesion was attributed to the gene — tissue plasminogen activator — acting as a nonspecific protease and cleaving extracellular matrix proteins responsible for attaching ECs to the graft (107). Vascular SMCs transfected with eNOS seeded onto LVAD grafts decreased platelet deposition and remained adherent (109).

The use of gene therapy augmented EPCs for cellular therapy has been a more recent therapeutic development. Early outgrowth EPCs have been transfected with genes to improve graft patency (plasminogen activator and hirudin (110)), neovascularization and blood flow recovery (VEGF and glycogen synthase kinase-3β(111)), and pulmonary hypertension (adrenomedullin (112)). Late outgrowth EPCs have been transduced with genes to reduce intimal hyperplasia (eNOS and heme oxygenase (113)), improve neovascularization (glycogen synthase kinase-3β) (111), and treat hemophilia (coagulation factor VIII)(114). Results have been promising as the EPCs can be easily isolated from peripheral blood and transfected *ex vivo* before therapeutic use, limiting the inflammatory response that occurs with *in vivo* vascular

transfection (115). To the best of our knowledge, there have been no studies to date utilizing transfected EPCs seeded on synthetic vascular grafts.

2.6 Thrombomodulin

Surface thrombogenicity is a significant problem for vascular grafts, particularly in the early healing stages after implantation arising from a thrombogenic graft surface that lacks intact endothelium or has adherent ECs that down regulate the expression of key anti-thrombotic and anti-inflammatory molecules (116-118). Systemic administration of anti-coagulants bears the risk of significant hemorrhagic complications (110), thus local administration of anticoagulant molecules is an appealing therapeutic option. Dr. Jeffery Lawson has proposed offsetting the down regulation of anti-thrombotic genes that occur in cardiovascular disease ((119-121)) by augmenting the expression of thrombomodulin (TM) in ECs. TM is a transmembrane glycoprotein expressed on the surface of ECs. TM is a major component in the protein C anti-coagulation pathway that includes the endothelial protein C receptor and protein C. During clot formation, TM binds thrombin, inhibiting its pro-coagulant potential while accelerating the conversion of protein C (PC) into activated protein C (APC). The thrombin-TM complex increases the rate of APC formation more than 1000-fold. APC in turn exerts anti-coagulant effects by binding protein S and inactivating factors Va and VIIIa which are responsible for generating thrombin (122, 123).

Thrombomodulin also has several important anti-inflammatory functions. When TM binds and inactivates thrombin, it prevents thrombin's activation of platelets, SMCs, and ECs (124). Second, TM acts as a critical cofactor in the production of APC which has anti-inflammatory properties of its own. For example, APC operates upstream to limit thrombin generation (122), reduces the expression of inflammatory cytokines (125-127), down regulates EC expression of adhesion molecules to block leukocyte adhesion (128), and inhibits EC apoptosis (129). Third, TM's lectin-like domain has been shown to inhibit leukocyte attachment to the activated endothelium (130).

During vascular injury or inflammation, pro-inflammatory cytokines such as TNF-α and IL-1β inhibit synthesis and promote the degradation of TM, predisposing the graft to thrombotic complications (131, 132). Furthermore, vessel distension caused by wall shear stress reduces TM production and leads to graft failure in autologous vein grafts for coronary artery bypass surgery (133). Researchers have used gene therapy to augment TM expression to improve the immediate vascular response after vessel injury. Local over expression of TM significantly decreased thrombosis after vein grafting (134) and vascular injury due to angioplasty in rabbit studies (135, 136). TM has also been shown to reduce intimal hyperplasia after 1) transfection of vein graft ECs (135), 2) mobilization of TM protein on a graft surface (137), or 3) systemically administration of soluble TM (138). Although hyperplasia was reduced in only selected studies, this may be because transfection was performed simultaneously with implantation so that acute

thrombosis or mechanical injury may already have initiated secondary growth factor and cytokine release (139). TM gene transfer prior to grafting may be more effective for preventing intimal thickening (139).

Chapter 3. Comparison of Endothelial Cell Phenotypic Markers of Late Outgrowth EPCs Isolated from Coronary Artery Disease Patients and Healthy Volunteers.

Original article co-authored with BS Grant, MA Brown, TJ Povsic, GA Truskey, and WM Reichert. Text excerpts and Figures are reprinted with permission from Mary Ann Liebert, Inc.

Stroncek JD, Grant BS, Brown MA, Povsic TJ, Truskey GA, Reichert. Comparison of Endothelial Cell Phenotypic Markers of Late Outgrowth EPCs Isolated from Coronary Artery Disease Patients and Healthy Volunteers, Tissue Engineering Part A. 15(11): 3473-86. 2009.

3.1 Synopsis

The lack of easily isolated autologous endothelial cell (EC) sources is one of the major challenges with vascular tissue engineering interventions. This manuscript examines the isolation and expansion of late outgrowth endothelial progenitor cells (EPCs) from 50 mL samples of peripheral blood drawn from patients with significant coronary artery disease (CAD) (n=13) versus healthy young adult volunteers (n=13). In cases where late outgrowth EPCs were successfully isolated, the cells were assayed *in vitro* for their expression of EC markers, proliferation potential, ability to endothelialize synthetic materials, form new blood vessels, and produce nitric oxide. Late outgrowth EPCs from patients with CAD and healthy volunteers exhibited critical endothelial cell markers and morphological characteristics that were analogous to a control population of human aortic ECs. To our knowledge, this is the first study to examine the suitability

of late outgrowth EPCs from patients with CAD for autologous endothelialization applications.

3.2 Introduction

A fully functional endothelial cell (EC) monolayer adherent to the lumen of synthetic or tissue engineered vascular grafts has been shown to increase the patency of the replacement vessel (29). Graft endothelialization requires harvesting autologous ECs that are: 1) isolated with minimal patient morbidity, 2) expandable to cell densities suitable for the application, 3) minimally contaminated with other cell types, 4) strongly and contiguously adherent to the vessel lumen, and 5) are functionally similar to intact endothelium.

The two most common sources of autologous ECs are cells harvested by trypsin and collagenase digestion from excised jugular or saphenous vein (78), and microvascular ECs isolated from liposuctioned fat (79) – both of which require significant interventional surgical procedures. Cell contamination, while often not a problem with EC isolation from excised vessels, is a concern with adipose-derived cells that are often heterogeneous and contaminated with other cell types (e.g. macrophages and fibroblasts) that are responsible for intimal hyperplasia and inflammation (80).

Autologous ECs isolated from peripheral blood would represent an essentially non-interventional source for endothelialization therapies. Asahara et al. (34) were first

to report that peripheral blood contains a population of bone marrow derived circulating cells that could differentiate into cells with some EC characteristics *ex vivo*, although the cells also displayed monocytic cell markers. These cells have been collectively termed endothelial progenitor cells (EPCs). Recent reports describe isolation of distinctly different EPC subpopulations from blood mononuclear cells (MNCs) dependent on the method of *ex vivo* culture (81-86). "Early outgrowth" EPCs (also known as Colony Forming Unit ECs) form spindle-shaped clusters of cells after only a few days following plating on fibronectin in angiogenic growth factor enriched media. Early outgrowth EPCs express multiple EC markers and secrete high levels of angiogenic cytokines (87); however, these cells have limited proliferation potential, express markers typical of macrophages, and show the ability to ingest bacteria indicating hematopoietic origin (88). In contrast, "late outgrowth" EPCs (also called endothelial colony forming cells or endothelial outgrowth cells) are a much rarer subpopulation isolated from MNCs (89). Late outgrowth EPCs are highly proliferative cells that express EC markers (83), exhibit no hematopoietic or monocytic character (90), and are capable of forming capillaries (89) and endothelializing denuded vessels when injected *in vivo* (91). Late outgrowth EPCs have been described as "true" EPCs because they are capable of generating ECs that express typical endothelial surface markers and exhibit typical EC function (92). It still needs to be clarified whether these cells are derived from the bone marrow or dislodged from the vessel wall (81, 93).

Flow cytometry has been used to sort and enumerate the abundant early outgrowth EPCs from MNC fractions through the use of a combination of surface markers, such as CD34+ /CD133+ /KDR+ that are predictive biomarkers for the extent of cardiovascular disease (140-144); in contrast, late outgrowth EPCs are too scarce to enumerate by cell sorting directly from peripheral blood, and are difficult to identify due to lack of unique cell markers to this cell subgroup (145). However, late outgrowth EPCs can be cultured to yield large numbers of cells that express endothelial cell antigens (84), which suggests suitability for endothelialization therapies. To date there has been little work in demonstrating whether autologous late outgrowth EPCs can be isolated and expanded in sufficient numbers from patients with significant coronary artery disease (CAD). It is also unclear if late outgrowth EPCs isolated from CAD patients exhibit differences in proliferation, adhesion, and angiogenic potential compared to healthy individuals.

In this study late outgrowth EPCs were isolated and expanded from peripheral blood drawn from patients undergoing cardiac catheterization in the Duke University Medical Center who had documented advanced coronary artery disease by angiography. In cases where EPCs were successfully isolated, the cells were assayed *in vitro* for their expression of EC markers, proliferation potential, ability to endothelialize synthetic materials, form new blood vessels, and produce nitric oxide (NO).

3.3 Methods and Materials

3.3.1 Donor Subjects

The Duke University Institutional Review Board approved the protocol for collection and use of human blood employed in the study. Patients undergoing left heart catheterization were approached for consent at Duke University Medical Center (n=13). In brief, all patients who have undergone cardiac catheterization, percutaneous coronary intervention, or cardiac surgery have had their demographic, clinical, angiographic, and procedural data entered into a standard database. All cardiac catheterization procedures are systematically reviewed in a standardized fashion by two operators, and the extent of coronary artery disease is documented. Enrolled CAD patients had documented advanced coronary artery disease by angiography. Clinical data was extracted from the patient's medical chart.

Young control individuals were normal healthy volunteers (n=13). Individuals had no history of chest pain and were surveyed for CAD risk factors including body mass index, smoking history, diabetes, smoking, hypertension, hyperlipidemia, and medication use.

3.3.2 Cell Isolation and Culture

Approximately 50 ml peripheral blood was drawn after arterial sheath insertion for patients with CAD and stored in K2 EDTA tubes (BD Labware, Franklin Lakes, NJ). For healthy individuals, approximately 50 ml peripheral blood was drawn by vein puncture. Blood samples were processed the same day of collection. Late outgrowth EPCs from CAD patients and healthy individuals were isolated and grown according to a previously described protocol (146). Mononuclear cells were resuspended in 12 ml complete EBM-2 + EGM-2 SingleQuots (Cambrex, Walkersville, MD) medium with 1% antibiotic/antimycotics solution (Gibco, Carsbad, CA) and seeded onto 3 separate wells of a 6-well tissue culture plate coated with type 1 rat tail collagen (BD Biosciences) at 37°C, 5% CO_2, in a humidified incubator. An average of $34x10^6$ MNCs were seeded per well. After 24 hours of culture, nonadherent cells were removed and complete EGM-2 medium was added to each well. Medium was changed daily for 7 days and then every other day following. Cells were used at passages 5-10 for all experiments.

Human aortic endothelial cells (HAECs) (Cambrex) were grown to confluence in T-25 or T-75 polystyrene flasks with endothelial basal media-2 supplemented with EGM-2 SingleQuots, 10% FBS, and 1% antibiotic/antimycotics solution. HAECs were used at passage 7-10 for all experiments.

3.3.3 Doubling Time

A 12-well plate was coated with 3.33 μg/ml of fibronectin (Millipore, Billerica, MA). Cells were trypsinized and seeded at an initial density of $5x10^3$ cells/cm^2 in complete EGM-2 media. After three days, cells were fixed with 3.7% paraformaldehyde and cell nuclei were stained with DAPI (Sigma, St. Louis, MO). Four pictures per well were taken and the number of EPCs were counted using ImageJ computer software (version 1.37a, National Institutes of Health).

3.3.4 Flow Cytometry

Cells were detached using 0.025% trypsin (Cambrex). Detached cells were resuspended in 10% goat serum with antibodies against: CD14 (BD Pharmingen), CD31 (Invitrogen), CD45 (BD Pharmigen), CD105-PE (Invitrogen) and CD133 (Miltenyi Biotec, Auburn, CA). Alexa Fluor 488 goat anti-mouse IgG (H+L) (Invitrogen) or Phycoerythrin (Sigma) goat anti-mouse IgG (H+L) were used as secondary antibodies. Appropriate control isotype antibodies were used. Flow cytometric analysis was performed with FACStar Plus flow cytometer (BD Biosciences).

3.3.5 Substrate for Measuring Cell Spreading and Adhesion

To test cell behavior on a material with similar chemistry to polytetra-fluoroethylene (ePTFE) vascular grafts, Teflon-AF™ (DuPont, Wilmington, DE) films

were spun-cast onto standard glass microscope slides (Gold Seal, Portsmouth, NH) as described previously (23). Prior to use, glass slides were cleaned by sonication with 2% PCC-54 detergent cleaning solution (*p*ierce, Rockford, IL) and a 1:1 mixture of MeOH:HCl.

3.3.6 Cell Spreading

Teflon-AF™ coated slides were incubated with 3.3 μg/ml human fibronectin (Millipore) in DPBS for 1 hour at 37°C. Cells were detached with 0.025% trypsin (Clonetics) for 5 minutes at 37ºC and neutralized with trypsin neutralizing solution (Clonetics) (twice as much trypsin neutralizing solution was used compared to trypsin), spun down, and stained with 5 μM Cell Tracker Orange (Invitrogen). Cells were washed, plated onto the fibronectin-coated Teflon- AF™ slide. 10 random images were taken, using fluorescence microscopy at 200X magnification (Nikon), at 1, 2, 3, 4, and 24 hours after seeding. The projected cell area was measured using ImageJ software. On average 50-100 cells were examined for each time point for each condition and four experiments were performed for each condition.

3.3.7 Strength of Adhesion

The strength of cell adhesion to Teflon-AF™ was measured as previously described (22). Briefly, Teflon-AF™ coated slides were incubated with 3.3 μg/ml

fibronectin in DPBS for 1 hour at 37°C. Cells were incubated with 0.025% trypsin for 5 minutes at 37ºC and neutralized with trypsin neutralizing solution (Clonetics), spun down, and stained with Hoechst 33342 (Invitrogen). The cells were then seeded onto slides for 10 minutes at room temperature. The slide was placed in a variable height flow chamber (147) and 5 pre and post flow images were taken at 5 different channel heights along the chamber. Steady laminar flow was applied for two minutes through the use of a programmable syringe pump (Harvard Apparatus, Holliston, MA). The total elapsed time from initial cell attachment to the onset of flow was typically 20 minutes. The flow media consisted of DPBS with varying amounts of dextran (average molecular weight 500,000; Fischer Scientific, Pittsburg, PA) in order to increase the viscosity to 2-5 centipoise. Four experiments were performed per cell type.

3.3.8 Surface Expression of $\alpha_5\beta_1$ and $\alpha_V\beta_3$ Integrins

The relative expression of $\alpha_5\beta_1$ and $\alpha_V\beta_3$ integrins present on each cell type was measured after using 0.025% trypsin. Detached cells were resuspended in DPBS, and incubated for 5 min. The cells were then incubated with 10 μg/ml of cycloheximide for 30 min in order to block protein synthesis (148). The cells were then rinsed, incubated with 10% goat serum (Sigma), incubated with either 10 μg/ml mouse-anti-$\alpha_5\beta_1$ or 20 μg/ml mouse-anti-$\alpha_V\beta_3$ antibodies (Chemicon), rinsed, incubated with Alexa fluor 488 goat-anti-mouse secondary antibody (Invitrogen), rinsed, and fixed in 3.7%

paraformaldehyde. The antibody concentration used was determined as the concentration to saturate the integrin binding sites (data not shown).

Fluorescence intensity per cell produced by the bound antibody was measured using a FACStar Plus flow cytometer (Becton Dickinson, San Jose, CA). Typically $1x10^4$ cells were collected and measured for fluorescence intensity. In addition, an isotype control was used for each sample condition, and the geometric mean fluorescent intensity found for the isotype control was subtracted from the geometric mean fluorescent intensity of the antibody bound cells in order to compensate for background fluorescence.

3.3.9 In Vitro Vasculogenesis Assay

Endothelial tube formation was assessed in Matrigel™ (BD Biosciences) (94). 150 μl Matrigel™ was pipetted into a 48-well plate and was incubated at 37ºC for 30 minutes to allow the polymerization of collagen. After solidification, $4x10^4$ cells per well were resuspended in 150 μL growth media and added to the well and incubated at 37ºC. At 4, 6, and 24 hours, three representative images were taken per well at 40x magnification (Nikon TE2000U, Tokyo, Japan). The total tube length per field was measured using ImageJ. Four to five independent experiments were performed for each cell type.

3.3.10 Effect of Shear Stress on Cell Morphology and Nitric Oxide Expression

Flow Setup. Cells were seeded onto SlideFlasks (NUNC, Rochester, NY) at a density of $50x10^3$ cells/cm^2. The following day, the slides were placed in a parallel plate flow chamber and connected to a circular flow consisting of a peristaltic pump (Cole Palmer, Vernon Hills, IL), pulse dampener (Cole Palmer), and flow chamber as described previously (147). The flow media used consisted of EBM-2 + 10% FBS + 1% antibiotic/antimycotic. Cells were exposed to 15 dyn/cm^2 for 48 hours. Controls consisted of cells under identical culture conditions, but not exposed to flow (static).

Staining. After exposure to flow, slides were removed from flow chambers and the cells were washed with DPBS and fixed in 3.7% paraformaldehyde for 10 minutes. Cells were permeabilized with 0.1% triton X, rinsed with DPBS, and incubated with 10% goat serum (Sigma) for 30 min at 37°C to block non-specific binding. Primary antibodies (PECAM 1:100, F-actin 1:20 (Invitrogen)) were incubated with the cells for 1 h at 37°C in 10% goat serum. Cells were rinsed multiple times and then incubated with a goat anti-mouse Alexa488-conjugated secondary antibody (1:500) (Invitrogen). Nuclei were stained with 10 μg/ml Hoechst 33342. Images were captured using a Nikon Eclipse TE2000-U (Nikon, Tokyo, Japan) inverted fluorescent microscope and a digital camera (DS-Qi1Mc, Nikon).

3.3.11 Quantitative real-time RT-PCR

Late outgrowth EPCs or HAECs were seeded onto polystyrene Slideflasks and placed to a parallel plate flow chamber flow loop as described above. The cells were exposed to shear stresses of 15 dyn/cm^2 for 48 hours after which the cellular RNA was isolated using the RNeasy Minikit (Qiagen, Germantown, MD). The quantity and purity of all RNA samples were measured using a NanoDrop Spectrophotometer (NanoDrop Technologies, Wilmington, DE). Reverse transcription of 50 ng total RNA was performed with cDNA kit (Bio-Rad, Hercules, CA) and a MyCycler (Bio-Rad). RT-PCR was performed using a SYBR-Green RT-PCR kit (Bio-Rad) and the MyIQ™ iCycler Optical Module (Bio-Rad). Whole-gene cDNA sequences of the target genes were obtained from PubMed, and primer sequences for Beta-2 microglobulin, KLF2, and endothelial nitric oxide synthase (eNOS) were generated using the online design program Primer3 (149). The melt curves of the primers were examined after reaction with reference RNA, and primers were selected that had uniform and single-product melt curves. After results were obtained, fold change from the reference RNA was calculated by the $2^{-\Delta\Delta CT}$ method. All samples were preformed in quadruplicate for all genes at each condition. Primer sequences are available upon request.

3.3.12 Nitric Oxide Assay

Media aliquots from 48 hour shear stress experiments were frozen and were lyophilized (Heto CT110, Appropriate Technical Resources, Laurel, MD). Nitric oxide concentration was determined by measuring breakdown products NO_2^- and NO_3^2 using a commercial assay (Active Motif, Carlsbad, CA) according to the manufacturers' instructions. Media samples were filtered through a 10,000 Dalton micropore filter (Millipore) prior to assay.

3.3.13 Statistical Analysis

Patient clinical characteristics are presented as mean and standard deviation. All other results are presented as means and standard errors. Categorical differences among clinical characteristics were analyzed by Fisher's exact test. Differences among cell sources, between cultures from patients with CAD, cultures from healthy individuals, and HAECs were carried out by multivariate ANOVA, with the significance of individual differences established by post hoc Fisher's Protected Least Significant Difference Test or t-test for comparing only two groups. For cell spreading and *in vitro* vasculogenesis assay, a repeated measure ANOVA was performed. *P* values below 0.05 were considered to indicate a statistically significant difference.

3.4 Results

3.4.1 Characteristics of Study Subjects and EPC Proliferation Potential

Twenty six total individuals were enrolled, 13 patients with extensive coronary artery disease and 13 healthy volunteers. The characteristics of the two donor groups are shown in Table 1. Enrolled patients with CAD had a mean age of 61.5 ± 10.5 years, while healthy donors had an average age of 26.2 ± 2.2. The patients with CAD averaged 2.1 ± 0.3 vessels with significant vessel stenosis and had significantly higher frequency of tobacco use, diabetes, hypertension, hyperlipidemia, and medication use. The healthy volunteers had no symptomatic indicators or self-reported any disease.

Table 1. Baseline donor characteristics of young healthy donors versus patients with coronary artery disease (CAD).

Characteristic	***Healthy Donors (n=13)***	***Patients with CAD***	***P-Value***
Male, n (%)	9 (69)	9 (69)	
Race, n (%)			
White	12 (92)	10 (77)	
Other (2 black, 2 Asian)	1 (8)	3 (23)	
Age, mean ± SD (range)	26 ± 3 (23–31)	62 ± 11 (44–75)	<0.001
Body mass index, mean ± SD	24.3 ± 2.6	29.0 ± 4.1	0.01
Smoking history, n (%)	0	5 (39)	0.04
Diabetes, n (%)	0 (0)	7 (54)	0.005
Hypertension, n (%)	2 (15)	10 (77)	0.005
Hyperlipidemia, n (%)	1 (8)	11 (85)	<0.001
Number of vessels with significant CAD, mean ± SD	—	2.1 ± 1.0	
Percutaneous transluminal coronary angioplasty, n (%)	0 (0)	9 (69)	<0.001
Coronary artery bypass graft, n (%)	0 (0)	7 (54)	0.005
Medication use, n (%)			
Beta blockers	0 (0)	13 (100)	<0.001
Statins	0 (0)	10 (77)	<0.001
Angiotensin-converting enzyme inhibitors	1 (8)	9 (69)	0.004

3.4.2 Frequency of Isolation

Table 2 shows the success rate of late outgrowth EPC isolation from CAD patients. No single clinical characteristic precluded the isolation of late outgrowth EPCs from patients with CAD. Colonies appeared after approximately 3 weeks in culture (Figure 1A). Colonies were successfully isolated in 7 out of 13 patients with CAD (54%

of total): 5 of 9 male CAD patients and 2 of 4 female CAD patients. Isolation success was not dependent on any of the measured variables. Late outgrowth EPC colonies were isolated in 9 of 13 healthy donors (69% of total): 6 of 10 from male donors and 2 of 3 from female donors.

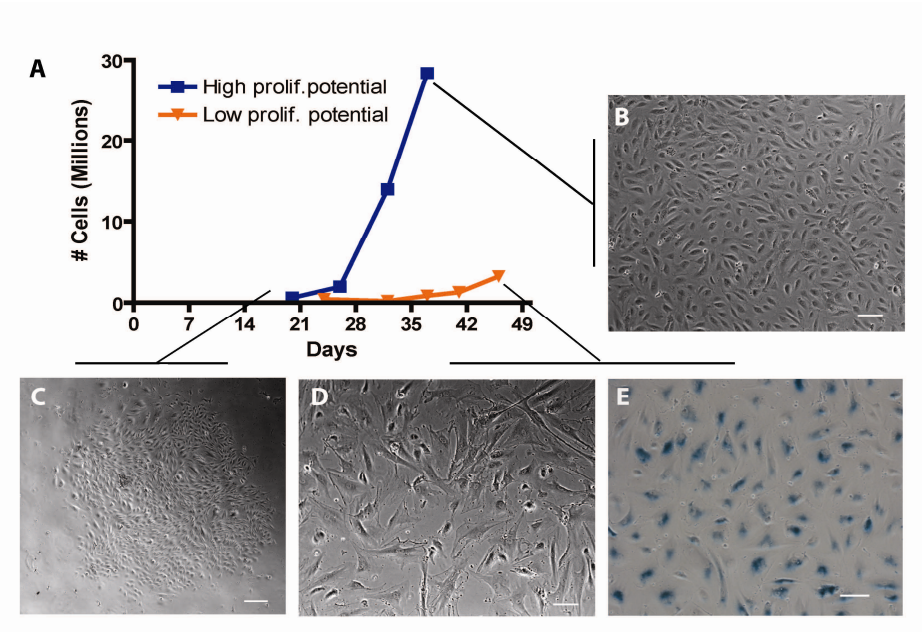

Figure 1. Representative growth and expansion of late outgrowth EPCs isolated from peripheral blood of CAD patients and healthy donors. Cultures had either high proliferation potential, low proliferation potential, or no colonies (A). Late outgrowth EPCs colonies appeared 2-3 weeks after plating peripheral blood mononuclear cells (C). Upon passaging, some cultures from CAD and healthy donors showed exponential growth. Cells typical EC cobblestone morphology while growing to confluence and were defined as high proliferation potential (A,B). In four healthy donors, cultures were unable to be expanded to over 10^7 cells and the cultures were defined as low proliferation potential (A). Cells from low proliferation cultures had a larger area and more irregular shape (D). Low proliferation cultures stained positive for β-galactosidase, a marker of cell senescence (E). Scale bar 100 μm (B,D,E), 200 μm (C).

Table 2. Characteristics of donor population with coronary artery disease.

		Late-Outgrowth EPC Colonies Obtained		
Characteristic	***All Subjects with CAD***	***Yes***	***No***	**P-*Value***
Subjects, n	13	7	6	
Male, n (%)	9 (69)	5	4	
Female, n (%)	4 (31)	2	2	
Race, n (%)				
White	10 (77)	5	5	
Other (2 Black, 1 Asian)	3 (23)	2	1	
Age, mean ± SD (range)	62 ± 11 (44–75)	61 ± 11 (44–75)	62 ± 10 (45–75)	0.80
Body mass index, mean ± SD	29.0 ± 4.1	27.9 ± 4.8	30.2 ± 3.0	0.25
Smoking history, n (%)	5 (39)	2	3	0.59
Diabetes	7 (54)	3	4	0.59
Plasma glucose, mg/dL	127 ± 45	126 ± 41	128 ± 52	0.94
Hypertension	10 (77)	4	6	0.19
Hyperlipidemia	11 (85)	5	6	0.46
Familial hypercholesterolemia, n (%)	4 (31)	2	2	>0.99
Number of vessels with significant CAD, mean ± SD	2.1 ± 1.0	1.7 ± 1.1	2.5 ± 0.8	0.18
Percutaneous transluminal coronary angioplasty, n (%)	9 (69)	5	4	>0.99
Coronary artery bypass graft, n (%)	7 (54)	3	4	0.59
Medication use, n (%)				
Beta-blockers	13 (100)	7	6	—
Statins	10 (77)	4	6	0.19
Angiotensin-converting enzyme inhibitors	9 (69)	4	5	0.56

Endothelial colonies grew in the original culture plates until 75% confluence and were passaged into T25 or T75 Flasks (Figure 1C). Passaged cells that grew to a cell population of over 10^7 cells over the course of 3-6 passages were defined as "highly proliferative" (Figure 1A,B) (Table 3). All 7 of the late outgrowth EPC cultures successfully isolated from CAD patients were highly proliferative. Five of 13 healthy donors yielded highly proliferative colonies: 3 of 10 from male donors and 2 of 3 from female donors; while the other 4 colonies isolated from healthy donors never attained > 10^7 cells (Figure 1A) (p = 0.096). These "limited proliferation" cultures displayed differing growth characteristics with cells which became larger and more irregular, and stained positively for β-galactosidase, a marker of senescence (Figure 1D,E) (150).

Table 3. Isolation frequency of late-outgrowth endothelial progenitor cells (EPCs).

	Young Healthy Donors	***Patients with Coronary Artery Disease***
Late-Outgrowth EPC Isolation Frequency	n (%)	
Highly proliferative colonies (>107 EPCs)	5 (38)	7 (54)
Limited proliferation colonies (<107 EPCs)	4 (30)	0 (0)
No colonies (no EPCs)	4 (30)	6 (46)

It took an average of 36 ± 5 days to reach 10^7 cells from CAD donors versus 40 ± 4 days for healthy donors (p = 0.64). There were no significant differences among donor groups in the initial number of MNCs counted (p = 0.54), nor were there significant

differences between the number of MNCs counted and the ability to isolate late outgrowth EPC colonies (i.e. high proliferation, low proliferation, or no colony cultures) ($p = 0.69$) (Table 4).

Table 4. Number of Mononuclear cells in collected peripheral blood samples.

	Young Healthy Donors	***Patients with Coronary Artery Disease***
	Number of Mononuclear cells ($x10^7$), (n)	
All cultures	98 ± 7 (13)	107 ± 12 (13)
Highly proliferative colonies (>10^7 EPCs)	113 ± 12 (5)	105 ± 22 (7)
Limited proliferation colonies (<10^7 EPCs)	83 ± 9 (4)	N/A (0)
No colonies (no EPCs)	93 ± 12 (4)	109 ± 9 (6)

Highly proliferative late outgrowth EPC colonies from CAD and healthy subject groups were passaged 4-6 times and frozen. The doubling times of thawed late outgrowth EPCs from CAD patients and from healthy volunteers were 2.3 ± 0.7 days and 2.5 ± 0.6 days, respectively ($p = 0.79$). Doubling time for control HAECs was 1.2 ± 0.1 days ($p = 0.15$ versus outgrowth EPC from patients with CAD).

3.4.3 Culture Phenotype

Flow cytometic studies were performed to assess the marker expression of expanded actively proliferating EPCs from several donors. Late outgrowth EPCs derived from CAD patients and healthy volunteers showed uniform expression of EC markers CD31, CD105. Cells were negative for the stem cell marker CD133 as well as

hematopoeitic markers CD45 and CD14, indicating the cultures were not contaminated with hematopoietic or monocytic cells (Figure 2). HAEC histograms were similar to both EPC groups for all markers.

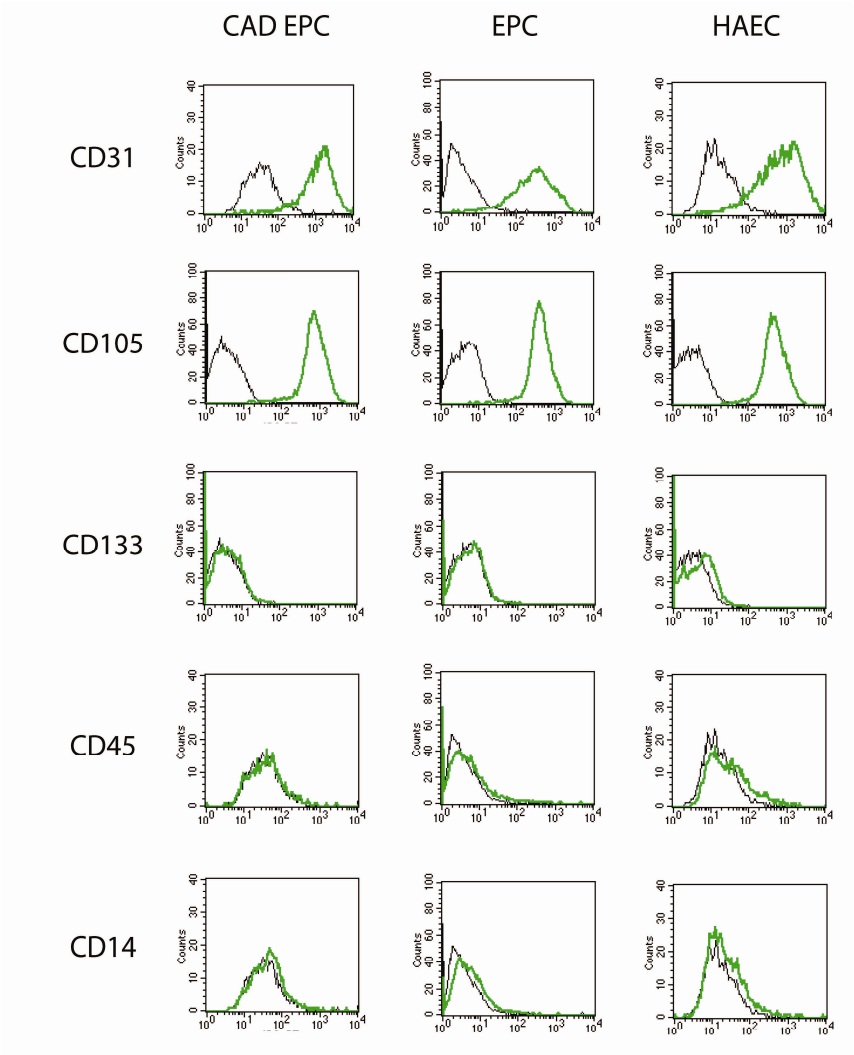

Figure 2. Immunotypic analysis of expanded late-outgrowth EPCs from patients with CAD (CAD EPCs), late-outgrowth EPCs from healthy donors (EPCs), and control human aortic ECs (HAECs) (black lines: fluorescent signals of isotypic controls, bold green lines: fluorescence signals of specific antigens). CAD EPCs, EPCs, and HAECs were positive for endothelial markers CD31 and CD105. CAD EPCs, EPCs, and HAECs showed no positive fraction for stem cell marker CD133 or hematopoietic markers CD45 and CD14. Shown are representative data from three

independent experiments using different CAD EPCs and healthy EPCs with similar results.

3.4.4 Cell Attachment to Teflon-AF™

3.4.4.1 Cell Spreading

Teflon-AF™ was used as a surrogate for ePTFE vascular graft material (23). Spreading rates of late outgrowth EPCs from patients with CAD were compared with cells isolated from healthy individuals on Teflon-AF™ surfaces that have the same hydrophobicity and nearly the same chemistry as expanded ePTFE. Teflon-AF™ surfaces were incubated with 3.3 μg/mL fibronectin for 1 hour to permit cell attachment. EPCs from healthy volunteers spread the fastest. Healthy EPCs were significantly larger in area than HAECs at 4 and 24 hours and significantly larger than EPCs from CAD patients at 24 hours ($p<0.05$) (Figure 3A).

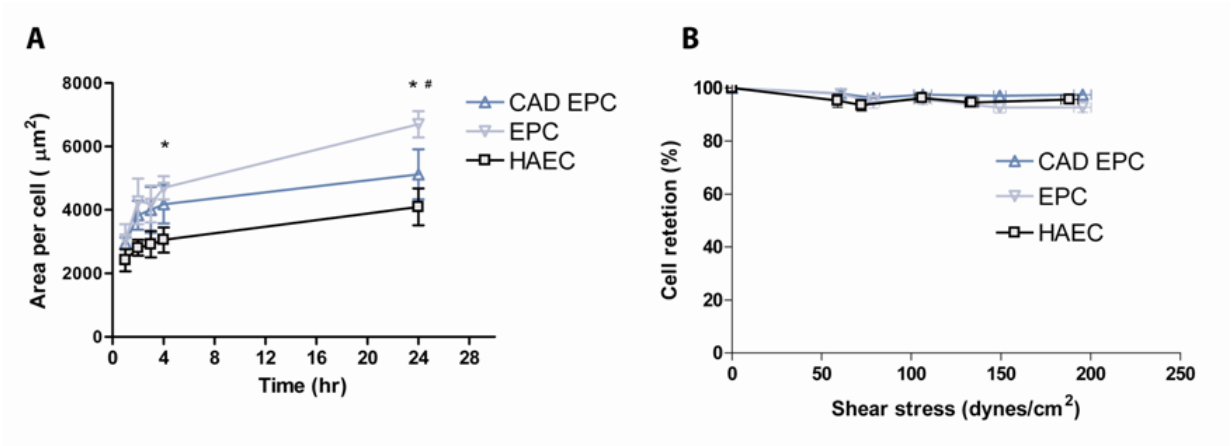

Figure 3. Cell spreading and adhesion on fibronectin-coated Teflon-AF. Late outgrowth EPCs from healthy donors spread at a higher rate than EPCs from CAD patients and HAECs (A). EPCs from healthy donors had a significantly larger area at 4 hours and 24 hours (*p<0.05 EPC vs HAEC, # p<0.05 EPC vs. CAD EPC). ECs were seeded onto Teflon-AF coated with fibronectin for 20 minutes. All three cell types had over 95% adhesion after exposure up to 187 dynes/cm² (B).

3.4.4.2 Cell retention

The ability of late outgrowth EPCs to remain adherent after exposure to fluid shear stress was tested by exposing the cells to short term super-physiological flow. Late outgrowth EPCs from CAD patients, healthy donors, and HAECs adhered firmly to fibronectin-coated Teflon-AF™ after exposure to high shear stresses in a variable height flow chamber. Both cell types showed greater than 95% retention after exposure to shear stress of 187 dynes/cm² (Figure 3B).

3.4.5 Integrin Expression

The primary integrins that mediate cell adhesion to extracellular matrix proteins such as fibronectin and collagen are $\alpha_v\beta_3$ and $\alpha_5\beta_1$. Late outgrowth EPCs from both donor groups expressed significantly higher levels of $\alpha_5\beta_1$ than HAECs ($p<0.05$). Late outgrowth EPCs from CAD patients expressed significantly higher levels of $\alpha_v\beta_3$ than cells from healthy donors and HAECs ($p<0.002$) (Figure 4).

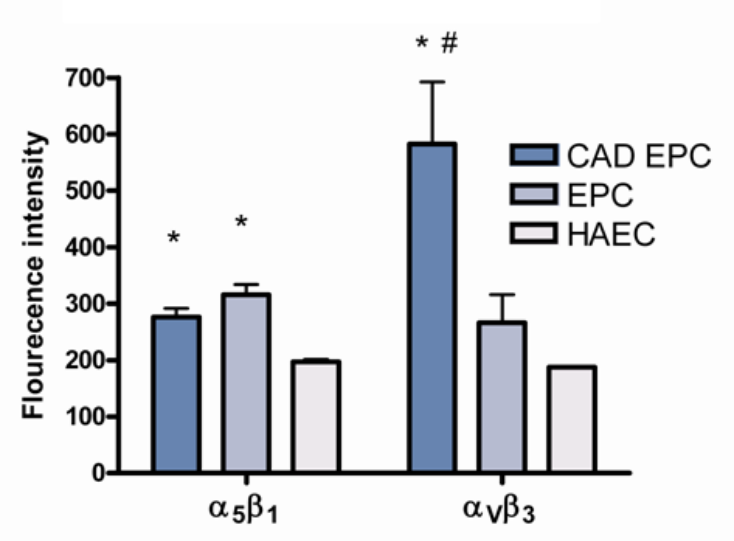

Figure 4. Late outgrowth EPCs from CAD patients and healthy donors expressed significantly higher levels of $\alpha_5\beta_1$ compared to HAECs. $\alpha_v\beta_3$ was expressed at significantly higher levels in CAD EPC (* p<0.05 versus HAEC, # p<0.05 versus EPC).

3.4.6 *In vitro* Vasculogenesis Assay

Both late outgrowth EPCs from CAD patients and healthy individuals spontaneously formed capillaries when plated on three-dimensional Matrigel™ extracellular matrix. At 4 hours, tube structures began to form (Figure 5A). After 24 hours, the cells coalesce and form more discrete tubes (Figure 5B). Vessel length was

significantly higher at 6 hours than 4 or 24 hours (p<0.003) but no significant differences between CAD EPCs, EPCs, and HAECs were observed (p = 0.46) indicating that kinetics of the of the vasculogenesis properties of the cell types in Matrigel™ are similar (Figure 6C).

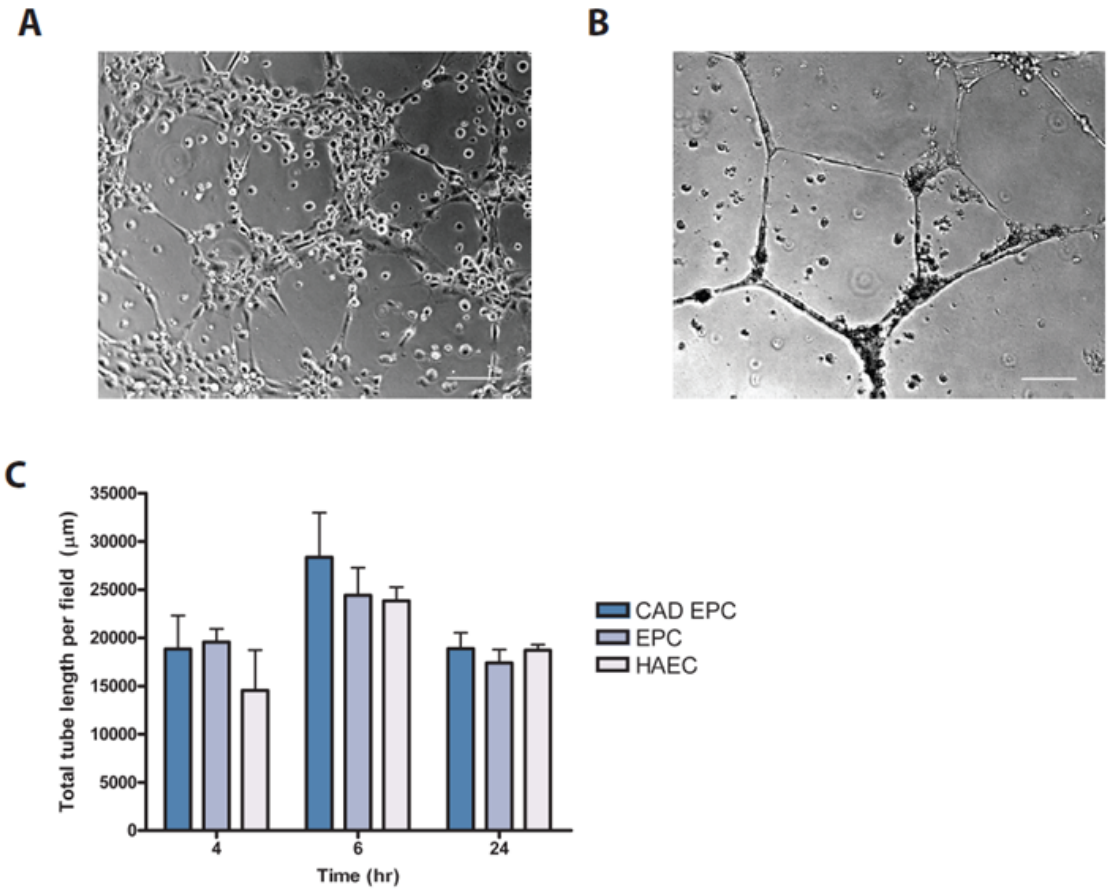

Figure 5. ***In vitro*** **vasculogenesis assay. Representative image of late outgrowth EPCs from CAD patient seeded onto Matrigel™ and viewed after 4 hours by phase contrast microscopy (A). Tubes were more defined after 24 hours (B). There were no significant differences in total vessel length versus cell type when measured at 4, 6, and 24 hours (C). Scale bar 200 μm (A), 100 μm (B).**

3.4.7 Effect of Shear Stress on Cell Morphology and Nitric Oxide Expression

Late outgrowth EPCs from both donors had typical EC cobblestone morphology under static conditions (Figure 6A,B). CD31 staining was similar in both donor groups and was localized to the cell-cell borders. After exposure to 48 hour laminar shear stress of 15 dynes/cm^2, cells elongated and f-actin oriented parallel to flow (Figure 6C,D).

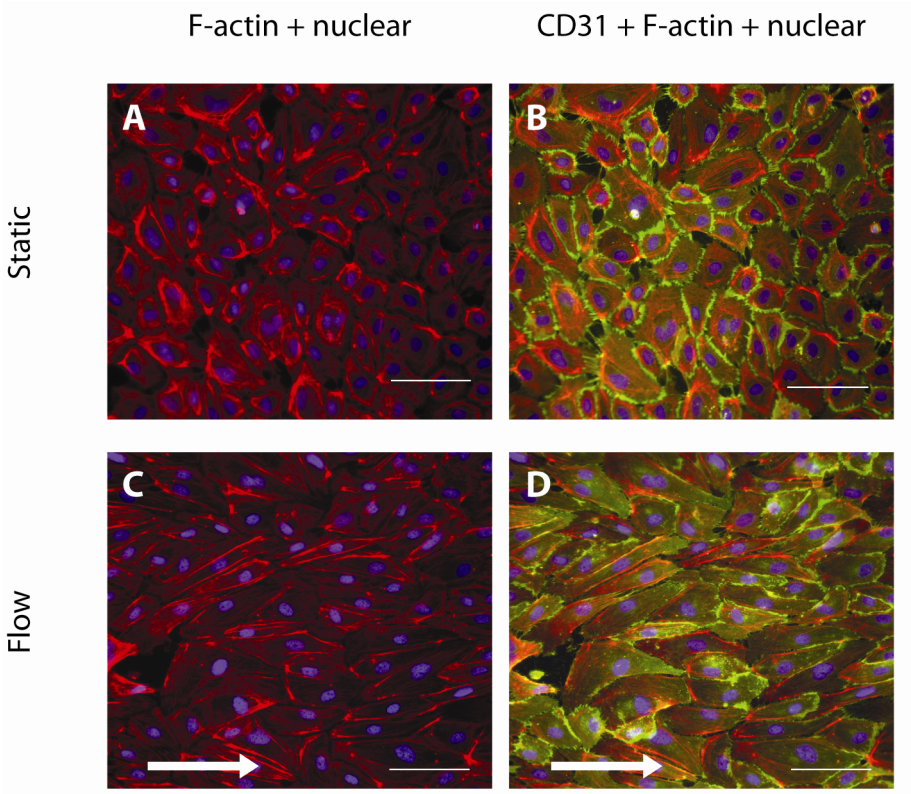

Figure 6. Effect of shear stress on cell morphology. Representative immunoflourescent images of late outgrowth EPCs from patient with CAD under static conditions stained for f-actin (A) and CD31 (B). Cultures were exposed to laminar shear stress (15 dynes/cm^2) for 48 hours. Late outgrowth EPCs tended to elongate and align parallel to the direction of flow (C,D). Scale bar 100 μm.

Late outgrowth EPCs from both healthy donors and donors with CAD cultured under static conditions expressed significantly lower levels of KLF2 and eNOS mRNA than HAECs (Figure 7A,B) ($p<0.05$). Upon exposure to laminar shear stress of 15 dynes/cm^2 for 48 hours, all cell groups increased mRNA levels for the flow responsive transcription factor KLF-2 and eNOS. EPCs from patients with CAD expressed significantly higher levels of KLF-2 than late outgrowth EPCs from healthy donors. However, all cell types cultured under static conditions expressed similar low basal levels of NO products (Figure 7C). Laminar shear stress of 15 dynes/cm^2 for 48 hours increased NO expression 150-fold over static conditions. No significant differences in NO production were observed between cell types ($p = 0.88$).

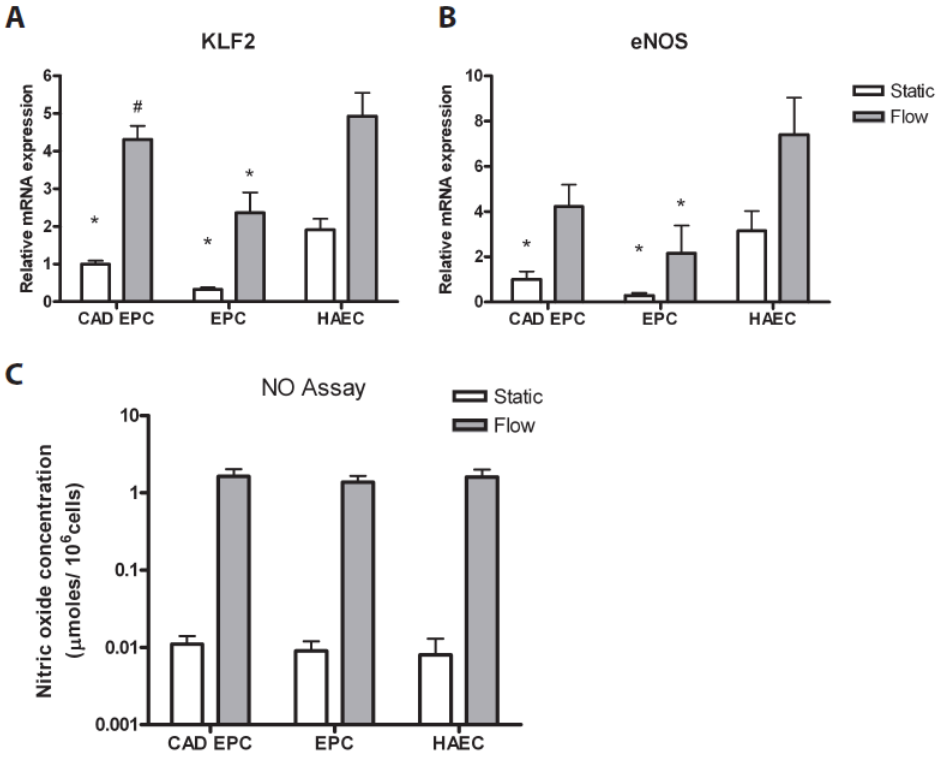

Figure 7. Effect of shear stress on flow responsive genes and nitric oxide expression. KLF2 and eNOS gene expression by patients with CAD and healthy donors were significantly lower than HAECs (A,B). Upon exposure to 48 hr laminar shear, KLF-2 and eNOS mRNA levels increased for all cell types, though expression was significantly reduced for healthy donors compared to HAECs (A,B) (* $p<0.05$ versus HAECs, # $p<0.05$ versus CAD EPCs). Late outgrowth EPCs from CAD patients, healthy individuals, and HAECs all increased their production of nitric oxide during exposure to flow (C). No significant differences were observed in NO release between the three cell groups.

3.5 Discussion

The lack of easily isolated autologous endothelial cell sources is one of the major challenges of vascular tissue engineering (78). The ability to isolate late outgrowth EPCs non-invasively from peripheral blood and expand the colonies in long term cultures is a

major development for autologous cell therapies. Late outgrowth EPCs have been pursued as an alternative cell source for endothelialization strategies (94-99). The 2-3 week time interval before EPC colonies are observed is a clinical drawback for emergency interventions, however the cells are highly proliferative, capable of undergoing over 30 population doublings while maintaining a stable endothelial phenotype during long-term culture justifying their use for elective procedures (84, 94).

If late outgrowth EPCs are to be used as an autologous source of ECs for vascular conduits, they will likely be procured from patients with extensive vascular disease. To our knowledge, the characteristics of late EPCs from these patients have not been fully characterized.

In the present study we compared the ability to isolate late outgrowth EPCs from peripheral blood donated by older patients with coronary artery disease and younger healthy volunteers. EPC isolation and expansion, EC marker expression, cell contamination, cell adhesion, and NO expression provided an essential set of characteristics needed to demonstrate the suitability of late outgrowth EPCs from patients with CAD for autologous endothelialization applications.

The frequency that late outgrowth EPC colonies were observed was similar for CAD and young healthy donors, though no limited proliferation potential colonies were recovered from patients with CAD. While the observation was initially surprising, it was not at odds with recent reports finding that the number of late outgrowth EPCs

isolated in culture increases with the extent of patient coronary artery stenosis (100). Another study quantifying late outgrowth EPCs from patients with age-related macular degeneration showed only 11% of the young control subjects had cultures of more than 10^7 cells, whereas 38% of patients with neovascular age-related macular degeneration had highly proliferative colonies (101).

Cell contamination is an important issue in EC harvesting as cultures can be contaminated with fibroblasts and myofibroblasts that are capable of outgrowing EC cultures. Moreover, endothelialization methods using heterogeneous cell sources increased the extent of neointimal hyperplasia (80). Highly proliferative late outgrowth EPC cultures from both donor types appeared homogeneous, with flow cytometry profiles closely resembling HAECs that were used as a positive EC control. Late outgrowth EPCs from both groups were mature and fully differentiated, displaying antigenic characteristics of ECs, but negative for stem and hematopoietic markers. Additionally, late outgrowth EPCs grown under static conditions had typical cobblestone morphology but were sensitive to shear stress, reorienting parallel to the direction of flow upon application of laminar flow at 15 dynes/cm^2 for 48 hours.

Since one of the causes of failure of endothelialized vascular grafts is cell detachment upon exposure to blood flow (21, 151), seeded ECs must rapidly adhere, spread, and withstand physiological stresses. Previously reported low trypsin conditions during subculture were used to maximize the extent of cell adhesion to

Fibronectin-coated Teflon-AF™ (22). In the current study, late outgrowth EPCs from CAD patients and healthy donors rapidly attached to the substrate and assumed a larger area than HAECs. All EPCs maintained firm adhesion as over 95% of seeded cells remained adherent after exposure to superphysiological shear stresses as high as 187 dynes/cm^2. Although only the highly proliferative EPC cultures were used for all experiments, the increased cell area of late outgrowth EPCs from healthy individuals compared to late outgrowth EPCs from CAD patients and HAEC could be due to decreased proliferation potential as seen in other studies where cell area increases with passage number and cell senescence (152).

The initial adhesion strength is dependent on the number of $\alpha_5\beta_1$ and $\alpha_v\beta_3$ interactions with the material (22). Late outgrowth EPCs from CAD patients and healthy individuals expressed more elevated levels of $\alpha_5\beta_1$ and $\alpha_v\beta_3$ than HAEC, helping to explain the high levels of attachment to Teflon-AF™. Late outgrowth EPCs from CAD patients had increased expression of $\alpha_v\beta_3$ over both HAECs and EPCs from healthy individuals. These integrins are not only important for cell-biomaterial adhesion but also adhesion to denuded arteries (153) and angiogenesis (154) and thus the high levels of $\alpha_5\beta_1$ and $\alpha_v\beta_3$ present may aid late outgrowth EPC homing and vessel formation.

We speculated that with increased expression of $\alpha_v\beta_3$ in late outgrowth EPCs from CAD patients, there may be differences in vessel forming ability between cell types. Capillary formation is important not only for revascularization of ischemic tissue

but also may improve performance of porous materials (5). The presence of CAD showed no effect cell vessel forming ability, as all cell types were able to spontaneously form vessels at comparable densities during *in vitro* vasculogenesis assays. Recent studies have shown that with late outgrowth EPCs, vessel formation decreases after cells are exposed to oxidative stress though it remains to be seen if there are differences versus patient disease state (155). A more selective vessel forming assay involving co-culture with fibroblasts may be more appropriate to evaluate the differences between cell types (156).

Vascular ECs are known to release NO when challenged with fluid shear stress. Reduction in nitric oxide production is believed to lead to early development of atherosclerosis (157). KLF2, a key transcription factor that regulates key factors in maintaining an antithrombotic EC surface, was significantly reduced in late outgrowth EPCs versus HAECs. EPCs exposed to 48 hours shear increased their transcription of KLF2 and eNOS, in agreement with studies showing that KLF2 acts as a regulator of eNOS and can be induced by biomechanical stimulation (158, 159). Late outgrowth EPCs from CAD patients and healthy individuals cultured under static culture conditions expressed low basal levels of NO end products; whereas outgrowth EPCs exposed to laminar shear stress over 48 hours expressed approximately 150-fold more NO over static conditions. No significant differences were observed between late outgrowth EPCs from CAD patients and healthy donors indicating that EPCs from both groups are

responsive to shear stress and have similar NO secretion rates *in vitro*. Levels of NO secreted by both donor groups were similar to HAECs, comparable to recent studies demonstrating no differences in NO release between porcine late outgrowth EPCs and porcine aortic ECs grown under static conditions (95).

A drawback of using autologous late outgrowth EPCs for endothelialization applications is their exceedingly rare presence in peripheral blood MNC populations. The frequency of late outgrowth EPCs in healthy volunteers was estimated by Yoder et al. as 0.017 colonies per 10^6 plated MNCs (89). With an average of $103 \pm 7 \times 10^6$ MNCs per subject observed in our study, we would estimate 1.75 endothelial colonies per 50 mL peripheral blood sample would be recovered. Others have similarly estimated 2.5 late outgrowth EPC colonies per 50 ml blood (100). Simply doubling the volume of blood collected should also increase the frequency of isolation. Alternatively, preselecting CD34+ CD45- MNCs before plating can enrich cell populations of late outgrowth EPCs by as much as 300-fold over non-sorted cord blood cultures (160). Methods to specifically capture late outgrowth EPCs using novel peptide ligands are also under development (161).

Limitations of this study

The goal of the current study was to assess the feasibility of isolating therapeutic late outgrowth EPCs from patients with known CAD, as indicated by angiography. Not surprisingly, this patient population differed in a range of clinical characteristics from

our healthy donor population. The majority of the patients were also on a range of medications at the time of catheterization. As such, we feel this study reflects the pool of patients with CAD that would likely be candidates for autologous endothelialization therapies.

Because the sample was small and random, we were unable to systematically determine the impact of clinical factors or medication use on the isolation and characterization of late outgrowth EPCs. Having said this, the impact of patient-specific factors merits consideration. It has previously been shown that acute myocardial infarction (162, 163) can cause mobilization of late outgrowth EPCs and that statin treatment can maintain elevated levels of late outgrowth EPCs within the vasculature (164). Patient age may also affect the ability to isolate late outgrowth EPCs (165). Our CAD population included only patients with stable CAD, therefore, we do not believe that this represents a population in which EPCs were mobilized by acute injury. It may be of interest in future work to assess the impact of acute or chronic statin therapy before isolation of EPCs. Our data shows that we were able to isolate functional late outgrowth EPCs from patients with CAD on and off statin therapy.

Finally, mononuclear cells derived from the bone marrow are multipotent with the ability to generate vascular or muscular cells (166). As such, culture conditions strongly influence their phenotypic destination (167, 168). Also, even mature ECs are known to change their surface marker expression during culture (169). Therefore,

subjecting both CAD and healthy late outgrowth EPCs to the same long-term culture conditions may have influenced the cells acquiring the same EC phenotypic characteristics. Practically speaking, this concern is less important than the ability to non-invasively obtain healthy cells suitable for autologous endothelialization therapy from the peripheral blood of patients with significant CAD.

3.6 Conclusions

Late outgrowth EPCs isolated from CAD patients are a potentially clinically relevant cell source for autologous endothelialization applications. The isolation of EPCs from peripheral blood is less invasive than harvesting endothelial cells from excised blood vessels and adipose tissue or late outgrowth EPCs isolated from bone marrow. Late outgrowth EPCs were capable of attaching, spreading, and maintaining firm adhesion to the underlying substrate and showed a functional response to flow by reorienting and increasing expression of NO. Once colonies were established and expanded from small volumes of peripheral blood, few differences were observed between late outgrowth EPCs isolated from CAD patients and those isolated from healthy individuals.

Chapter 4. *In Vitro* Functional Testing of Endothelial Progenitor Cells that Overexpress Thrombomodulin

Original article co-authored with Y Xue, N Haque, JH Lawson, and WM Reichert. Text excerpts and all figures are reprinted with permission from Mary Ann Liebert, Inc. Figure 12 and Figure 13 were added since the original manuscript submission.

Stroncek JD, Y Xue, N Haque, JH Lawson, and WM Reichert. In Vitro Functional Testing of Endothelial Progenitor cells that Overexpress Thrombomodulin, Tissue Engineering Part A [accepted].

4.1 Synopsis

This study investigated the augmentation of endothelial progenitor cell (EPC) thromboresistance by using gene therapy to overexpress thrombomodulin (TM), an endothelial cell membrane glycoprotein that has potent anti-coagulant properties. Late outgrowth EPCs were isolated from peripheral blood of patients with documented coronary artery disease and transfected with an adenoviral vector containing human TM. EPC transfection conditions for maximizing TM expression, transfection efficiency, and cell viability were employed. TM-overexpressing EPCs had a 5-fold increase in the rate of activated protein C production over native EPCs and EPCs transfected with an adenoviral control vector expressing β-galactosidase ($p<0.05$). TM upregulation caused a significant 3-fold reduction in platelet adhesion compared to native EPCs, and a 12-fold reduction compared to collagen I coated wells. Additionally, the clotting time of TM-transfected EPCs incubated with whole blood was significantly extended by 19% over native cells ($p<0.05$). These data indicate that TM-overexpression has the potential

to improve the anti-thrombotic performance of patient-derived EPCs for endothelialization applications.

4.2 Introduction

Endothelial cells (ECs) make up the inner lining of all natural blood vessels and perform critical functions in thromboregulation and mediation of vascular health. The seeding of ECs onto the blood-contacting surface of synthetic materials has been shown to improve the performance of biomedical implants such as synthetic vascular grafts (170), vascular assist devices (109), and heart valves (171). Effective endothelialization of the material surface requires that a fully confluent monolayer of ECs remain adherent and express a healthy, quiescent EC phenotype (25). A subconfluent monolayer of ECs can lead to a thrombogenic surface (172), while injured or activated adherent ECs expose tissue factor and down regulate key anti-thrombotic and anti-inflammatory molecules (117, 118), increasing the risk of thrombosis and intimal hyperplasia due to smooth muscle cell activation.

We and others have shown that rare peripheral blood-derived EC-like cells, termed late outgrowth endothelial progenitor cells or endothelial colony forming cells, can be isolated from patients with coronary artery disease (CAD) (100, 173). In this study EC-like late outgrowth endothelial progenitor cells are simply referred to as "EPCs".

The isolation of EPCs from peripheral blood, a method less invasive than surgical harvest of ECs from large veins or adipose tissue, is a significant development for autologous endothelialization of vascular grafts (34, 81, 84). EPCs can be expanded to higher densities with minimal contamination with other cell types, maintain firm adhesion to the underlying substrate, and can express a healthy quiescent EC phenotype *in vitro* (173). EPCs have been shown to mediate clot formation, releasing anti-thrombotic molecules to prevent platelet activation and reduce thrombus formation (174, 175). Proof-of-principle studies have shown that animal-derived EPCs can improve the patency rates of synthetic small diameter vascular grafts (96, 97, 176). While harvesting EPCs from CAD patients is attractive, there is concern that both CAD and aging may lead to decreased functional activity of these cells (119) and detract from a healthy anti-thrombogenic phenotype (120, 121).

Thrombomodulin (TM) is an endogenous anti-thrombotic molecule that is expressed at the surface of ECs that plays a key role in mediating endothelial thromboresistance. TM acts in two manners: first by scavenging excess thrombin, and second by accelerating the production of activated protein C (APC). Inhibiting thrombin activity reduces fibrin formation and the activation of platelets, leukocytes, and smooth muscle cells (124); whereas increased APC production acts upstream and limits thrombin generation (123), reduces the expression of inflammatory cytokines (125-127),

down regulates EC expression of adhesion molecules to prevent leukocyte adhesion (128), and inhibits EC apoptosis (129).

Because TM is decreased in patients with diabetes and atherosclerosis (177, 178) we hypothesized that overexpression of TM by patient-derived EPCs would enhance their performance for vascular graft endothelialization protocols. The inhibition of thrombin activity through TM overexpression may reduce the number of thrombosis-caused failure events occurring in vascular constructs within the first week post-implant while also reducing inflammation and the progression of atherosclerosis (179, 180). The objective of the current study was to assess *in vitro* the feasibility of augmenting the expression of TM in patient-derived EPCs to create a short-lived enhancement of the intrinsically anti-thrombotic phenotype of healthy ECs. EPCs isolated from patients with documented CAD were transfected *ex vivo* with the gene for human TM in the attempt to create a transient increase in TM expression. EPCs were evaluated for their expression of TM over time and their ability to (1) remain adherent after exposure to laminar flow, (2) produce APC, (3) prevent platelet adhesion, and (4) extend the clotting time of whole blood.

4.3 Methods and Materials

4.3.1 EPC Isolation and Cell Culture

All cells designated as "EPCs" in the current study were late outgrowth EPCs isolated and expanded from peripheral blood drawn from patients undergoing cardiac catheterization in the Duke University Medical Center who had documented advanced coronary artery disease by angiography. Patient clinical characteristics have been described previously (173). The Duke University Institutional Review Board approved the protocol for collection and use of human blood employed in the study.

EPC cultures were isolated and expanded (n=5) from 50 mL of peripheral blood as previously described (181). Late outgrowth EPCs were grown in endothelial complete media consisting of EBM-2 supplemented with EGM-2 SingleQuots (Lonza, Walkersville, MD), 10% FBS (HyClone, Logan, UT) and 1% antibiotic/antimycotics solution (Gibco, Carsbad, CA). Cells were used at passages 5-10 for all experiments.

EPC cultures were previously characterized to confirm EC phenotype, which has been published elsewhere (173). EPCs expressed a similar phenotype to a control population of human aortic ECs (Lonza). EPCs had uniform expression of EC markers CD31, CD105. Cells were negative for the stem cell marker CD133 as well as hematopoietic and monocytic markers CD45 and CD14. EPCs also expressed nitric oxide and were capable of forming tubular structures in Matrigel.

4.3.2 Virus Production

Two different adenoviral vectors were used in this study. First, replication deficient adenoviral expressing human thrombomodulin (AdTM) was a gift from Dawn Bowles, Duke University. Human cDNA for the TM gene was obtained from American Type Culture Collection (ATCC). The AdEasy system (Stratagene, La Jolla, CA) was used to insert the human TM gene with a cytomegalovirus promoter into an adenoviral vector. Recombinants plasmids were identified by restriction digest and mass-produced in the recombination-deficient XL10-Gold ultracompetent bacterial strain (Stratagene). Purified recombinant Ad plasmid DNA was linearized and used to transfect an adenovirus packaging cell line, AD–293 cells, for large scale viral production. Recombinant adenovirus was purified using cesium chloride gradients, aliquoted, and stored at -80ºC for later use. The presence of replication-competent adenovirus was excluded by assessment of infectivity in COS1 cells and tested for replication competent virus by PCR for E1a prior to use.

Second, replication deficient β-galactosidase adenovirus "control vector" (AdCV) was purchased (Eton Bioscience, San Diego, CA). AdCV stained cells blue after incubation with X-gal in proportion to the degree of transfection and also served as an experimental control to account for effects associated with transfection.

4.3.3 Adenoviral Transfection Optimization

Transfection. EPCs were transfected in EBM-2 with 2% FBS, and 1% antibiotic/antimycotics solution for either 4 or 24 hours at 37 ºC with multiplicity of infections per cell (MOI) of 500, 100, 20, or 0. After transfection, cells were washed three times with DPBS and fresh endothelial complete media was added. Following transfection optimization testing, a viral concentration of 100 MOI for 4 hrs was used for all subsequent experiments (n=4).

Transfection Efficiency and Thrombomodulin Surface Expression. Transfection efficiency of EPCs was assessed by flow cytometry. EPCs were seeded into 12-well plates and transfected at confluency. 24 hours after AdTM transfection, EPCs were detached using 0.025% trypsin (Lonza). Detached cells were resuspended 1:4 by volume with PE-conjugated mouse anti-human CD141 (BD Biosciences, San Jose, CA) and 10% goat serum for 40 minutes at 37 ºC. Cells were fixed in 3.7% formaldehyde and flow cytometric analysis was performed with FACSCalibur (BD Biosciences). A fluorescence intensity threshold gate was set so that 1% of single native EPC cell events had fluorescence intensities falling above the gate. For all AdTM-EPC transfection conditions, the percentage of cells gated with respect to the initial threshold gate was recorded (n=4).

In the same experiment, surface expression of TM after transfection was assessed by flow cytometry with CD141-PE as described above. Mouse PE conjugated IgG_1 was used as isotype control (BD Biosciences). Geometric mean fluorescence intensity of CD141-PE each sample was subtracted from the respective isotype control for all experiments (n=4).

Cell Proliferation. EPCs were seeded into 12-well plates and allowed to grow for one day to reach a confluent density of 50,000 cells/cm^2. The cells were transfected with AdTM for 4 or 24 hours with 500, 100, 20, or 0 MOI. 24 hours later, in order to mimic seeding the transfected cells onto new material at less than confluent density, EPCs were trypsinized and each well was transferred to a T-25 flask to allow room for cell expansion. Media was changed the following day. Four days after transfection (three days after typsinization from 12-well plate), EPCs within T-25s were trypsinized and counted in trypan blue solution to exclude dead cells (n=3).

4.3.4 Long-term Thrombomodulin Expression

EPCs were seeded into 6-well plates at a density of 30,000 cells/cm^2. Cells were transfected with AdTM on the following day. Cultures were trypsinized 1, 3, 7, 14, and 21 days after transfection. Detached cell populations were divided into two groups: half were used to evaluate mRNA expression of TM, and half were used for evaluate surface

expression of TM as described above using PE-conjugated mouse anti-human CD141 primary antibody (BD Biosciences). Media was changed every other day during the experiment (n=3).

Cellular RNA was isolated using the RNeasy Minikit (Qiagen, Germantown, MD). The quantity and purity of all RNA samples were measured using a NanoDrop Spectrophotometer (NanoDrop Technologies, Wilmington, DE). Reverse transcription of 50 ng total RNA was performed with cDNA kit (Bio-Rad, Hercules, CA) and MyCycler (Bio-Rad). RT-PCR was performed using a SYBR-Green RT-PCR kit (Bio-Rad) and the MyIQ™ iCycler Optical Module (Bio-Rad). Whole-gene cDNA sequences of the target genes were obtained from PubMed, and TM and Beta-2 microglobulin primer sequences were generated using the online design program Primer3 (149). The melt curves of the primers were examined after reaction with reference RNA, and primers were selected that had uniform and single-product melt curves. After results were obtained, fold change from the reference Beta-2 microglobulin RNA was calculated by the $2^{-\Delta\Delta CT}$ method (n=3).

4.3.5 Effect of Shear Stress on Cell Adhesion and Morphology

Cells were seeded onto SlideFlasks (NUNC, Rochester, NY) at a density of 50,000 cells/cm^2 and transfected at confluency. The following day, the slides were placed in a parallel-plate flow chamber and connected to a circular flow setup consisting of a

peristaltic pump (Cole Palmer, Vernon Hills, IL), pulse dampener (Cole Palmer), and parallel-plate flow chamber as described previously (147). The flow media used consisted of EBM-2 + 5% FBS + 1% antibiotic/antimycotic. Cells were exposed to 15 dynes/cm^2 for 48 hours. A mean shear stress of 15 dynes/cm^2 represented a mean wall stress value larger or comparable in magnitude to human medium to large arteries such as the common carotid artery, aorta, femoral artery, and brachial artery (182). Controls consisted of cells under identical culture conditions, but not exposed to flow (static).

After exposure to flow, cells were fixed with 3.7% paraformaldehyde, permeabilized with 0.1% Triton X, and non-specific binding was blocked with 10% goat serum (Sigma). Primary antibodies for CD31 (Invitrogen) (1:100) were incubated with the cells for 1 hour at 37°C. Cells were rinsed multiple times and then incubated with a goat anti-mouse Alexa488-conjugated secondary antibody (1:500) (Invitrogen). F-actin was visualized with rhodamine phalloidin according to the manufacturers' instructions (Invitrogen). Nuclei were stained with 10 μg/ml Hoechst 33342 (Invitrogen). Images were captured using a Nikon Eclipse TE2000-U (Nikon, Tokyo, Japan) inverted fluorescent microscope and a digital camera (DS-Qi1Mc, Nikon). The angle of cellular orientation was determined using ImageJ for 50 cells across 4 locations for each condition (n=4).

4.3.6 Assessment of TM Function

APC production. The biological activity of EPC TM was assessed by measuring the rate protein C is cleaved by the TM-thrombin complex to form APC (n=4). EPCs were seeded into 24-well plates and transfected when confluent. One day after transfection, cultures were washed with Tyrodes buffer and 5nM thrombin (Haematologic Technologies Inc (HTI), Essex Junction, VT) was added for 5 min at 37ºC. 400nM human protein C (HTI) was added and duplicate 50μL supernatant aliquots were removed at 0, 1, 5, 10, 15, 20, 30, 40, 50, and 60 minutes. Free thrombin was inhibited with equal volumes of TM stop solution (5U/mL hirudin (Calbiochem, San Diego, CA), 1μM human antithrombin III (HTI), and 5U/mL porcine heparin (Sigma-Aldrich, St. Louis, MO) in Hank's buffered salt solution. A standard curve of APC (HTI) ranging from 0 to 25nM was prepared and added to the 96-well plate. The APC formed was quantified with the addition of 100μL/well of 400mM Spectrozyme PCa (American Diagnostica, Stamford, CT) in a microtiter plate reader (BioTek Instruments, Winooski, VT) by the change in absorbance with time at 405nm (n=4).

Leukocyte adhesion. EPCs were seeded onto SlideFlasks (Nunc, Rochester, NY) and transfected at confluency. The following day, Slideflasks were incubated for 4 hr with endothelial complete media or endothelial complete media with IL-1β (10 μg/mL). Slides were placed in a parallel plate flow chambers and HL-60 cells (2 x 10^6 cells/mL) stained with Cell Tracker Orange (Invitrogen) were infused over the EPCs for 5 minutes

at a shear rate of $55s^{-1}$ and shear stress of 0.5 dynes/cm^2 using a syringe pump (Harvard Apparatus, Holliston, MA). The slide was then washed by infusing DPBS for 5 minutes at a shear rate of 110 s^{-1} and fixed in 3.7% paraformaldehyde. A series of 12 images per slide were captured on a fluorescent microscope (Nikon Eclipse TE2000-U, Tokyo, Japan) and the number of adherent HL-60 cells were quantified with ImageJ (n=5).

Platelet adhesion. EPCs were seeded onto 12-well plate and transfected at confluency, 24 hours before blood collection. For use as a positive control, rat-tail collagen I (BD Biosciences) at 100μg/mL in DPBS, was plated overnight at 37°C. Blood from healthy human volunteers was drawn from the antecubital vein directly into blood collection tubes containing acid citrate dextrose for anticoagulation. All blood samples were used the same day.

Blood samples were centrifuged at 300g for 10 min at room temperature and platelet-rich plasma was collected. Platelet-rich plasma (0.5 ml per well) was gently pipetted into each well. After incubation for 30 min at 37°C, wells were washed with DPBS three times to thoroughly remove free platelets and the wells were fixed with 3.7% paraformaldehyde. Wells were blocked with 10% goat serum then incubated for 30 min with mouse anti-human CD41 primary antibody (BD Pharmingen). Cultures were rinsed in DPBS 3x and incubated with a goat anti-mouse Alexa488-conjugated secondary antibody (1:500) (Invitrogen). Five fields from each well were randomly selected and imaged with phase contrast and fluorescence to view EPC and platelet coverage

respectively. The percent area covered with adherent platelets was assessed with ImageJ (n=4).

Clotting assay. EPCs were seeded into 6-well plates and transfected at confluency. The following day, blood was drawn from healthy individuals who had not taken any anti-coagulant medication within the past week and placed into vacutainers filled with 3.2% buffered sodium citrate (BD). Wells were washed twice with DPBS without calcium chloride and magnesium chloride. The anti-coagulant citrate was reversed just prior to the assay by adding calcium chloride (0.105M) at a 1:10 ratio to blood. Blood was added to each well and the plate was placed on a digital shaker (IKA, Staufen, Germany) at 200 rpm at room temperature and the time required for clot formation was recorded. All donated blood was used within 4 hours after drawing (n=4).

4.3.7 Statistics

Differences among groups were carried out by multivariate ANOVA, with the significance of individual differences established by post hoc Fisher's Protected Least Significant Difference Test. *P* values below 0.05 were considered to indicate a statistically significant difference.

4.4 Results

4.4.1 EPC Isolation and Transfection Optimization

Cultures of EPCs from patients with CAD were isolated and expanded in 7 out of 13 donors from 50 mL of blood, obtaining over 10 million late outgrowth EPCs in 7 out of 13 patients (173). Although EPCs cultures were typically frozen at lower passages (P3-P5), extrapolating the number of cells capable of being expanded from a frozen vial, it would be possible to have over 30 million cells in less than six weeks for 5 out of 7 CAD patients having EPC colonies. Some patient-derived cultures could be expanded to significantly higher number of cells; in one patient for example, over 350 million EPCs could be obtained after 6 weeks. A total of 20-30 million EPCs would likely be sufficient for seeding the lumen of a small diameter synthetic vascular graft used for coronary artery bypass surgery (10-15 cm long x 0.4 cm inner diameter, with seeding density of 1.5×10^6 cells/cm^2) (183) .

After confirming that EPC cultures expressed EC markers and were negative for hematopoietic and monocytic markers as previously described (173), the cells were transfected with an adenoviral vector. Transfection efficiency was determined by infecting EPCs with an adenoviral vector expressing human thrombomodulin (AdTM) and performing flow cytometry Figure 8A,B. The percentage of transfected cells having fluorescent intensities higher than native cells increased significantly with dosage of

viral particles (20, 100 and 500 MOI) (p<0.0001). There was no significant difference in percent transfected versus incubation time (4 hr versus 24 hr; p=0.78). At the intermediate vector dosage of 100 MOI, 4 hour incubation resulted in 83% cellular transfection, while 24 hour incubation increased efficiency to 91%.

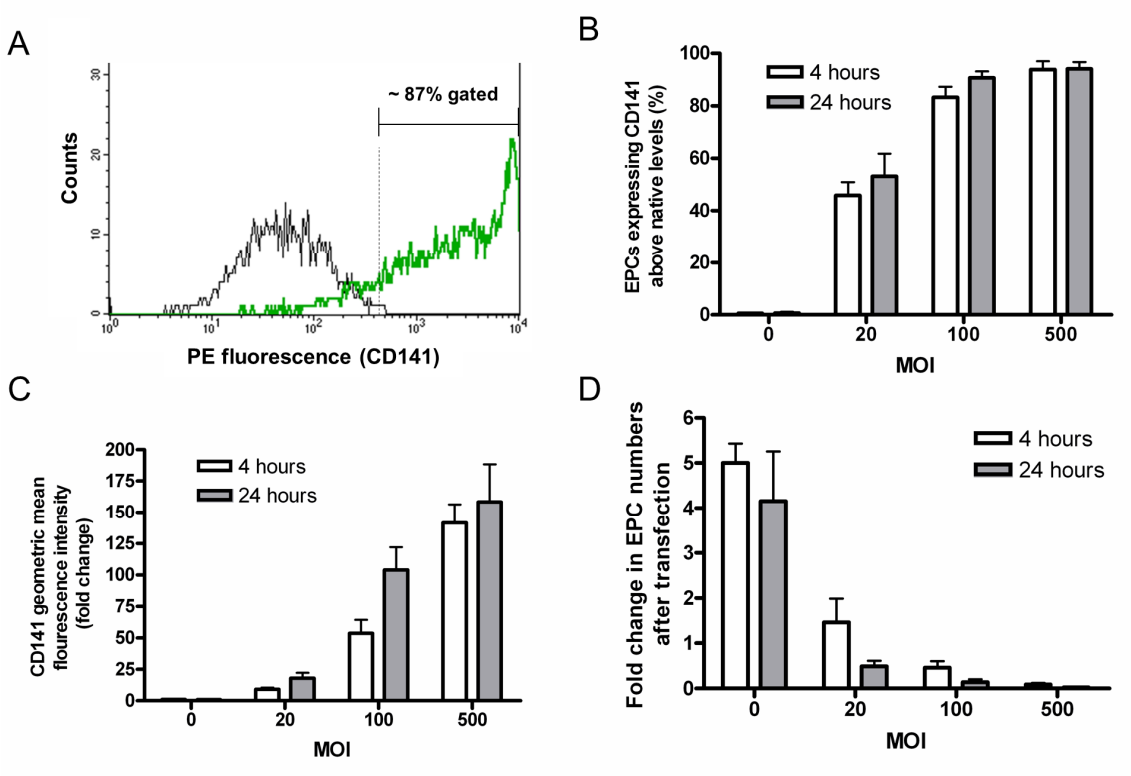

Figure 8: Optimization of adenoviral transfection of EPCs. EPCs were assessed for transfection efficiency after AdTM by flow cytometry for CD141-PE. Representative image of native EPCs (black line) and EPCs transfected 4 hours with 100 MOI (green bold line) (A). The percentage of EPC expressing CD141 higher than native EPCs increased with viral concentration (white bars: 4 hour transfection time; gray bars: 24 hour transfection time) (B). Surface expression of CD141 was increased with greater vector concentrations (C). Four days after transfecting EPCs with AdTM, EPC numbers were decreased versus native EPCs (all cultures initially had 1.9 x 10^5 cells at transfection) (D).

Transfection of EPCs with the gene for human TM (AdTM) increased the surface expression of TM substantially above the basal level measured of native EPCs ($p<0.0001$) (Figure 8). CD141 geometric mean fluorescence intensity, measured by flow cytometry, was used to determine the TM expression at the cell surface. Transfection with AdTM resulted in augmentation of TM expression with increasing viral dosage; however, this increase was essentially the same at 4 and 24 hour incubation times. Specifically, 4 hours incubation with 20 MOI had a 9-fold increase, 100 MOI had a 53-fold increase, and 500 MOI had a 140-fold increase, with similar increases observed with 24 hour incubation ($p = 0.16$).

Transfection of EPCs with AdTM also caused a decrease in overall cell numbers as measured by average live cells per flask post transfection (Figure 8D). EPCs were transfected in a 12-well plate using 20, 100 and 500 MOI for 4 and 24 hours. To mimic the seeding of the transfected cells onto a new material at subconfluent density, 24 hours post transfection 190,000 cells were transferred to a T-25 flask and allowed to grow for three additional days before they were detached and counted. EPCs designated 0 MOI referred to those that underwent the same 4 day procedure minus the actual transfection step.

For 0 MOI EPCs, the number of cells increased by more than 4-fold from the initial number of cells before transfection (Figure 8D). In contrast, other than 20 MOI for 4 hours, all AdTM dosages and incubation times inhibited the growth and decreased

viability of EPCs relative to the 4-day proliferation of native cells. There was no significant difference in cell numbers overall between 4 and 24 hour transfection (p = 0.43). Control experiments with the replication-deficient AdCV revealed a similar decrease in cell numbers (data not shown), indicating that this effect arose from the transfection and not TM expression.

Clearly, an increase in per cell TM expression and loss of cell proliferation and viability presented a trade-off. A viral concentration of 100 MOI for 4 hours was used for all subsequent experiments.

4.4.3 Time Course of TM Expression

Figure 9 shows the three week time course of TM expression for EPCs with a 4-hour incubation of 100 MOI AdTM for fold changes in both TM mRNA expression measured by RT-PCR and surface TM protein expression measured by flow cytometry. Both mRNA and protein expression peaked at 3 days before decreasing to close to native levels after 21 days. All cultures remained confluent over the course of 21 days, indicating that there was no loss in cell coverage over time due to transfection.

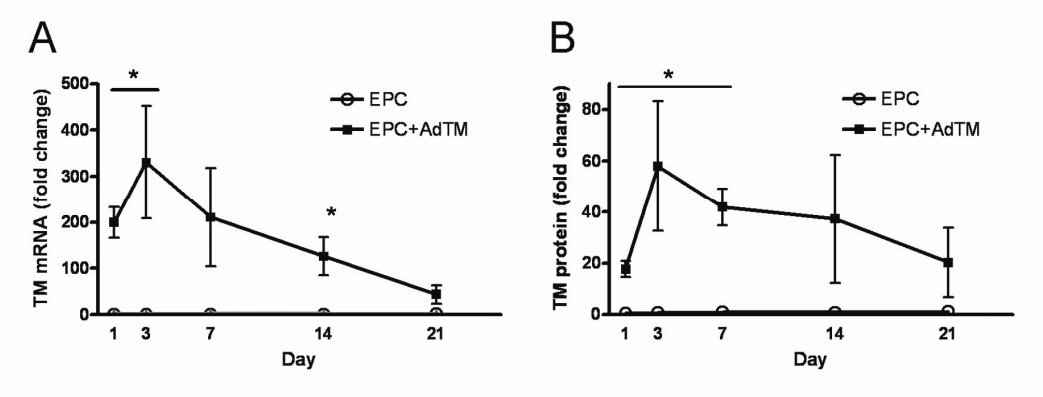

Figure 9. Long-term thrombomodulin expression measured through TM mRNA expression (A) and TM surface expression (B) in native and AdTM-transfected EPCs (*p<0.05 versus native EPCs).

4.4.4 Orientation of EPCs Subject to Flow

Figure 10 shows EPCs transfected with 100 MOI AdTM for 4 hours before and after exposure to 48 hour *in vitro* laminar shear stress of 15 dynes/cm^2. Cells were stained with CD31 (green) to indicate cell-cell borders, rhodamine phalloidin (red) to indicate F-actin, and Hoechst (blue) to indicate nuclei. Pre-flow cells show a typical cobblestone morphology (Figure 10A) while post-flow cells became elongated in the direction of flow (Figure 10B). Table 5 contains the angle between the major and minor axis of the cells averaged over 50 cells for native untransfected cells, and cells transfected with AdCV and AdTM. All pre-flow cases exhibited average angles of 42-47 degrees indicating random cellular orientation, while all post-flow cases showed average angles of 10-17 degrees indicating cellular alignment parallel to the direction of flow. The change in cellular orientation pre and post-flow for all conditions was significant

(p<0.0001), although there was no significance between native and transfected cells (p = 0.78). EPCs across all transfection conditions remained adherent during 48 hour exposure to flow.

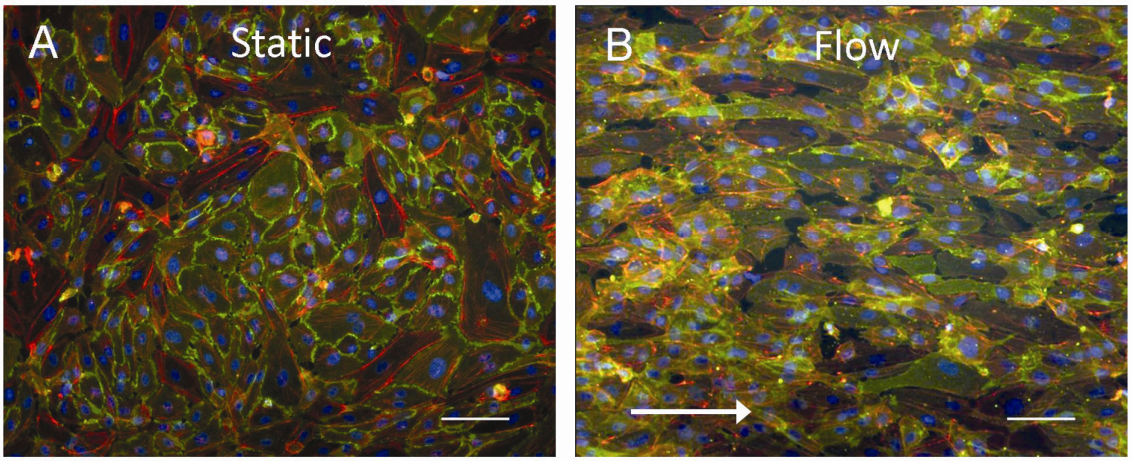

Figure 10. Transfected EPCs maintain firm adhesion and reorient in the direction of flow. Before the exposure to flow, AdTM EPCs had a random orientation and stained for PECAM (green), F-actin (red), and nuclei (blue). After 48 hours of laminar flow, AdTM-transfected EPCs remained adherent and aligned with the direction of flow (white arrow) (B) (scale bar 100 μm).

Table 5. EPC angle of orientation pre and post exposure to 48 hour laminar flow (*p<0.0001 vs static condition).

	Average Angle of Cell Orientation	
	Static	**Flow**
EPC	46.9 ± 3.0	*16.6 ± 4.4
EPC + AdCV	41.9 ± 4.4	*10.5 ± 1.0
EPC + AdTM	45.6 ± 4.3	*11.7 ± 2.7

4.4.5 APC Activity

Figure 11 shows the biological activity of TM protein expressed by EPCs transfected with 100 MOI AdTM or AdCV for 4 hours, compared to basal expression measured for untransfected cells EPCs. Bare tissue culture polystyrene (TCPS) wells were used as the negative control. All cells expressed significantly higher rate of APC production than did TCPS bare wells. TM activity of AdTM-transfected EPCs was 5-fold greater than both native EPCs ($p<0.05$) and EPCs transfected with AdCV.

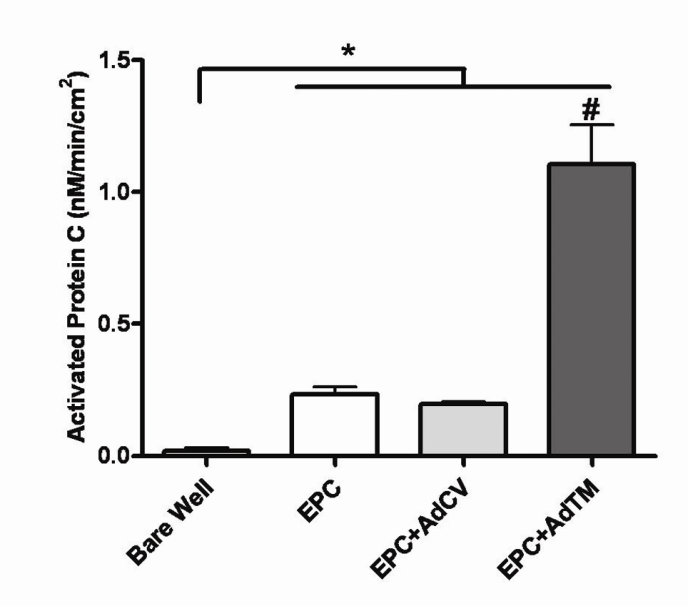

Figure 11. APC production rate of bare wells, EPCs, EPCs + AdCV, and EPCs + AdTM (*p<0.05 versus bare well, #p<0.05 versus native EPCs and EPCs + AdCV).

4.4.6 Leukocyte Adhesion

Neutrophil adhesion onto EPC cultures was tested under short term laminar flow. Neutrophils derived from a human neutrophil cell line, HL-60 cells, were infused

at a rate of 0.5 dyne/cm^2 for 5 minutes and washed at a rate of 1 dynes/cm^2 for 5 minutes before fixing and imaging. Without IL-1β stimulation, few HL-60 cells were able to adhere to native EPCs or transfected EPCs. When cells were pre-stimulated with IL-1β, TM-transfected EPCs had 43% fewer neutrophils per cm^2 compared to native EPC cultures (p<0.05) (Figure 12).

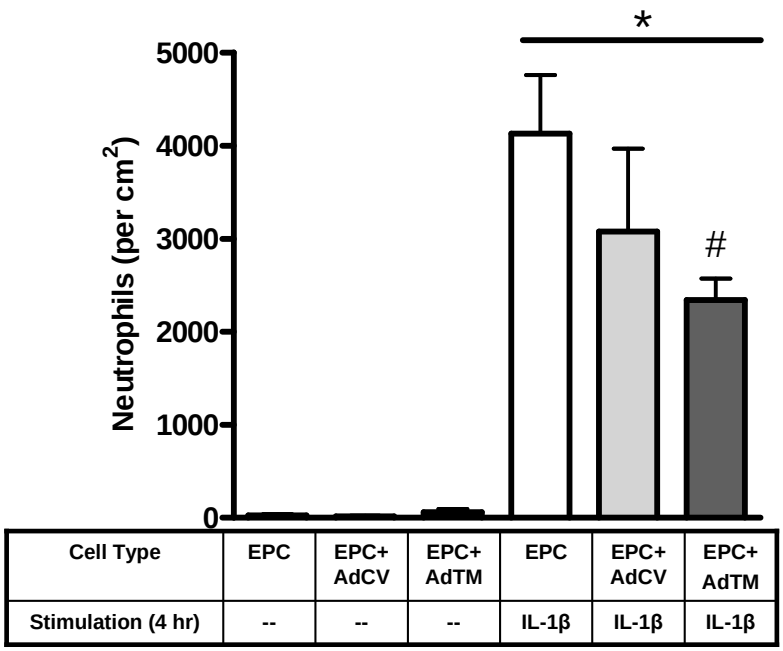

Figure 12. Dynamic neutrophil adhesion to confluent layers of EPCs. Unstimulated EPCs had low levels of neutrophil adhesion. IL-1β prestimulation resulted in increased neutrophil adhesion (*p<0.0001 versus no stimulation) and TM-transfected EPCs had significantly fewer neutrophils compared to native EPCs (#p<0.05 versus native EPCs).

We attempted to determine if there were differences in pro-inflammatory molecule expression in native versus transfected cells in order to explain why

differences were observed in leukocyte adhesion. Flow cytometry data showed that the expression of proinflammatory EC markers ICAM-1, VCAM-1, and E-Selectin increased after stimulation with IL-1β but there was no difference in expression between native and transfected EPCs (Figure 13).

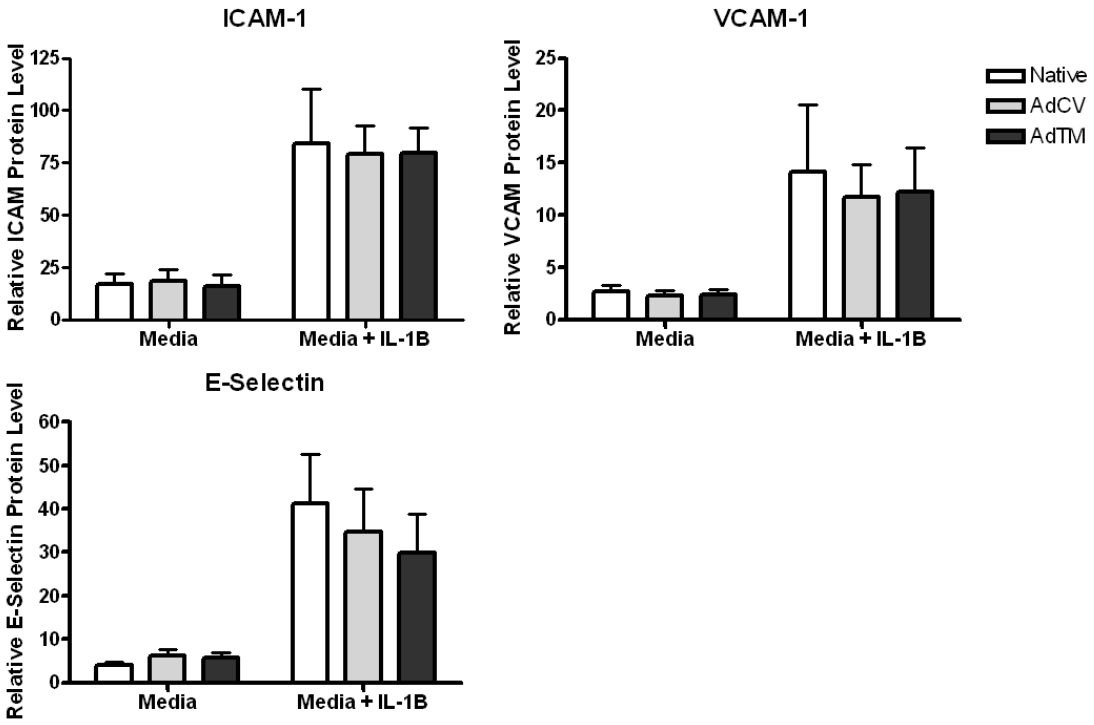

Figure 13. Surface expression of ICAM-1, VCAM-1, and E-Selectin on native or transfected EPCs assessed by flow cytometry. EPCs were either unstimulated (Media) or stimulated (Media + IL-1β) for four hours prior to running the assay.

4.4.7 Platelet Adhesion

Figure 14 contains overlaid fluorescent and phase contrast images of immunolabeled platelets adherent to collagen I positive control (Figure 14A) and to confluent layers of untransfected EPCs (Figure 14B), AdCV transfected EPCs (Figure 14C) and AdTM transfected EPCs (Figure 14D). The collagen control and AdTM transfected EPCs showed the highest and lowest levels of platelet coverage, respectively, with platelets on collagen having appearing the most spread.

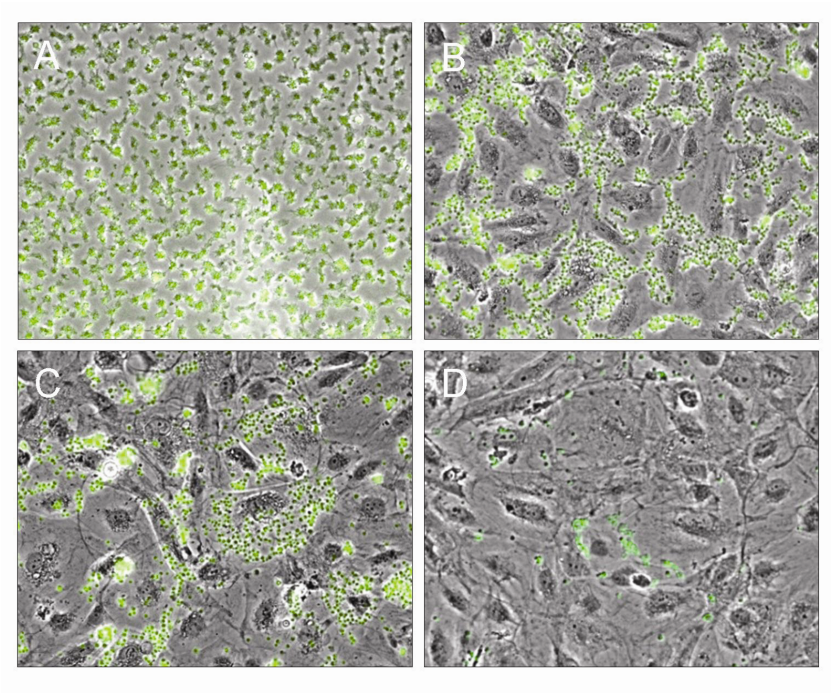

Figure 14. Platelet area coverage was determined after 30 minute incubation with platelet rich plasma. Representative phase contrast and fluorescent images showing EPCs and CD41-labeled platelets (green). Collagen I coated wells had highest coverage (A), followed by EPCs (B), EPCs+AdCV (C), and EPCs+AdTM (D).

The percent area covered by platelets was averaged over five fields of view for each of the conditions is shown in Figure 15. Native EPCs and EPCs transfected with

AdCV both had reduced platelet adhesion compared to collagen I coated wells ($p<0.05$), while EPCs with AdTM showed a 3-fold reduction in platelet adhesion compared to native EPCs ($p<0.05$) and a 12-fold reduction compared to collagen-coated wells ($p<0.0001$).

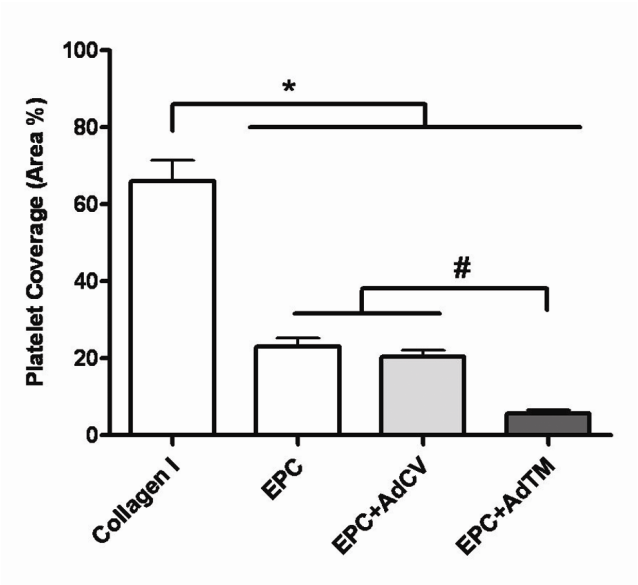

Figure 15. Percent platelet area coverage was determined after 30 minute incubation with platelet rich plasma (* p<0.0001 versus collagen coated well, #p<0.05 versus native EPCs or EPCs+AdCV).

4.4.7 Clotting times

Figure 16 demonstrates the anticoagulant character of TM overexpressing EPCs by determining whole blood clotting times in TCPS wells seeded with EPCs. Wells coated with native, untransfected EPCs and AdCV-transfected EPCs both extended the clotting time of bare wells by two minutes ($p<0.05$); whereas wells coated with AdTM-

transfected EPCs extended clotting times of bare wells by four minutes (p<0.01). Collagen-coated wells had longer clotting times than both bare TCPS wells and EPC-coated wells (EPCs clotted approximately 1 minute before collagen-coated wells; data not shown) and were not considered as a positive control.

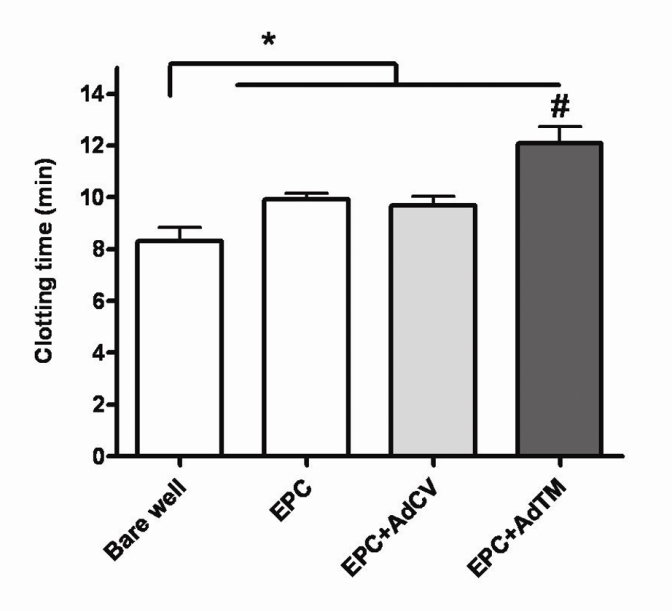

Figure 16. The clotting time of activated whole blood was measured on TCPS, and confluent layers of EPCs, EPCs+AdCV, and EPCs+AdTM (* p<0.05 versus bare well, #p<0.05 versus native EPCs and EPCs+AdCV).

4.5 Discussion

Lining biomaterials with autologous ECs is well-known to improve the anti-thrombogenicity of blood-contacting implants. Human EPCs are an attractive autologous cell source for endothelialization therapy because they express key anti-thrombotic molecules and maintain adhesion to vascular materials while under

physiological flow (174, 175), and because they can be harvested non-invasively. EPC expression of thrombomodulin in an important intrinsic anti-thrombotic mediator; however, aging and the presence of cardiovascular disease can alter cellular EC phenotype (10-12) and reduce overall TM expression (20,21). Because cells isolated from patients with cardiovascular disease would be used for autologous vascular material endothelialization strategies, we investigated whether it was beneficial to augment the antithrombotic properties of patient-derived EPCs with the human gene for TM.

In the present study, patient-derived EPCs were transfected with an adenoviral vector for human TM. This system provided high levels of TM mRNA and TM protein expression over the first week, followed by a decrease in expression to basal levels over 21 days, which may be beneficial for the initial pro-thrombotic and pro-inflammatory environment found following the surgical implantation of a vascular construct.

TM expressed by EPCs transfected with AdTM was biologically active and increased the rate of APC production relative to untransfected EPCs by five-fold, an increase similar in magnitude to previous studies with TM-transfected vein graft segments (134-136, 139) and twice that of a human aortic endothelial cell control group (data not shown).

Functional testing of transfected EPCs involved reduction of platelet adhesion on TM-transfected EPC by three-fold compared to untransfected EPCs, and by 12-fold compared to a collagen-coated well. We also observed that platelets adhering to

collagen had increased spreading whereas platelets on EPCs tended to appear rounded and attached preferentially at cell-cell junctions, a trend observed elsewhere (184).

The significantly increased clotting time with TM-transfected EPCs was in agreement with prior studies demonstrating extended clotting time by ECs with adenoviral overexpression of the TM-promoter (159), and by material surfaces immobilized with TM at high densities (185). Surprisingly, blood clotting time on collagen-coated wells was longer than both TCPS and untransfected EPCs. The difference in clotting times between bare TCPS and collagen-coated wells may be due to the increased surface concentration of oxygen on TCPS which has been shown to reduce clotting times (186). The disparity in clotting times of endothelialized surfaces and collagen-coated materials has also been observed elsewhere (187). Overall the relatively modest differences in clotting time observed between conditions in this work may be due to a large fraction of the blood-contacting surface area being TCPS versus the EPC monolayer in all cases (188).

We contend that the reduced platelet adhesion and extended clotting times by AdTM transfected EPCs was due to increased thrombin inactivation and production of APC. This observation is similar in trend to the reduced platelet adhesion observed with biomaterials coated with thrombin inhibitors such as heparin and hirudin (189-192). Clotting studies of materials presenting anithrombotic molecules such as tissue plasminogen activator, hirudin, and heparin can also delay clot formation (193-196).

Maintaining cell adhesion under flow conditions is also critical for long-term performance of endothelialized constructs that will be placed within the vasculature. TM-transfected EPCs remained adherent and reoriented during long term physiological flow, showing no deleterious effects on cell adhesion due to TM gene overexpression. Some strategies to bolster the anti-thrombogenicity of ECs involve the overexpression expression of proteolytic anti-thromboic molecules such as tissue plasminogen activator, but this technique results in reduced EC adhesion due to the gene product cleaving extracellular matrix proteins responsible for attaching ECs to the material (107).

TM overexpression may improve the *in vivo* performance of EPC-endothelialized vascular materials such as small diameter vascular grafts. Previous studies using TM overexpressing autologous vein grafts have reduced thrombosis (135, 136), decreased intimal hyperplasia (135), and the endothelium may also be protected from inflammatory conditions that attenuate expression of TM (131, 132). TM also has been immobilized on biomaterials (49, 137, 197) with recent studies showing decreased thrombosis and intimal thickening in stent grafts (137).

In sum, this study showed the feasibility of using TM-overexpression to improve the anti-thrombotic performance of patient-derived late outgrowth EPCs. The adenoviral vector system employed here allowed us to deliver the TM gene to EPCs with high transfection efficiencies and robust protein expression similar to previous work (198). Transfection at an optimal viral concentration of 100 MOI for 4 hours

resulted in 83% EPC transfection. This viral concentration was 5 to 10 fold lower than that used in previous adenoviral gene therapy studies and human EPCs (199). While adenoviral vectors are well suited for examining efficacy in vitro, as we did here, there are several limitations with the use of this transfection vector that may prohibit their adoption for cardiovascular therapies in the clinic.

First, EPCs in the current study had altered cell growth following transfection and were unable to undergo subsequent expansion when replated at subconfluent density. The decreased cell numbers contrasts to work with lentiviral vectors where transfection results in no decrease in EC proliferation with cells capable of undergoing many population doublings following transfection (200). These data indicate that approximately 2-fold greater EPC numbers (compared to native EPCs) would be required before adenoviral transfection and material seeding. When transfected EPCs were seeded at confluent densities, we did not observe any change in total cell coverage over 21 days in our long term TM expression tests or 2 day laminar flow experiments, suggesting that the transfected cells remain adherent.

Second, adenoviral transfection can also result in adaptive immune responses against viral proteins produced by the transfected cells resulting in inflammation and tissue necrosis (201). Third, transfection may be inhibited in many patients as the body contains preexisting immunity against the adenoviral vector. Approximately 50% of adults in the United States have neutralizing antibodies towards adenovirus type 5 (202,

203). Clearly another transfection vehicle will have to be employed before human trials can be considered.

4.6 Conclusion

This study showed the feasibility of using TM-overexpressing ECs to improve the anti-thrombotic performance of patient-derived late outgrowth EPCs. A combined cellular and gene therapy approach whereby blood-contacting materials such as small diameter vascular grafts are endothelialized with autologous cells exhibiting enhanced function may help avoid the systemic administration of anticoagulants while effectively preventing graft thrombosis though local expression of anti-thrombotic molecules. These data provide support for future *in vivo* testing of endothelialized synthetic vascular grafts overexpressing thrombomodulin.

Chapter 5. *In Vivo* Testing of Small Diameter Vascular Grafts Lined with Endothelial Progenitor Cells that Overexpress Thrombomodulin

5.1 Synopsis

This study investigated the use of patient-derived late outgrowth endothelial progenitor cells (EPCs) on small diameter expanded polytetrafluoroethylene (ePTFE) vascular grafts. Grafts (1mm inner diameter) were denucleated and sodded with native EPCs, EPCs transfected with an adenoviral vector containing the gene for human thrombomodulin, or EPCs transfected with an adenoviral vector containing the gene for β-galactosidase. Native and transfected EPCs maintained robust adhesion to grafts after in vitro testing. TM-transfected EPCs improved the rate of activated protein C (APC) production by the graft 4-fold over grafts sodded with untransfected EPCs ($p<0.05$). Grafts were implanted bilaterally into the femoral arteries of athymic rats for 7 or 28 days. Bare and denucleated grafts had low patency rates after 7 days, failing due to graft thrombosis (patency rate 25% (2/8) for bare grafts and 25% (2/8) for denucleated grafts). EPC sodding increased the patency rates to 89% (8/9) over 7 days. Grafts implanted for 28 days showed high patency rates with EPC sodded grafts had 88% (7/8) patency versus 75% (6/8) patency for grafts containing TM-transfected EPCs. Neointimal hyperplasia was observed near both the proximal and distal anastomoses in all EPC sodded graft conditions. Hyperplasia was most extensive in grafts sodded with

EPCs transfected with β-galactosidase ($p<0.05$). These in vivo data suggest human blood-derived EPCs can be used to improve the performance of small diameter vascular grafts.

5.2 Introduction

Vascular bypass surgery is a leading treatment option for coronary artery and peripheral vascular disease. Each year, however, over 100,000 patients lack the healthy venous or arterial vessels necessary for this critical procedure (2). While synthetic grafts are suitable for large diameter vessels (>6 mm), small diameter synthetic grafts remain incapable of being used clinically due to unacceptable patency rates caused by luminal surface thrombosis and neointimal hyperplasia.

The presence of a functional endothelium improves the patency of synthetic small diameter grafts (27, 170). However, endothelialized synthetic grafts have not received widespread adoption in part due to difficulties with the autologous sourcing of endothelial cells (ECs). ECs with high proliferation potential can be isolated non-invasively from the peripheral blood (81, 84). These cells, termed late outgrowth endothelial progenitor cells (EPCs) or endothelial colony forming cells, are capable of being isolated from patients with extensive cardiovascular disease (100, 173). Late outgrowth EPCs can be expanded to higher densities with minimal contamination by other cell types, maintain firm adhesion to the underlying substrate, and express a

healthy quiescent EC phenotype *in vitro* (173). Human EPCs can mediate clot formation, releasing anti-thrombotic molecules to prevent platelet activation and reduce thrombus formation (174, 175).

A key mediator in EC thromboresistance is thrombomodulin (TM), a membrane-bound glycoprotein that is central to the protein C anti-coagulation pathway (122). During clot formation, TM binds with free thrombin, inducing a conformational change in thrombin that inhibits its pro-coagulant potential. The TM-thrombin complex then acts as a cofactor that binds with protein C, catalyzing its conversion to activated protein C (APC). APC in turn inhibits clotting by binding protein S and proteolytically cleaving two coagulation factors responsible for generating thrombin: Factor Va and Factor VIIIa (122, 123).

While proof-of-principle studies have shown that animal-derived late outgrowth EPCs can improve the patency rates of synthetic small diameter vascular grafts (96, 97, 176), there has been limited *in vivo* testing of patient-derived EPCs. Because TM expression by ECs is decreased in patients with diabetes and atherosclerosis (177, 178), we previously showed the feasibility of augmenting the expression of TM in EPCs isolated from patients with CAD (Chapter 4). The benefit of TM-overexpression to improve the performance of small diameter synthetic vascular grafts is uncertain; however, autologous vein grafts with ECs overexpressing TM had reduced thrombosis (135, 136) and decreased intimal hyperplasia (135).

In the current study, EPCs derived from patients with CAD overexpressing TM were sodded onto small diameter expanded polytetrafluoroethylene (ePTFE) grafts and tested *in vivo*. Grafts were implanted into the femoral artery of athymic rats for 7 or 28 days and the performance of the grafts were compared between the following conditions: 1) bare grafts, 2) bare grafts with air removed, 3) grafts sodded with patient-derived EPCs, 4) grafts sodded with patient-derived EPCs overexpressing β-galactosidase, and 5) grafts sodded with patient-derived EPCs overexpressing TM. We hypothesized that grafts sodded with EPCs overexpressing TM would have the highest patency rates with reduced thrombosis and intimal hyperplasia.

5.3 Methods and Materials

5.3.1 EPC Isolation and Cell Culture

All cells designated as "EPCs" in the current study were late outgrowth EPCs isolated and expanded from 50 mL of peripheral blood drawn from patients undergoing cardiac catheterization in the Duke University Medical Center who had documented advanced coronary artery disease by angiography. EPCs were grown (n=5) and characterized as described in Chapter 3. EPCs were used at passages 5-10. The Duke University Institutional Review Board approved the protocol for collection and use of human blood employed in the study.

5.3.2 Adenovirus Virus and Transfection Conditions

Two different adenoviral vectors were used in this study as described in Chapter 4. First, replication deficient β-galactosidase adenovirus "control vector" (AdCV) was purchased (Eton Bioscience, San Diego, CA). Second, replication deficient adenoviral expressing human thrombomodulin (AdTM) was a gift from Dawn Bowles, Duke University. EPCs were transfected with AdTM or AdCV for 4 hours at 100 MOI (multiplicity of infection) one day before graft sodding.

5.3.3 Vascular Graft Conditions

Five vascular graft conditions were tested in the study: 1) bare off the shelf ePTFE vascular grafts (1mm inner diameter, 30 μm internodal distance, International Polymer Engineering, Tempe, AZ), 2) denucleated grafts (grafts having air removed by immersing in 100% ethanol and drawing a vacuum until no bubbles were released from the graft), 3) grafts endothelialized with native EPCs, 4) grafts endothelialized with EPCs transfected with AdCV, and 5) grafts endothelialized with EPCs transfected with AdTM.

5.3.4 Vascular Graft Endothelialization

The graft endothelialization method used in this study was similar to Kidd et al. (204) where cells are sodded onto the porous graft lumen. ePTFE vascular grafts were

placed in vacutainers containing 2.5 mg/mL tridodecylmethylammonium chloride (TDMAC, Polysciences, Warrington, PA), a cationic surfactant, in ethanol at room temperature. A vacuum was drawn to remove residual air. Complete denucleation was assumed when air bubbles were no longer released from the graft and the graft sank to the bottom of the solution. Denucleation reduces material thrombogenecity (205) and TDMAC increases protein adsorption on hydrophobic materials such as ePTFE (206). The graft was washed three times in DPBS and transferred to a solution of human fibronectin (20 μg/mL). The grafts were incubated in fibronectin at 37 °C for approximately 1 hour.

EPCs were detached (0.025% trypsin, Lonza, Walkersville, MD) in preparation for graft sodding. EPCs had been transfected with AdTM or AdCV the day prior at 100 MOI. The graft was cannulated with a 19-guage needle and the distal end of the graft was clamped with titanium vascular clips (Teleflex medical, Research Triangle Park, NC). Detached cells were resuspended in 5 mL media and placed into a 5 mL syringe to achieve an effective graft luminal seeding density of 1.5×10^6 cells/cm^2. The cell suspension was infused into the graft at a rate of 0.5 mL per minute using a programmable syringe pump (Harvard Apparatus, Holliston, MA). The cell solution was flushed through the graft and cells were trapped in the graft interstices. The flow-through solution was collected into a separate container and showed few cells, indicating the majority of the cells were present on the graft. Optimal sodding density

was determined by sodding cells at densities ranging from 0.5 - 2.5x10^6 cells/cm^2. Following sodding, the cannula and vascular clamps were removed and the graft was placed into a 6-well plate containing EBM-2 complete media and cultured for 2 days before *in vitro* or *in vivo* testing.

5.3.5 EPC Adhesion Assessment

To assess the potential extent of EPC loss during handling, cell coverage on the graft was assessed after exposure to surgical clamping and super-physiological flow. Grafts were sodded as described above. Fresh EBM-2 complete media was used to cover the graft while in a 6-well plate. Microvascular clamps (S&T AG, Neuhausen, Switzerland) were placed each end of the graft. Every 5 minutes, the position of the clamps were adjusted along the length of the graft to simulate the suturing movements. This procedure was performed for 30 minutes and the 6-well plate was maintained at 37°C using a heated stage (Pathology Devices, Westminster, MD). After 30 minutes, the graft was either fixed with 3.7% paraformaldehyde (Clamped+Static) or exposed to 5 minutes of laminar flow at 100 dynes/cm^2 with a peristaltic flow setup as described above and fixed (Clamped+Flow). SEM was used to obtain images at 4 randomly selected visual fields of the graft luminal surface at 1000x magnification. Cell coverage was quantified by overlaying a 10 x 13 grid on the image and counting the fraction of grid intersection points occupied by cells.

5.3.6 APC Production

The biological activity of EPCs on vascular grafts was assessed by measuring the rate at which protein C was cleaved by the TM-thrombin complex to form activated protein C (APC). EPCs were sodded onto 7 mm long grafts as described above. Grafts were placed into wells of a 24-well plate and incubated with 5mM thrombin (Haematologic Technologies Inc (HTI), Essex Junction, VT) and 400 mM human protein C (HTI) as previously described (Chapter 4).

5.3.7 *In Vivo* Testing

5.3.7.1 Animal Selection

The experimental protocol was approved by the Duke University Institutional Animal Care and Use Committee. Thirty-two male athymic rats weighing 180-280g (Charles River Laboratories, Wilmington, MA) underwent bilateral femoral artery interpositional grafting with ePTFE grafts. One of two identical grafts (1 mm diameter, 7 mm long and same experimental condition) was implanted into each side of the animal. Grafts were explanted at 7 or 28 days.

5.3.7.2 Femoral Artery Interposition Grafting

Animals were anesthetized with isoflurane (4% induction, maintained with 2%). The ventral side of the rat was shaved and the femoral artery was dissected from the

femoral vein. The femoral artery was clamped with vascular clamps and approximately 3 mm of the artery was excised. A 7 mm length ePTFE graft was anastomosed interpositionally using standard microsurgical technique with 10-0 nylon interrupted sutures (Ethicon, Somerville, NJ) under an operating microscope. The graft and surgical site was bathed in heparanized saline (12.5 U/mL) throughout the procedure. Once the sutures were in place the vascular clamps were released and hemostasis was achieved within 2-3 minutes. Blood flow through the graft was monitored using a Laserflo BPM^2 Blood Perfusion Monitor (Vasamedics, St. Paul, MN) for 30 minutes following suturing. Patency was additionally confirmed distal to the graft though a "milking test" where the artery distal to the graft was clamped a section further downstream was gently milked with a forceps to push the remaining blood distally. When clamp closest to the graft was removed, the distal artery was observed. If it filled with blood, the graft was considered patent. No anticoagulants were administered post-operatively and pain was managed by bupivacaine and flunixin (2 mg/kg) for 2 days post-operative.

5.3.7.3 Explant

After 7 or 28 days, grafts were explanted. Rats were placed under general anesthesia, grafts were isolated, and graft patency was evaluated by laser Doppler flow measurements and the milking test. Grafts were explanted and washed in heparinized saline for 5 minutes, placed in 10% formalin overnight, and transferred to 70% ethanol

prior to paraffin embedding. No differences in animal behavior were observed prior to explant with animals having patent versus non patent grafts.

5.3.8 Histology

Tissue samples were embedded in paraffin and sectioned for histological evaluation. A series of 5 μm cross-sections were obtained so that each graft was assessed by visualizing four to five unique cross-sections covering the length of the 7 mm graft. Additional sections were obtained of the native artery (proximal to the graft), the proximal artery-graft anastomosis, the distal graft-artery anastomosis, and the native artery (distal to the graft). All sections were removed of paraffin using Sub-X (Surgipath Medical, Richmond, IL) and stained with H&E. Masson's trichrome staining was used to evaluate neointimal hyperplasia of 28 day graft samples.

The thrombosis index for each sample was calculated by measuring the area of clot within the graft lumen divided by the area of the graft. The hyperplasia index was calculated by measuring the area of intimal hyperplasia divided by the area of the graft.

Sections were stained for endothelial cells after antigen retrieval with a rabbit anti human von Willebrand Factor (vWF, 1:50 dilution) (Dako, Carpinteria, CA) antibody. vWF sections were incubated with a biotinylated horse anti rabbit secondary antibody for peroxidase staining (1:200 dilution) (Vector Labs, Burlingame, CA). Human cells were distinguished after antigen retrieval though staining with mouse anti

human MHC class I antibody (1:50 dilution) (Santa Cruz Biotechnology, Santa Cruz, CA). MHC-I staining was visualized with Alexaflour goat anti mouse secondary antibody (1:500 dilution) (Invitrogen). Negative controls in both cases consisted of sections with no primary antibody incubation.

Sections were imaged with a Nikon TE2000U microscope and NIS Elements software (Nikon). The percent graft thrombosis was measured by the area of the clot divided by the luminal area of the ePTFE graft. The percent graft hyperplasia was defined as the area of the neointima divided by the luminal area of the ePTFE graft.

5.3.9 Computational Model

An idealized geometry of the femoral artery interpositional graft was created in three dimensions. The femoral artery had a vessel diameter of 0.62 mm and the ePTFE graft diameter was 1 mm by 7 mm long (diameter mismatch of 1:1.6). Walls were considered non-compliant. The flow was mathematically characterized by Navier-Stokes equations and solved using CFDesign software (Blue Ridge Numerics Inc, Charlottesville, VA). Blood was considered incompressible and non-Newtonian. Flow was considered laminar.

The inlet boundary condition was based on blood flow rates measured through the right femoral artery of a 410 g rat as described previously by Rickard et al. (207). The outlet boundary condition was set to a gauge pressure of zero. The velocity values at all

wall boundaries were set to zero. A time step size of 0.001 seconds was used for all simulations.

5.3.10 Statistics

Statistical differences in graft patency were assessed with Fisher's Exact Test. All other statistical analysis was performed with a one-way ANOVA followed by a Tukey-Kramer post hoc test. All error bars represent the standard error of the mean. *P* values below 0.05 were considered to indicate a statistically significant difference.

5.4 Results

5.4.1 Vascular Graft Sodding

EPCs formed a confluent endothelial layer onto small diameter vascular grafts within two days after graft sodding. EPCs transfected with the control vector could be visualized by β-galactosidase staining with positive cells labeled blue (Figure 17A,B). We previously showed that approximately 50% of EPCs stained positively for β-galactosidase following 100 MOI for 4 hours (Chapter 4). Cell coverage was uniform throughout the length of the graft (Figure 17A) and SEM images showed that sodded grafts typically contained approximately 90% endothelial coverage (Figure 17D).

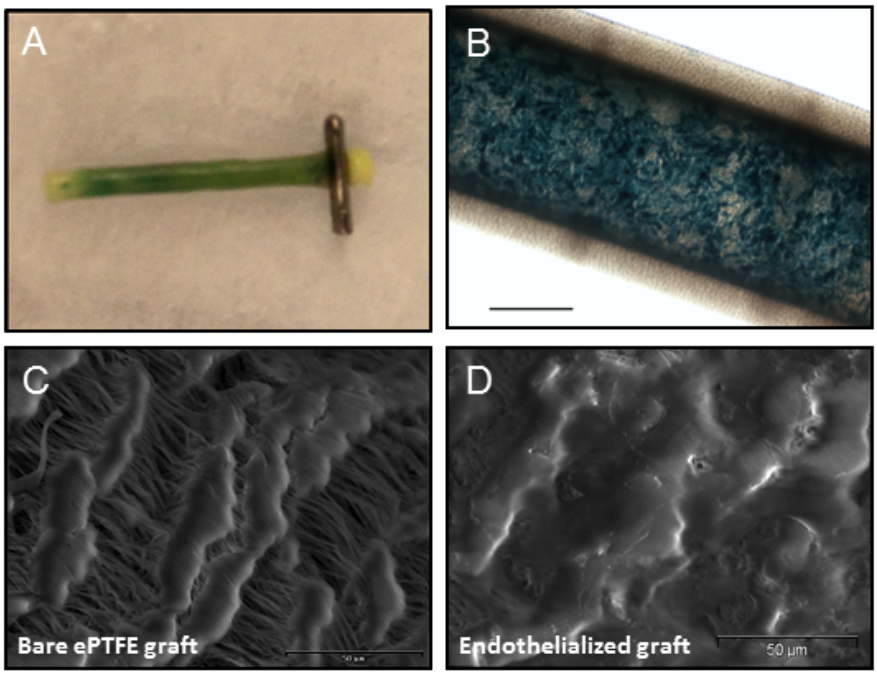

Figure 17: EPC sodding of 1 mm inner diameter ePTFE vascular grafts. Transfection with AdCV one day prior to sodding allowed the visualization of transfected EPCs grossly (A) and though bright field microscopy at 100x magnification (B) (scale bar 500 µm). SEM images show the lumen structure of a bare graft (C) and a graft sodded with EPCs (D) (scale bars 50 µm).

5.4.2 EPC Adhesion on ePTFE Grafts

An *in vitro* experiment was designed assess EPC graft coverage after exposure to conditions attempting to mimic a surgical implantation procedure. After allowing EPCs to culture on grafts for two days, sodded grafts were exposed to 1) clamping along the length of the graft for 30 minutes and 2) short term super-physiologic flow of 100

dynes/cm² for 5 minutes. Figure 18 shows that EPCs sodded onto vascular grafts had approximately 90% graft coverage in the control static conditions. EPCs maintained strong adhesion to the fibronectin-coated ePTFE grafts as 100 dynes/cm² flow caused little decrease in overall cell coverage versus static conditions (p=0.35). Clamping along the length of the graft with vascular clips and exposing the grafts to flow reduced EPC graft coverage a maximum of 5%. There was no difference in cell coverage between native and transfected EPCs (p=0.78).

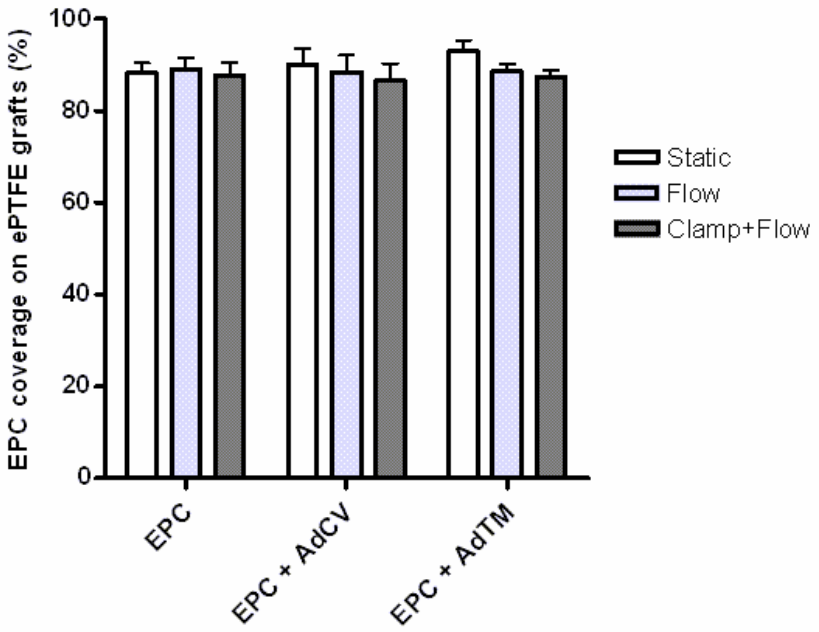

Figure 18: EPC graft coverage after 30 minutes of vascular clamping and exposure to short term flow at 100 dynes/cm² (n =4).

5.4.3 APC Production

EPCs sodding improved the anti-thrombotic performance of small diameter vascular grafts. Figure 19 shows the rate of graft APC production. Sodding grafts with native EPCs or EPCs transfected with AdCV had significantly higher rates of APC production over bare grafts ($p<0.05$). The rate of APC production between native and AdCV EPCs was similar, showing no detrimental effect of the adenoviral control vector on APC production. Sodding grafts with EPCs overexpressing TM increased the rate of APC production an additional 4-fold over grafts containing native EPCs ($p<0.05$).

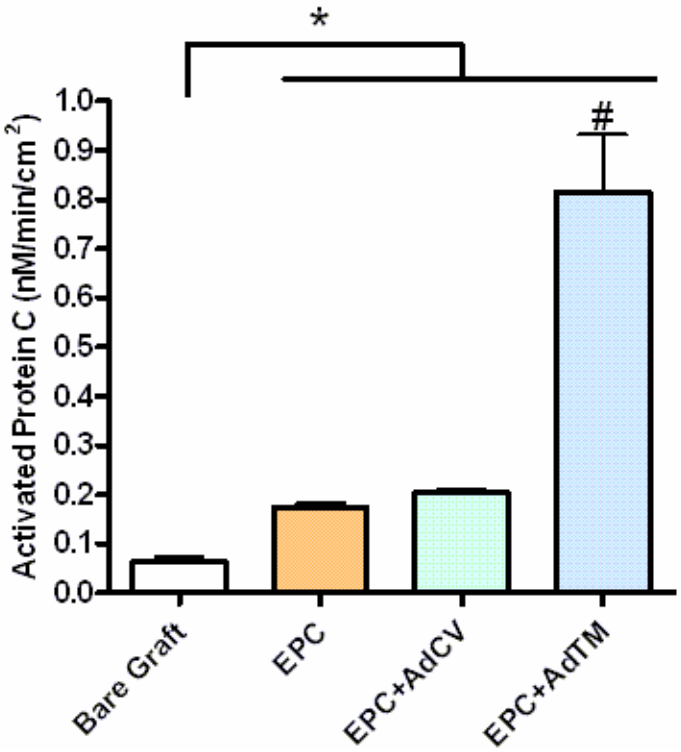

Figure 19: APC production rate of Bare, EPC, EPC + AdCV, and EPC+ AdTM sodded grafts (* p<0.05 versus bare grafts, #*p*<0.05 versus grafts with native EPC and EPC+AdCV) (n=4).

5.4.4 *In Vivo* Testing

To determine the impact of graft sodding with native EPCs and TM-transfected EPCs *in vivo*, grafts were implanted bilaterally into the femoral arteries of athymic rats. Standard microsurgical technique was used to suture 7 mm grafts as interpositional segments (Figure 20A, B). Upon removal of the vascular clamps, bleeding was limited to the anastomosis site for 1-2 minutes before hemostasis was achieved (Figure 20C). Grafts were observed for approximately 30 minutes before closing of the surgical site.

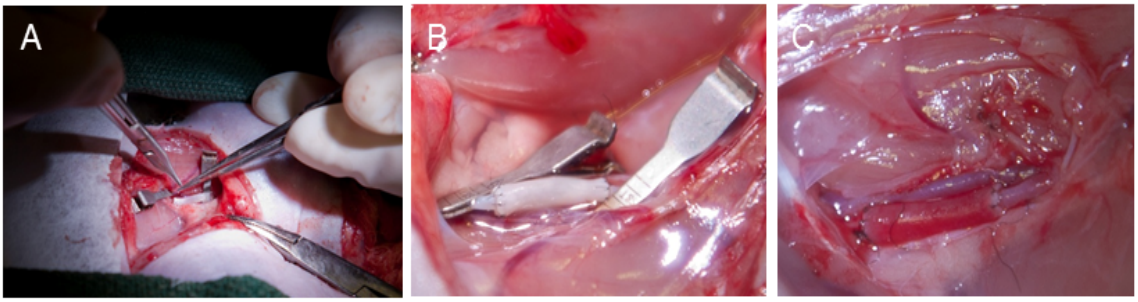

Figure 20: Surgical procedure for implanting 1 mm ID grafts into the femoral arteries of athymic rats (A). 7 mm long grafts were sutured interpositionally (B). Vascular clamps were removed allowing grafts to fill with blood (C).

Table 6 shows the patency rates of grafts implanted 7 or 28 days. Non-endothelialized grafts had poor patency after 7 days: 25% (2/8) bare grafts and 25% (2/8) denucleated grafts were patent. Grafts sodded with EPCs transfected with AdCV had improved patency rates versus the bare and denucleated grafts (62.5% (5/8)). Sodding with native EPCs or EPCs overexpressing TM significantly improved 7 day patency

rates, with 89% (8/9) of EPC sodded grafts patent and 88% (7/8) of AdTM grafts patent ($p<0.05$). It should be noted that within the same animal subject, graft patency in one leg did not appear to affect the patency in the other leg.

Table 6: Patency rates of grafts implanted 7 or 28 days (*$p<0.05$ versus Bare Graft and Denucleated Graft).

Condition	7 Day Implant Patency	28 Day Implant Patency
Bare Graft	25% (2/8)	---
Denucleated Graft	25% (2/8)	---
EPC	89% (8/9)*	88% (7/8)
EPC + AdCV	63% (5/8)	75% (6/8)
EPC + AdTM	88% (7/8)*	75% (6/8)

Figure 21 shows the presence of cells within the graft vascular wall after 7 days *in vivo*. The interstitial space of the ePTFE of the bare grafts appeared filled with red blood cells (Figure 21A). Non-sodded denucleated grafts contained greater numbers of mononuclear cells (Figure 21B). EPC sodded grafts contained high number of mononuclear cells throughout the thickness of the wall and additionally had a cellular lining on the luminal surface of the graft (Figure 21C-E).

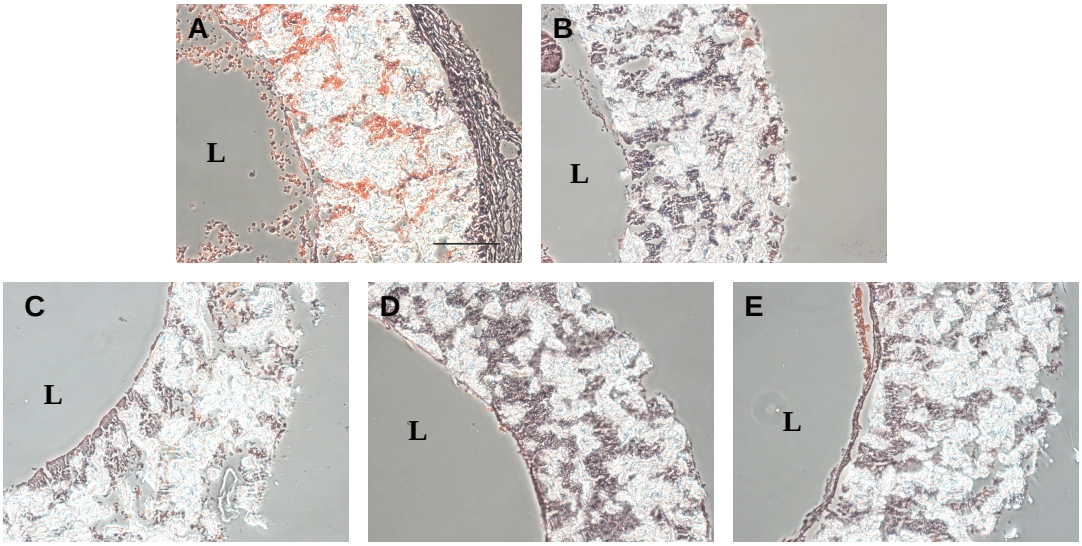

Figure 21: Representative H&E vascular graft wall images of bare (A), denucleated (B), EPC sodded (C), EPC + AdCV sodded (D), and EPC + AdTM sodded (E) graft after 7 days *in vivo* (graft lumen: "L" and scale bar: 100 μm).

Cross-sections from 7 day implants showed that the non-patent bare and denucleated grafts had extensive thrombus formation within the graft lumen, whereas grafts containing EPCs had patency and limited thrombus within the graft (Figure 22). Patent grafts were analyzed for thrombus coverage across the length of the graft. Because only 2/8 of each the bare grafts and denucleated grafts were patent, they were excluded from analysis. Of the EPC sodded graft conditions, there were no significant differences in thrombosis coverage (p = 0.32); however, grafts sodded with AdTM EPCs had slightly less thrombus present than native EPCs or ADCV EPCs (Figure 23).

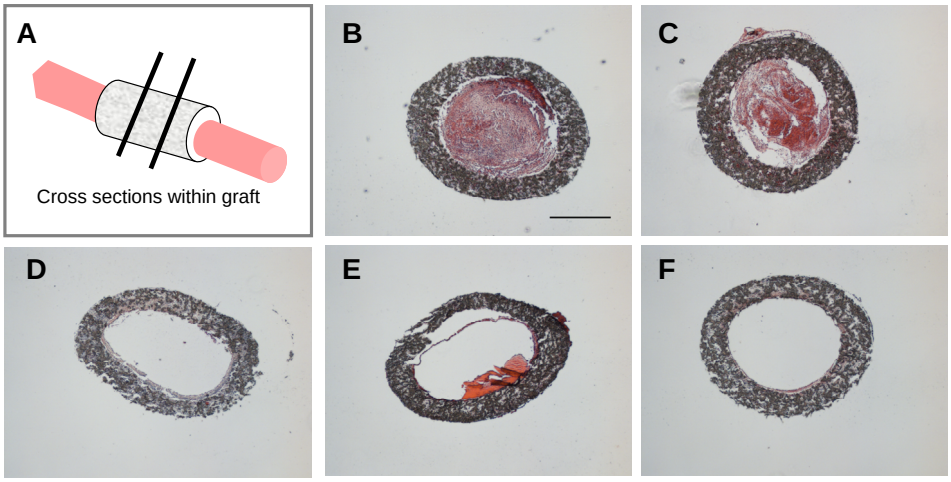

Figure 22: Representative midgraft H&E ePTFE vascular graft cross sections after 7 days *in vivo*. Location of the serial graft cross-sections (A). Bare (B) and denucleated (C) grafts had extensive thrombus. Grafts sodded with native EPCs (D), AdCV EPCs (E), and AdTM (F) had little thrombus present (scale bar 500 μm).

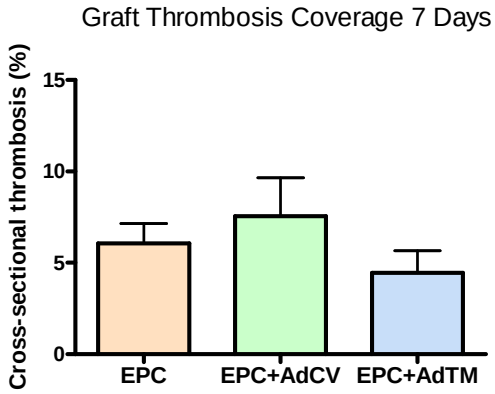

Figure 23: Analysis of graft cross-sectional thrombosis after 7 days (n=7 for EPC, n=5 for EPC+AdCV, n=6 for EPC+AdTM).

EPC-sodded grafts maintained high patency rates after 28 days with no significant differences in patency rates between native EPCs (7/8), AdCV EPCs (6/8), and

AdTM EPCs (6/8) (Table 6). Because the poor patency of bare and denucleated grafts, they were not utilized in 28 day implant experiments.

Sectioning of the 28 day implants revealed intimal hyperplasia within the graft near both the proximal and distal anastomoses (Figure 24). Grafts were evaluated for the index of intimal hyperplasia within three regions: proximal, middle, and distal section as shown in Figure 25A. The distal regions of the grafts had the greatest hyperplasia response followed by the proximal region. Hyperplasia was significantly reduced in the proximal and mid graft regions for EPC sodded and EPC+AdTM sodded grafts versus EPC+AdCV ($p<0.05$).

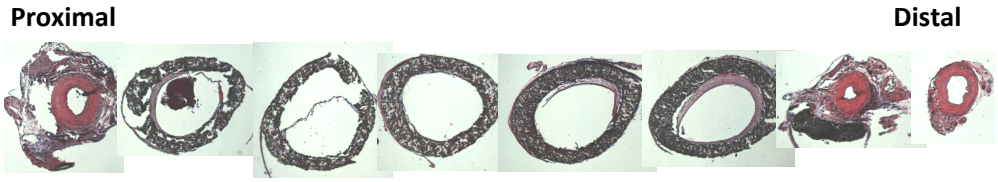

Figure 24: Representative of serial cross-sections of single EPC-sodded implant from the proximal to distal end.

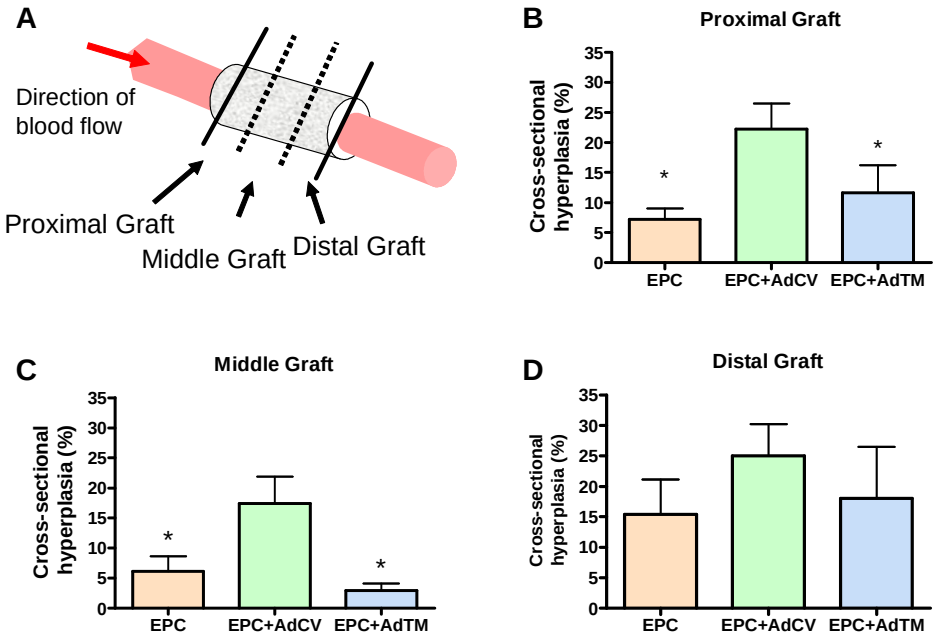

Figure 25: Analysis of graft cross sectional neointimal hyperplasia split by section.

Figure 26 shows H&E and Masson's trichrome staining of the distal regions of EPC sodded grafts after 28 days. Regions of hyperplasia tended to stain blue, a positive marker of extracellular matrix protein. All grafts showed little thrombus formation at 28 day time points.

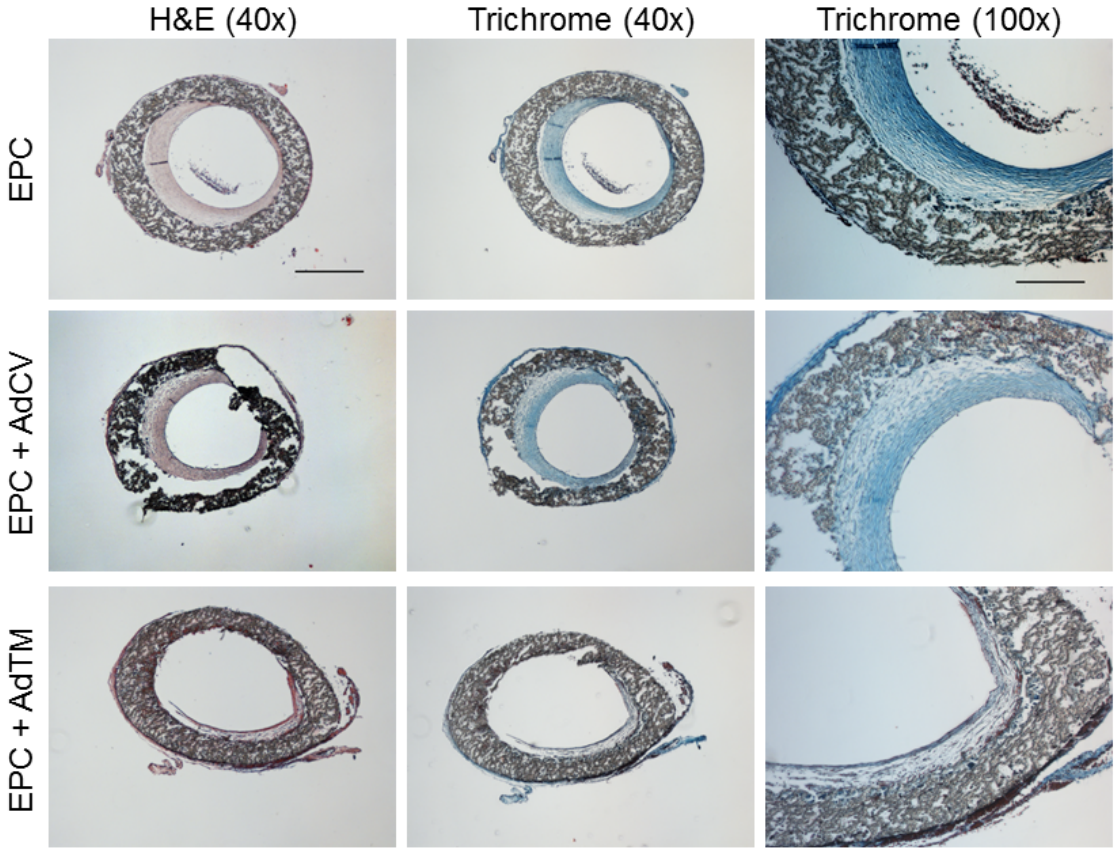

Figure 26: Representative H&E and Masson's Trichrome staining of distal ePTFE vascular graft cross sections after 28 days *in vivo*. All EPC sodded graft conditions had regions of neointimal hyperplasia near the proximal and distal anastomosis. Scale bar 40x images: 250 μm; 100x images: 500 μm.

Figure 27 shows representative H&E and Masson's trichrome stains of the distal graft-to-artery anastomosis. We were unable to obtain sections for analysis for all patent graft conditions due to difficulties in sectioning grafts perpendicular the graft axis at the anastomosis. As a result, histologic analysis for the distal anastomosis was limited.

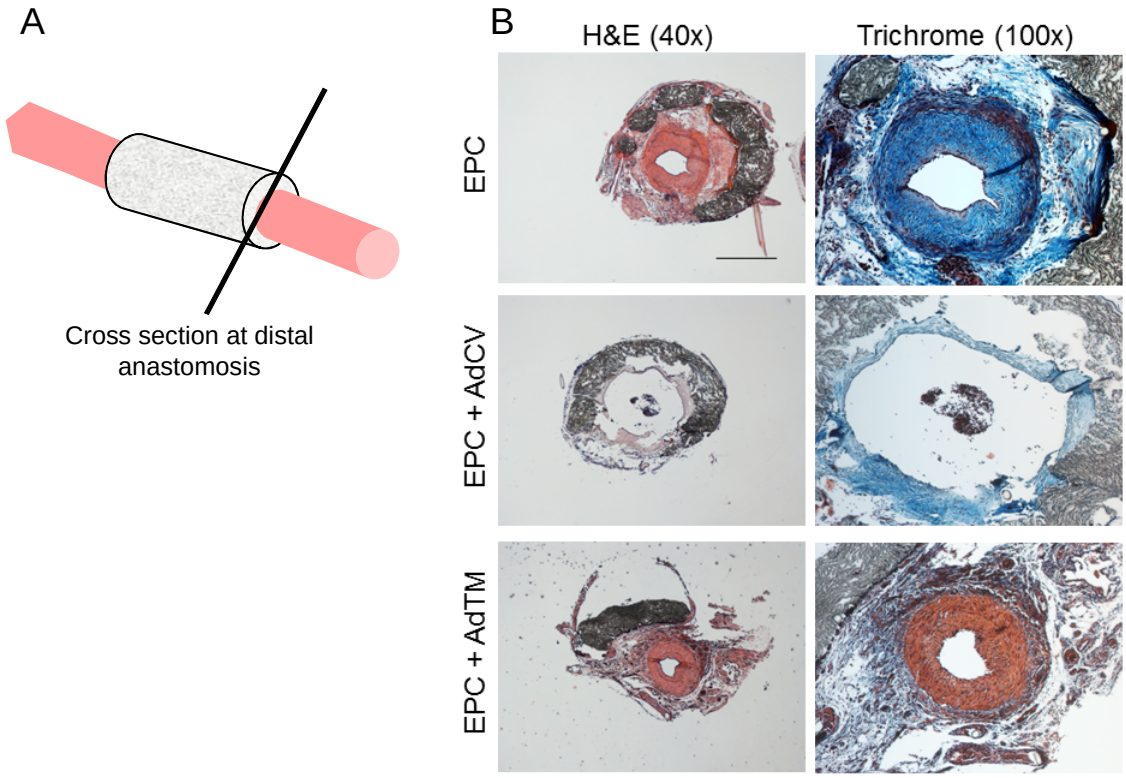

Figure 27: Diagram showing the location of the distal graft-to-femoral artery anastomosis (A). Representative H&E and Masson's trichrome staining of distal anastomosis after 28 days (B).

Confluent layers ECs remained present on the lumen of EPC sodded grafts after 7 and 28 days, visualized through vWF staining (Figure 28). Positive vWF staining was also present on the surface of grafts with neointimal hyperplasia(Figure 28C,D). Because vWF was non-specific for rat or human ECs, human MHC-I staining was performed to determine the contribution of the sodded EPCs. Bare grafts were negative for MHC-I staining (Figure 29A) while grafts sodded with human EPCs showed positive staining within the graft lumen after 7 (Figure 29B) and 28 days (Figure 29C,D). 28 day

images showed that the neointimal area was likely made up of rat-derived cells as MHC-I staining was negative in the area of hyperplasia (Figure 29D).

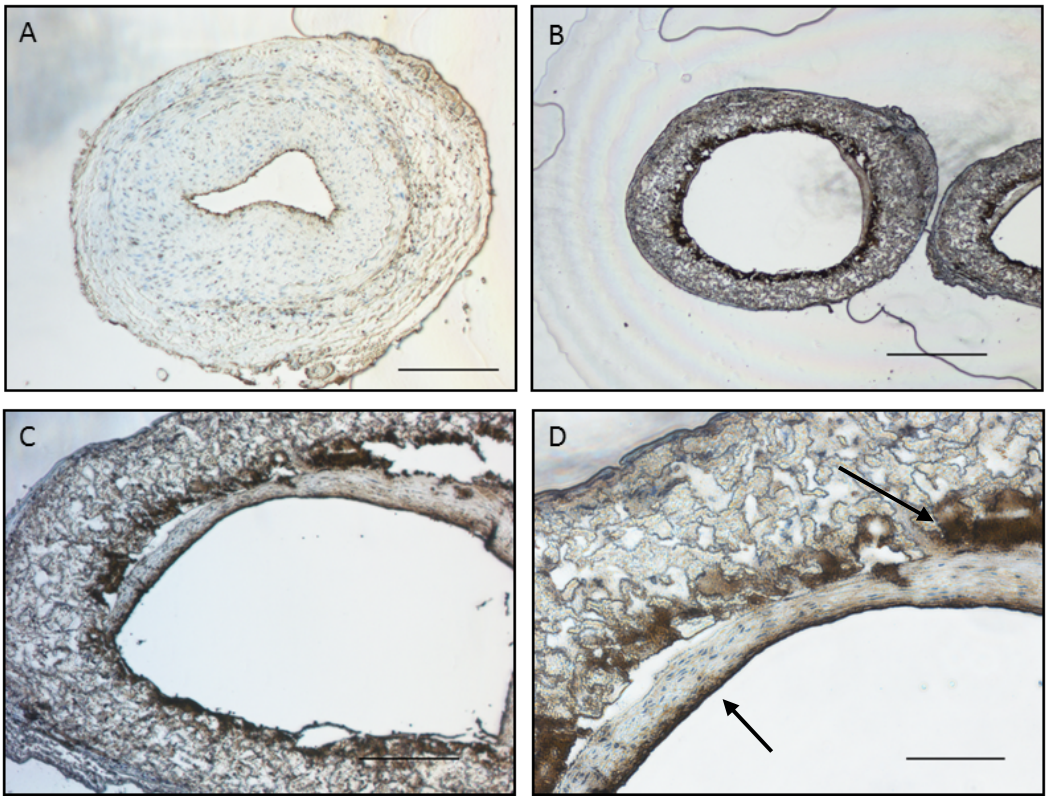

Figure 28: Representative images of von Willebrand Factor (vWF) staining. ECs lining the control femoral artery stained positively for vWF (A) (scale bar 200 μm). EPC Sodded grafts showed confluent EC coverage luminal coverage at 28 days (B) (scale bar 500 μm). EPC sodded graft having neointimal hyperplasia also stained positive for vWF (C,D). Arrows point to positive both within graft and along region of hyperplasia (scale bars were 200 μm (C) and 100 μm (D)).

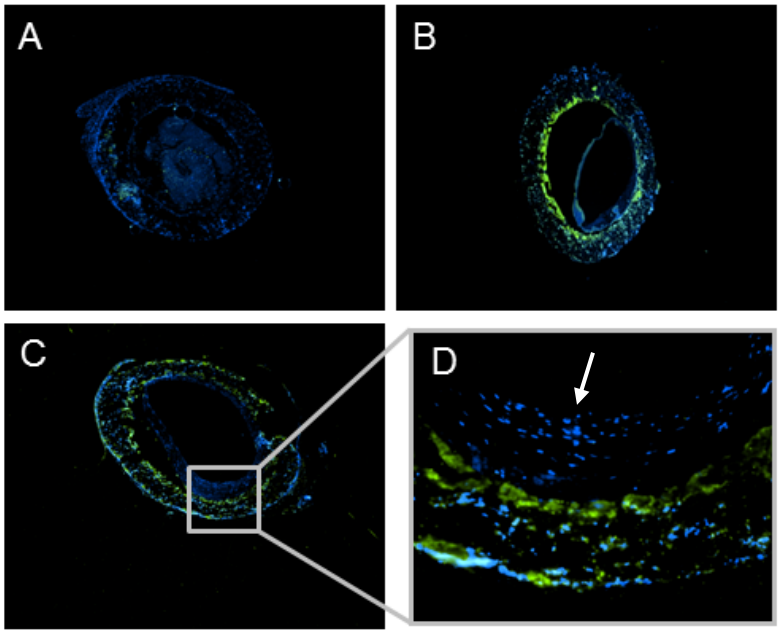

Figure 29: Staining of ePTFE grafts for human MHC-I (green) and cell nuclei (blue). Bare grafts had cell nuclei lining the outer walls of the graft and within the clot but showed no human MHC-I staining (A). Grafts sodded with native EPCs showed positive MHC-I staining near the graft lumen 7 days after implantation and nuclei were observed on the lumen and within the graft wall (B). After 28 days, sodded human EPCs remained on the graft original ePTFE lumen but not on the region of hyperplasia (C,D).

5.4.5 Computational Modeling

In order to better characterize the fluid profile though the interpositional graft, computational analysis was performed using a finite element method solver. An idealized geometry of the femoral artery to graft anastomosis used for analysis can be seen in Figure 30.

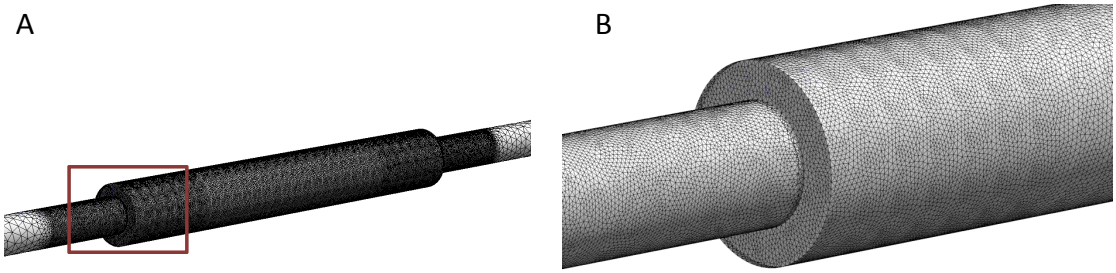

Figure 30: Computational model geometry and mesh showing the entire construct (A) and at higher detail at the proximal graft anastomosis (B).

The model was run for 0.60 seconds with time steps of 0.001 seconds. For clarity, a single pulse from 0.27 to 0.40 second was used for analysis. Particle traces of blood flow over time are shown in Figure 31. The corresponding wall averaged shear stresses over time are shown in Figure 32.

At the start of the start of the pulse, recirculating flow is present at the proximal anastomosis as the diameter of the vessel abruptly changes from 0.62 mm to 1 mm. At the peak of the systole at 0.29 seconds with 12.54 mL/min, flow is fully developed and maximal shear stresses are observed (150 dynes/cm^2 in the femoral artery and 53 dynes/cm^2 in the graft).

After the pulse, the fluid flow rapidly decelerates to 3-4 mL/min and a region with increased shear stress is found near the proximal anastomosis. Shear stresses continue to decrease until they reach their minimum values at 0.4 seconds, 30 dynes/cm^2 in the femoral artery and approximately 1 to 4 dynes/cm^2 in the graft. The flow recirculation zone at this point extended 1.2 mm from the proximal anastomosis.

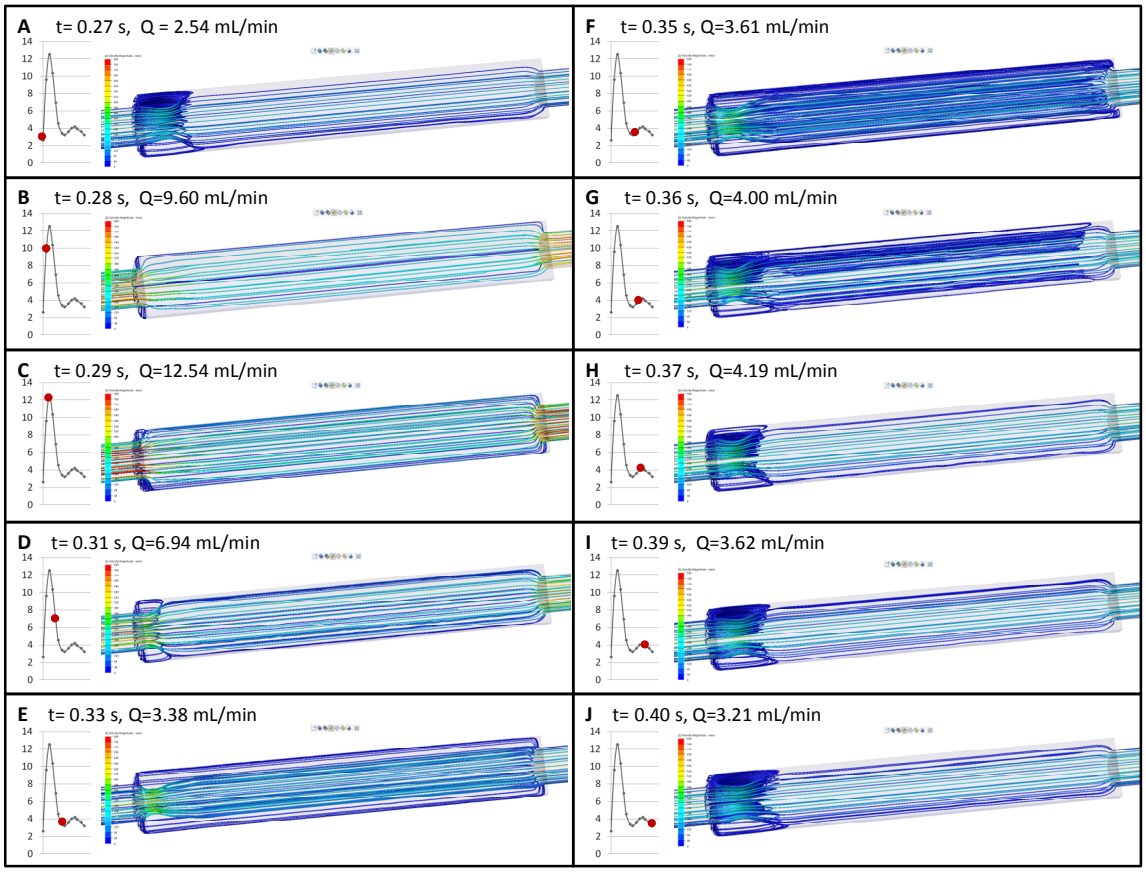

Figure 31: Fluid flow lines over one pulse from 0.27 to 0.40 seconds. Lines are colored by fluid velocity.

In contrast to the proximal anastomosis, no flow recirculation was observed at the distal anastomosis. A small 0.2 mm long region at very distal end of the graft showed lowered shear stresses compared to the rest of the graft.

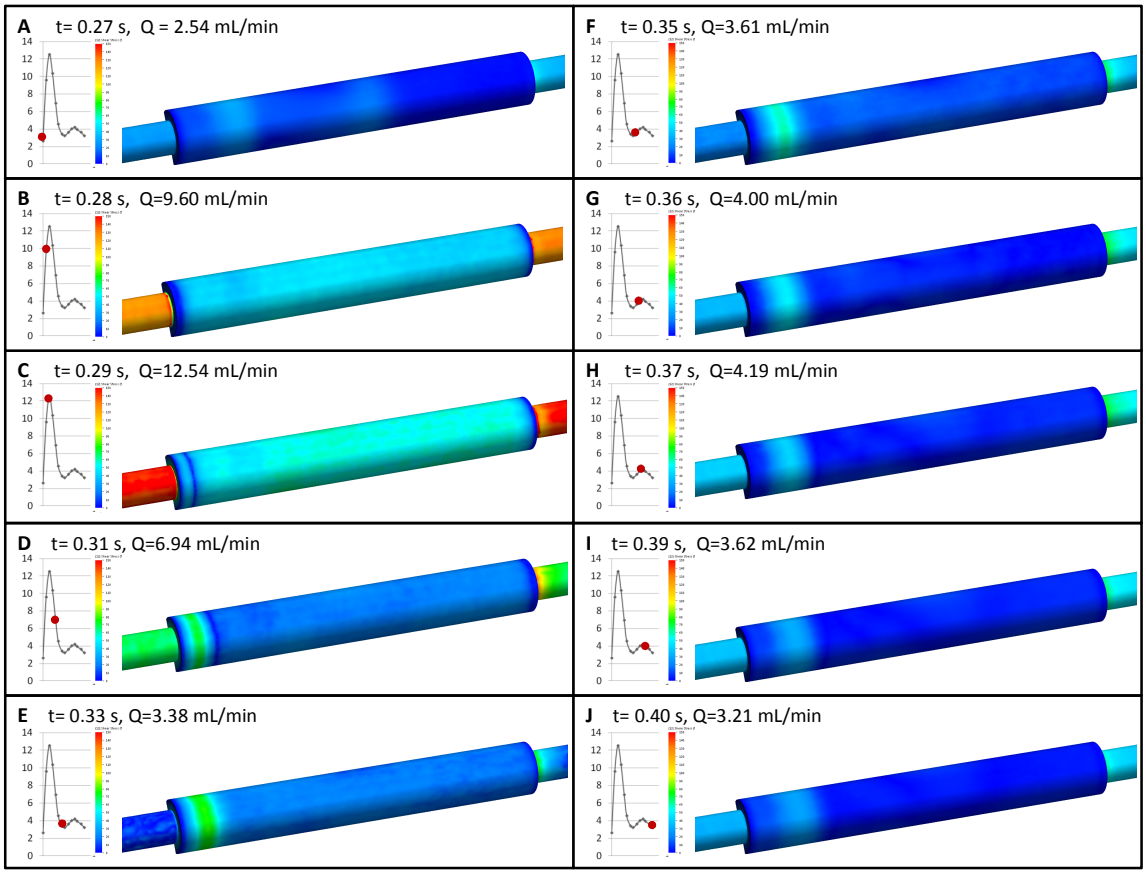

Figure 32: Shear stress over one pulse from 0.27 to 0.40 seconds. Color bar ranges from 150 to 0 dynes/cm^2.

5.5 Discussion

Vascular graft endothelialization is well known to improve the patency of small diameter vascular grafts (27, 170). These and other studies, however, rely on harvesting autologous blood vessels or microvascular tissue, an invasive procedure that introduces donor site morbidity. (27, 170, 208). In contrast, EPCs can be isolated non-invasively from small samples of peripheral blood of patients with documented CAD (Chapter 3).

Previous studies using animal derived EPCs indicate EPCs can improve the performance of synthetic vascular grafts (96, 97, 176). To date, however, only one study has tested the use of human peripheral blood-derived EPCs on vascular grafts *in vivo* (98). The goal of the present study was to assess the patency rates of small diameter vascular grafts containing patient-derived EPCs *in vivo*. To the best of our knowledge, this is the first *in vivo* study of testing vascular grafts utilizing human EPCs that were isolated from patients with CAD disease. We additionally assessed the impact enhancing the anti-thrombotic phenotype of patient EPCs prior to graft sodding. Previous *in vitro* work (Chapter 4) showed TM-transfected EPCs had increased APC production, reduced platelet adhesion, and prolonged clotting times over native EPCs.

Bare ePTFE grafts and denucleated grafts serving as control groups had low patency rates. While the removal of air from vascular graft materials can decrease clot formation (205) and enhance cell adhesion *in vivo* (209), no difference in patency rates were observed between the two control groups after 7 day testing. Sodding EPCs on the graft lumen significantly increased graft patency rates over the control grafts after 7 days. High patency rates of sodded grafts were retained in long term 28 days testing. Sodded patent grafts across all groups generally had low levels of cross-sectional thrombosis. While absent at 7 days, intimal hyperplasia was observed across all groups after 28 days.

Transfected EPCs appeared to remain adherent during *in vitro* testing. These results agreed with our previous observations that transfected EPCs would remain adherent after both long term physiological flow (Chapter 4) and short term graft clamping and super-physiological flow (Figure 18). Analysis of *in vivo* cross-sections remains unclear. Human specific MHC I staining results showed that a portion of graft EC coverage positive for vWF may have been attributed to the sodded human EPCs that were retained up to 28 days. In regions of hyperplasia at 28 days, the lumen appeared to stain positively for vWF but negative for human MHC-1. We speculate that the the inner lining may consist of ECs of rat origin rather than the originally sodded human EPCs. The migration of ECs from the anastomosis is commonly observed in vivo, and is more pronounced in animal models than in humans (8). It is less likely that the rat EC derived from rat circulating EPCs (210), or ECs from migrating through the graft wall as the ePTFE was low porosity (5).

After sodding onto grafts, EPCs transfected with AdTM expressed TM that was biologically active and increased the rate of graft APC production 4-fold relative to grafts endothelialized with native EPCs. APC production per graft luminal area was about 30% lower than APC production than on flat TCPS (Chapter 4). The 4-fold increase in APC production rate due to TM-transfection was similar in magnitude to previous studies with TM-transfected vein graft segments (134-136, 139).

Previous *in vivo* studies with autologous vein grafts overexpressing TM had reduced thrombosis (135, 136) and intimal hyperplasia (135). Knowing that the overexpressed TM was functional, it was surprising no differences in thrombosis or neointimal hyperplasia were observed between grafts containing TM-transfected versus native EPCs.

There are a number of possible reasons for the lack of improvement in graft patency and intimal hyperplasia between native EPCs and TM-transfected cells. Longer durations of TM expression may be necessary to reduce neointimal hyperplasia. *In vitro* characterization studies of the AdTM showed TM levels were significantly upregulated for only one week (Chapter 3).

Second, TM-mediated anti-thrombotic activity may have decreased due to the differences in human TM activity compared to the rat coagulation substrates. Human TM is capable of binding rat thrombin and accelerating the conversion of human protein C to APC (data not shown). It remains unknown, however, whether human TM bound to rat thrombin can accelerate the activation of rat protein C. Pig TM, for example, activates human protein C at only 10% of the rate of human TM (211). Roussel et al. suggested that the positioning and conformation of the pig TM active site may not be optimal for interacting with bound human protein C (211). Additional studies using human TM in rats showed that soluble human TM was capable of binding thrombin but unable activate rat protein C (212). That said, it is important to note that human TM

overexpression has been used in rat (139) and rabbit (135, 136) animal models with beneficial effects.

Blood flow dynamics is another important consideration due to the femoral artery and vascular graft diameter mismatch. As blood travels from the native artery into a graft of larger diameter, the sudden expansion results in a decrease in blood velocity that can result in eddy formation and reciprocating shear stress. Blood in this region is described as disturbed blood flow. Disturbed blood flow is often found at the vascular anastomosis and is widely acknowledged to contribute to intimal hyperplasia [reviewed by Chiu et al. (213)]. Computational simulations were performed to better characterize the flow characteristics of the end-to-end anastomosis between the rat femoral artery and the 1 mm inner diameter ePTFE graft.

We utilized transient blood flow data from the rat femoral artery obtained by Rickard et al. to determine the flow profile though an idealized model of our in vivo graft geometry (207). While intimal hyperplasia is most often observed at the distal graft-to-artery anastomosis, numerical modeling indicated the presence of disturbed blood flow in the proximal region of the graft which may have contributed the formation of intimal hyperplasia in the proximal region observed in the current study.

Disturbed blood flow may have also caused a reduction in TM expression in our graft. Animal models with narrowing lesions within their lumen have decreased expression of KLF-2, a key transcription factor that regulates TM expression, in regions

of disturbed flow (214). Additional antithrombotic and anti-proliferative molecules such as eNOS are reduced (215) while pro-inflammatory molecules such as ICAMs and VCAMs that are involved in white blood cell recruitment are increased (216).

Endothelialization of small diameter vascular grafts remains an effective method to improve the performance of small diameter vascular grafts. Herein we show that patient-derived ECs called EPCs can be isolated noninvasively from small samples of peripheral blood, expanded to higher cell densities, and sodded onto the lumen of small diameter grafts to enhance graft patency in challenging animal models. Additional work remains testing these cells in a larger animal model with more physiologically relevant geometries and flow profiles that more closely mimic an arteriovenous shunt or bypass surgery applications.

5.6 Conclusion

In conclusion, the present study shows that the sodding of EPCs derived from patients with CAD can effectively improve the patency rates of small diameter ePTFE vascular grafts. Sodded vascular grafts with enhanced TM expression had augmented production of human APC. *In vivo* testing indicated patient derived EPCs enhance short and long term graft patency with no detectable benefit to utilizing of TM-transfected EPC.

Chapter 6. Overview and Future Studies

6.1 Overview

The need for easily isolated autologous endothelial cell sources for vascular tissue engineering interventions was a major motivation for this work. The ability to isolate ECs non-invasively from small samples of peripheral blood would potentially eliminate the need for a two-step procedure whereby, in the first step, ECs are surgically isolated from autologous tissue, and in the second step occurring weeks later, vascular grafts containing the autologous ECs are implanted.

Researchers had recently demonstrated the possibility of obtaining late outgrowth EPCs from both umbilical cord blood and peripheral blood ((34, 81, 84)). EPCs were appealing for autologous regenerative medicine strategies because they are highly proliferative cells that express EC markers and exhibit no hematopoietic or monocytic character. However, because EPCs capable of forming high proliferation colonies are exceedingly rare in peripheral blood, there was skepticism regarding the ability to isolate and expand these cells from older patients who may have cardiovascular disease and along with other co-morbidities. For example, while flow cytometry had been used to sort and enumerate the abundant early outgrowth EPCs from mononuclear cell fractions as biomarkers for the extent of cardiovascular disease (140-144), late outgrowth EPCs were too scarce to enumerate by cell sorting directly from peripheral blood, and were difficult to identify due to lack of unique cell markers

to this cell subgroup. Accordingly, there had been little work in demonstrating whether autologous late outgrowth EPCs could be isolated and expanded in sufficient numbers from patients with cardiovascular disease for tissue engineering applications. It was also unclear if late outgrowth EPCs isolated from CAD patients exhibit differences in proliferation, adhesion, and angiogenic potential compared to healthy individuals.

In Chapter 3, a study was designed to assess differences in EPC isolation frequency and cellular phenotype of EPCs isolated from young healthy individuals versus patients who had documented coronary artery disease. Mononuclear cells were isolated from 50 mL blood samples of 26 people: 13 young healthy volunteers and 13 patients with CAD. Seeding mononuclear cells onto collagen-I coated plates, EPCs appeared after approximately 3 weeks and were expanded to higher numbers for characterization studies. While we were able to obtain EPC colonies at a higher frequency from healthy patients, it was interesting that patients with CAD had a similar frequency of EPC isolates that could be expanded to high numbers. After colonies were established and expanded from small volumes of peripheral blood, few phenotypic differences were observed between late outgrowth EPCs isolated from CAD patients and those isolated from healthy individuals. EPCs were capable of attaching, spreading, and maintaining firm adhesion to the underlying substrate and showed a functional response to flow by reorienting and increasing expression of NO.

For the purposes of utilizing autologous EPCs in patients with cardiovascular disease, there was the concern that the environmental conditionals in which the cells are placed can lead to decreased functional activity of the cells (119) and detract from a healthy anti-thrombogenic phenotype (120, 121). Chapter 4 describes the process of augmenting the anti-thrombotic capacity of patient derived EPCs though the overexpression of human thrombomodulin (TM). Through the use of an adenoviral vector, TM expression was significantly increased over native untransfected EPCs. TM-transfected patient derived EPCs expressed increased levels of activated protein C, had reduced platelet adhesion, and prolonged clotting times.

Chapter 5 describes the use of native and TM-transfected EPCs to improve the performance of synthetic small diameter vascular grafts. EPCs were sodded onto the inner lumen of 1 mm inner diameter ePTFE vascular grafts. The sodding technique resulted in approximately 90% graft cellular coverage. Native and TM-transfected EPCs remained adherent to the ePTFE graft after in vitro surgical clamping and short term super-physiologic flow. TM-overexpression improved graft anti-thrombogenicity as grafts containing TM-transfected cells had a 4-fold increased rate of APC production over grafts containing native cells. Bare grafts and EPC sodded grafts were implanted bilaterally into the femoral arteries of athymic rats. The femoral artery model had lower flow rates than the more commonly used aorta interpositional model, allowing for a rigorous assessment of graft thrombogenicity. Bare and denucleated grafts had poor

patency rates after 7 days, whereas EPC sodding with native or AdTM-EPCs improved graft patency significantly. Due to their poor patency, bare grafts were not tested for longer than 7 days. 28 day experiments showed EPC sodded grafts maintained high patency rates, and there was no detectable benefit to graft patency by incorporating TM-transfected cells. Histologic analysis at 7 days post-implant revealed the presence of graft thrombosis with increased frequency in unsodded versus EPC sodded grafts. 28 day histology sections of EPC sodded grafts revealed the presence of neointimal hyperplasia near the proximal and distal anastomoses. There was no significant difference in graft narrowing between native and TM-transfected EPCs.

Endothelialization of small diameter vascular grafts is an effective method to improve the performance of synthetic small diameter vascular grafts. The findings in the present study indicate patient-derived EPCs can be isolated noninvasively from small samples of peripheral blood, expanded to higher cell densities, and sodded onto the lumen of small diameter grafts to enhance graft patency in challenging vascular thrombosis animal models.

6.2 An Ideal Small Diameter Vascular Graft

We attempted to improve the performance of clinically utilized ePTFE vascular grafts though the incorporation of non-invasively isolated adult endothelial progenitor cells. This project met many of the design criteria considered to be important for clinical

success of a small diameter vascular graft, but the graft was still less than ideal. An ideal small vascular graft should satisfy the following essential parameters: 1) a tubular scaffold with correct diameter and mechanical properties necessary to prevent bursting, 2) a non-thrombogenic lumen to prevent blood activation and clot formation throughout the lifetime of the implant, 3) a resistance to intimal hyperplasia that can gradually lead to graft failure, and 4) an ability to be easily handled and sutured. Less than critical but still important features include: 5) graft compliance matching or similar to the native vessel, 6) ability to undergo remodeling and grow over time with the patient, and 7) available off-the-shelf with a long shelf life.

In the present study a cellular approach to improve standard ePTFE vascular grafts. Autologous cells ECs are appealing because they can produce a variety of therapeutic factors to maintain vascular patency. Anti-thrombotic drug releasing grafts, while capable of reducing thrombosis and hyperplasia have yet to show robust enough performance for small diameter graft applications over the long term. ePTFE vascular grafts were used as the scaffold material in the present work because they remain widely utilized clinically for grafts of medium diameter (6-8 mm ID) applications. Additionally, over the past decade, the labs of Monty Reichert, George Truskey, and Bruce Klitzman at Duke University have developed significant expertise in optimizing EC adhesion to ePTFE. The mechanical properties of the grafts are well characterized with the strength and suturability sufficient for the application.

There are several limitations with the use of ePTFE for future studies. The compliance of the ePTFE graft was not comparable to the intended location of the graft in the rat femoral artery. In addition, because ePTFE is non-degradable, vascular graft remodeling was limited. Remodeling is also influenced by the structure of the graft wall. The low porosity ePTFE graft utilized in this study prevented significant remodeling as the small pore sizes present in ePTFE grafts with 30 μm internodal distance are too small to allow capillary ingrowth from the outer graft wall. Alternatively, grafts with higher porosity have the additional challenges of blood seepage and require altered methods of EC seeding.

Until regenerative medicine technologies have a greater clinical presence, the ability have a graft that is ready off the shelf is an added benefit. The time required before implantation of our EPC sodded graft depends on the time to isolate EPCs. At the current rate, we would be able to obtain sufficient numbers of cells for seeding a 10-15 cm long coronary artery bypass graft segment at high densities after approximately 1-2 months. That said, we were unable to isolate EPCs in 50% of the patients and thus there is a clear need for improvement of EPC isolation methods. In a different scenario, it may be possible to draw blood for a patient before they necessitate surgery, isolate EPCs over a period of months, and bank the cells for future use. As the regenerative medicine field continues to grow this approach may become more feasible as cellular therapy centers become more common.

6.2 Future Work

6.2.1 Retrospective Evaluation of Experimental Design

The overarching goal of the current work was to show the feasibility of using human EPCs from the patient population that would be candidates for vascular tissue engineering interventions. Due to our focus on utilizing human cells, we were limited to animal models that would not mount an immune response and reject the cells. An athymic rat model allowed us to test our human EPCs without the risk of rejection. The use of human EPCs was promising as graft sodded with EPCs improved both short and long term graft patency. One aspect we were unable to assess, however, was the difference in graft anti-thrombotic performance caused by utilizing human versus rat cells. Human TM is capable of binding rat thrombin but may be unable activate rat protein C (212). This may have impacted our *in vivo* studies as increased rat activated protein C would reduce thrombotic events by preventing the generation of thrombin and activation of platelets, leukocytes, and smooth muscle cells (124).

Additional *in vivo* experiments with small diameter grafts containing EPCs over expressing rat TM could further our understanding of TM-overexpression. Ideally the following conditions would be included for graft sodding: 1) native rat EPCs, 2) rat EPCs overexpressing rat TM, 3) rat EPCs overexpressing human TM. In addition to the work involved to produce a new adenoviral vector containing the gene for rat TM, one

of the major challenges would be to obtain sufficient number of rat EPCs necessary to seed the graft. Human EPCs were isolated from 50 mL of blood, a volume far exceeding the possibilities from a rat, with total blood volumes of 10-16 mL per animal (217).

Another modification to future in vivo studies would involve better tracking of the sodded cells. Staining for human MHC class I antigens was used to differentiate between rat and human cells within the graft at time of explant. A different approach would have entail transfecting EPCs with a lentiviral vector containing GFP to allow long term tracking of sodded EPCs. We did use β-galactosidase to visualize EPCs that had been transfected with the control vector during *in vitro* testing. For animal studies, however, grafts were embedded in paraffin to preserve morphology for histological analysis of thrombosis and intimal hyperplasia. After fixation and paraffin embedding, we were unable to stain for β-galactosidase.

6.2.2 Vector System Used for Gene Therapy

The adenoviral system used in the present study allowed high EPC transfection efficiencies with high levels of transgene expression. Potential drawbacks of the vector system were the short duration of expression and the body's potential immunogenic response to viral proteins. The use of adeno-associated or lentiviral vectors could be used for long term expression with decreased immune response (103). An additional

consideration is the use of an endothelial specific (218) or an inducible promoter to activate gene overexpression only in ECs or when overexpression is called upon (219).

6.2.3 Vascular Graft Scaffold

The primary goal of *in vivo* studies was to determine the benefit of EPC endothelialization of a small diameter vascular graft in a challenging animal model. ePTFE was used as the Klitzman, Truskey, and Reichert labs have extensive experience in obtaining strong EC adhesion, and ePTFE remains a common clinically utilized vascular graft material. ePTFE grafts were stiffer and less elastic than the native arteries. This difference in compliance between the graft and the native artery has been suggested to contribute to the failure of synthetic vascular grafts (58, 59). It would be of interest to perform additional in vivo experiments with a small diameter vascular graft with mechanical properties more similar to a native artery. Porous polyurethanes and decellularized blood vessels are two example scaffold materials having better compliance properties that would be worth testing. Compliant vascular grafts releasing anti-thrombotic molecules also show promise (220) (221).

6.2.4 EPCs Isolation Efficiency

A drawback of using EPCs for material endothelialization applications is their exceedingly rare presence in peripheral blood MNC populations. We were able to

obtain high proliferation EPC colonies in less than 50% of patients having CAD. The frequency of late outgrowth EPCs in healthy volunteers was estimated by Yoder et al. as 0.017 colonies per 10^6 plated MNCs (89). With an average of 103 ± 7 x10^6 MNCs per subject observed in our study, we would estimate 1.75 endothelial colonies per 50 mL peripheral blood. A different study estimated 2.5 late outgrowth EPC colonies per 50 ml blood (100). While simply doubling the volume of blood collected should increase the frequency of isolation, strategies are needed to increase EPC isolation frequency.

Preselecting CD34+ CD45- MNCs before plating can enrich cell populations of late outgrowth EPCs by as much as 300-fold over non-sorted cord blood cultures (160). Other methods have been developed specifically capture late outgrowth EPCs using novel peptide ligands (161). Finding a unique or combination of markers to enrich cellular populations for late outgrowth EPCs populations from peripheral blood could have clinical benefits.

Finally, recent work has shown that late outgrowth EPCs may have lowered immunogenicity than mature ECs, suggesting that EPCs from mismatched donors could potentially be used when autologous ECs are unavailable. Rat derived late outgrowth EPCs had low levels of immunogenicity, expressing significantly lowered levels of MHC-I and MHC-II molecules compared to a population of rat aortic ECs (222). When cells were used *in vivo* in an abdominal aortic graft, use of allogeneic EPCs resulted in fewer T-cells and lowered neointima formation compared to allogeneic ECs. It should

be noted that EPCs were only tested over the course of two weeks, and there was more T-cell staining with grafts seeded with allogeneic EPCs than autologous ECs (222).

6.2.5 Induced Pluripotent Stem Cells (iPSCs)

The generation of pluripotent cells directly from a patient's own cells could be an enabling technology for the field of regenerative medicine. These cells, termed induced pluripotent stem cells (iPSCs), are created through the introduction of multiple transcription factors directly into a patient's own skin cells ex vivo, potentially avoiding the issue of immune rejection (223, 224). Fibroblasts have been reprogramed and differentiated into a variety of cell types including neurons, cardiomyocytes, and endothelial cells (225-227). Major challenges for clinical translation include preventing the formation of undifferentiated teratomas, generating iPSCs without the use of integrating viral vectors, developing more efficient methods to differentiate iPSCs, and eliminating the use of animal products in iPSC culture (228).

Although we are likely years away from cellular therapy products using iPSCs for material endothelialization applications, there has been a recent preliminary study focusing on the creation of ECs from iPSCs. Li et al. studied the differences in phenotype between ECs derived from embryonic stem cells (ESCs) versus iPSCs (227). Both cell types were capable of differentiating into ECs, expressing critical EC markers and forming blood vessels *in vivo*. iPSCs, however, gradually lost expression of key EC

markers over time and had lowered proliferation rates compared to ESCs. Morphology of iPSC derived cells was also altered, appearing fibroblast-like while ESCs exhibited typical EC cobblestone morphology. Both iPSCs and ESCs showed significantly lower expression of eNOS compared to a control EC population suggesting the cells were not fully differentiated. While ECs derived from iPSC are promising, additional work is needed to achieve a phenotype closer to native ECs before these cells can be used for regenerative medicine applications.

Appendix A

This is a write up of microarray experiments performed in collaboration with Dr. Ping Jin at the National Institutes of Health. The work here was written by undergraduate researcher and Duke Pratt Fellow, Enping Hong, and was submitted for graduation with honors at Duke University in May 2009.

Genetic Characterization of Late-Outgrowth Endothelial Progenitor Cells for Use in Synthetic Vascular Grafts

Authors: Enping Hong, John D. Stroncek, Ping Jin, William M. Reichert

ABSTRACT

Late outgrowth endothelial progenitor cells (EPCs) present an autologous, easily obtained, and highly proliferative cell source for the endothelialization of small-diameter synthetic vascular grafts. We investigate the possibility of using EPCs from patients with coronary artery disease (CAD) can be used to endothelialize synthetic bypass grafts implanted in these patients. To this end, we hypothesize that healthy and CAD EPCs will respond similarly to physiological shear stress in terms of gene expression and functional response. Using DNA microarray and RT-PCR techniques, we investigated the gene expression profiles of EPCs from healthy and diseased patients in response to 48 h of laminar shear stress at 15 dyn/cm^2. We found that differences within the results were dominated by flow condition rather than cell type. Healthy and CAD EPCs appear to be very similar, especially in the areas of cell adhesion and the

vasodilatory response, which were confirmed by functional assays of adherence under superphysiological shear stress and a nitric oxide assay respectively. While our investigation is still ongoing, these results provide promising support for the use of CAD EPCs in synthetic vascular grafts.

INTRODUCTION

Small-diameter synthetic vascular grafts have had considerably lower success than their larger-bore brethren used in aortic or iliac grafts. While expanded polytetrafluoroethylene (ePTFE) and Dacron® grafts used as prostheses for these larger vessels have yielded good results (25), small- (< 4 mm) to medium-sized (< 7 mm) grafts still have low patency rates due to neointimal hyperplasia and ongoing surface thrombogenicity (8). In these smaller grafts, neither transmural ingrowth through the graft wall nor transanastomotic ingrowth from the adjacent artery is able to form a functional endothelium beyond the immediate anastomotic region.

Over the last twenty years, it has been recognized that the presence of a functional endothelium improves the patency of synthetic small-diameter grafts. Endothelial cells (ECs) are highly antithrombotic and therefore provide an excellent local environment for preventing thrombus formation. When used in combination with synthetic materials of appropriate physical properties, ECs can result in synthetic vascular grafts having performance similar to autologous vein (229). Studies by Peter

Zilla's group have shown that medium-sized vascular grafts seeded with ECs maintain and intact endothelium even after several years, and show good patency rates four to seven years after implantation (170, 230). These and other studies, however, rely on harvesting autologous veins for endothelial cells, an invasive procedure that introduces donor site morbidity. Microvascular ECs taken from adipose tissue provides another common source, but these cells are often heterogeneous and contaminated with cell types that contribute to intimal hyperplasia and inflammation (80).

Endothelial progenitor cells (EPCs) have emerged as a promising alternative cell source for mature ECs in tissue engineering applications. Derived from the bone marrow, EPCs circulate in the peripheral blood and can differentiate into cells with EC characteristics ex vivo (34). EPCs have since been shown to improve the patency of both synthetic and decellularized grafts (96, 97), forming an autologous, non-thrombogenic luminal surface with vasomotor activity to physiological stimuli (97), and also reducing intimal hyperplasia due to induced trauma (96). Recent studies have identified two subpopulations of EPCs depending on the method of culture, "early outgrowth" EPCs with limited proliferative potential and bear macrophage markers, and "late outgrowth" EPCs that are highly proliferative and have vasculogenic potential *in vivo* (92).

In this study we continue our characterization of late outgrowth EPCs from patients with significant coronary artery disease (CAD) for the autologous endothelialization of synthetic small-diameter vascular grafts. To our knowledge, these

are the first such studies investigating the suitability of EPCs from CAD patients for graft seeding. In our previous work, we demonstrated that EPCs taken from such patients exhibited the same critical cell surface markers and morphological characteristics as EPCs from healthy patients and a control group from human aortic ECs (173). This manuscript compares the gene expression of healthy EPCs and EPCs taken from CAD patients in their response to sustained physiological shear stress, similar to conditions present *in vivo*. Late outgrowth EPCs were obtained from CAD patients and healthy donors, and the cells were exposed to laminar shear at physiological flow conditions in parallel plate flow chambers. RNA expression levels were compared using microarray and real-time reverse transcriptase polymerase chain reaction (RT-PCR), using RNA human aortic ECs as reference RNA. These results were also compared to several functional assays to verify the effects of the genes studied.

MATERIALS AND METHODS

Coronary Artery Disease Patient Enrollment. The use of human blood described in the study was approved by the responsible ethical committee at Duke University. Patients undergoing left heart catheterization were approached for consent at Duke University Medical Center. We studied 13 patients having coronary artery disease (9 men and 4 women; mean age: 61.5 ± 10.5 years; range: 44-75 years). After arterial sheath

insertion, approximately 50 ml peripheral blood was removed and stored in EDTA tubes.

Healthy Volunteer Enrollment. 50 ml of peripheral blood was drawn from 13 young healthy volunteers (9 men and 4 women; mean age: 26.2 ± 2.5 years; range: 23-31 years) and stored in EDTA tubes.

Late outgrowth EPC isolation and culture. Each blood sample was processed on the same day it was collected. Blood was diluted 1:1 with Hanks balanced salt solution (HBSS; Invitrogen, Grand Island, NY) and overlaid onto an equivalent volume of Histopaque-1077 (Sigma, St. Louis, MO). The mixture was centrifuged for 30 minutes at room temperature at 740g. Buffy coat mononuclear cells were isolated and washed 3 times in EBM-2 (Cambrex, Walkersville, MD) with 10% fetal bovine serum (FBS; Hyclone, Logan, UT). Mononuclear cells were resuspended in 12 ml complete EBM-2 + EGM-2 SingleQuots (Cambrex) medium with 1% antibiotic/antimycotics solution (Gibco, Carlsbad, CA) and seeded onto 3 separate wells of a 6-well tissue culture plate coated with type 1 rat tail collagen (BD Biosciences, Bedford, MA) at 37°C, 5% CO_2, in a humidified incubator. An average of 34×10^6 MNCs were seeded per well. After 24 hours of culture, nonadherent cells were removed and complete EGM-2 medium was added to each well. Medium was changed daily for 7 days and then every other day following. Cells were used at passages 5-10 for all experiments.

Human aortic endothelial cell culture. Human aortic endothelial cells (HAECs) (Cambrex) were grown to confluence in T-25 or T-75 polystyrene flasks with endothelial basal media-2 supplemented with EGM-2 SingleQuots, 10% FBS, and 1% antibiotic/antimycotics solution. HAECs were used at passage 7-10 for all experiments, and were not cultured under exposure to shear stress.

Flow experiments. Cells were seeded onto SlideFlasks (NUNC, Rochester, NY) at a density of $50x10^3$ cells/cm^2. The following day, the slides were placed in a parallel plate flow chamber and connected to a circular flow setup consisting of a peristaltic pump and pulse dampener (Cole Palmer, Vernon Hills, IL), and a flow chamber. The flow media used consisted of EBM-2 + 10% FBS + 1% AB/AM. Cells were exposed to 15 dyn/cm^2 for 48 hours in the incubator, also at 37°C and 5% CO_2. Controls consisted of cells under identical culture conditions, but not exposed to flow (static). For each cell type (diseased or healthy), 4 highly proliferative cell cultures were expanded and used.

Isolation of cellular RNA. Cellular RNA was isolated using the RNeasy Minikit (QIAGEN) and stored at -80°C. Optional on-column DNase digestion was not employed. Reference RNA was obtained from human aortic endothelial cells (HAECs) of a 22-year old healthy male individual purchased from Cambrex (Walkersville, MD).

Microarray performance and statistical analysis. Through a collaboration with Dr Ping Jin at the NIH Clinical Center, the extracted RNA was analyzed on an oligonucleotide microarray. RNA quality was tested with the Agilent Bioanalyzer 2000

(Agilent Technologies) and amplified into antisense RNA (aRNA)(231). Total RNA from PBMCs pooled from six normal donors was extracted and amplified into aRNA to serve as the reference. Pooled reference and test aRNA were isolated and amplified in identical conditions to avoid possible interexperimental biases. Both reference and test aRNA were directly labeled using ULS aRNA Fluorescent Labeling kit (Kreatech) with Cy3 for reference and Cy5 for test samples. Whole-genome human 36K oligo arrays were printed in the Infectious Disease and Immunogenetics Section of Transfusion Medicine, Clinical Center, NIH (Bethesda, MD) using oligos purchased from Operon. The Operon Human Genome Array-Ready Oligo Set version 4.0 contains 35,035 oligonucleotide probes, representing approximately 25,100 unique genes and 39,600 transcripts excluding control oligos. The design is based on the Ensembl Human Database build (NCBI-35c), with a full coverage on NCBI human Refseq dataset(04/04/2005). The microarray is composed of 48 blocks, with one spot printed per probe per slide.

Hybridization was carried out in a water bath at 42°C for 18 to 24 hours. The arrays were then washed and scanned on a GenePix 4000 scanner at variable photomultiplier tube to obtain optimized signal intensities with minimum (<1% spots) intensity saturation. Resulting data files were uploaded to the mAdb database(http://nciarray.nci.nih.gov/) and further analyzed using BRBArrayTools

developed by the Biometric Research Branch, National Cancer Institute (http://linus.nci.nih.gov/BRB-ArrayTools.html) and Cluster and TreeView software.

A brief summary of the microarray procedure is outlined as follows. The raw data set was filtered according to standard procedure to exclude spots with minimum intensity that arbitrarily was set to an intensity parameter of 200 for in both fluorescence channels. If the fluorescence intensity of one channel was great than 200 and that of the other but was below 200, the fluorescence of the low intensity channel was arbitrarily set to 200. Spots with diameters < 20μm and flagged spots were also excluded from the analyses. Filtered data was normalized using Lowess Smoother.

The gene array data was analyzed using the Ingenuity® software, which examined key functions and pathways that were activated or suppressed. For data analysis, a univariate paired T-test was used at a normal significance level of 0.005. Only genes that had differences significant at this level were reported.

RT-PCR. RT-PCR was used to investigate gene expression levels more closely. cDNA was produced using a cDNA kit (Biorad) and the RNA extract as a template, and stored at 4°C. RT-PCR was performed using a SYBR-Green RT-PCR kit (Biorad) and the MyIQ™ iCycler Optical Module (Biorad). Whole-gene cDNA sequences of the target genes were obtained from PubMed, and primer sequences generated using the online design program Primer3 (149). The melt curves of the primers were examined after reaction with reference RNA, and primers were selected that had uniform and single-

product melt curves. After results were obtained, fold change from the reference RNA was calculated by the $2^{-\Delta\Delta CT}$ method.

The primer sequences for the genes described in this paper are listed in Appendix B.

Nitric oxide assay. Flow experiments were conducted with EPCs as above, but using flow media consisting of phenol red-free EBM medium (Cambrex) + 10% FBS + 1% AB/AM. After exposure to shear stress for 48 hours, the media was collected and frozen at -80°C. Media aliquots were lyophilized and nitric oxide concentration was determined by measuring breakdown products NO_2^- and NO_3^2 using a commercial assay (Active Motif, Carlsbad, CA) according to the manufacturers' instructions. Media samples were filtered through a 10,000 Dalton micropore filter (Millipore) prior to assay.

RESULTS

Gene array results

Global differential gene expression. When healthy EPCs were exposed to physiological flow conditions, 740 genes were found to be differentially expressed as compared to the control (static) condition (Table 7). At the 0.005 significance level, the probability of getting at least this number of genes significant by chance is 0.03125. Of these genes, 337 of them had an expression level ratio >2 or <0.5. Thus, for 45.5% of the

differentially expressed genes, the difference between flow and static conditions dominates the difference between individual patients.

Similar analyses were performed for EPCs isolated from patients with CAD, and differential gene expression between EPCs from CAD patients and healthy donors were separately compared for flow and static conditions. The results are shown below in Table 7. It can be immediately noticed that the number of differentially expressed genes is considerably smaller between CAD and healthy EPCs than in the comparison between flow and static conditions.

Table 7: Differential gene expression from gene array across different conditions.

Condition Comparison	**Differentially expressed genes**	**Probability of this number by chance alone**	**% of genes with expression levels >2 or <0.5**
Healthy EPC: Flow/Static	740	0.03125	45.5%
CAD EPC: Flow/Static	575	0.125	40.7%
Flow: CAD/Healthy	117	0.2	47.9%
Static: CAD/Healthy	112	0.22857	54.5%

When the four conditions above were compared for shared genes, it was found that CAD and healthy EPCs shared 225 genes that were differentially regulated by flow out of pools of 575 and 740 genes respectively; when genes were examined for

differential expression due to cell type, only 19 genes were found to be shared between cells exposed to flow and static conditions. These results are represented graphically in Figure 33.

Functional analysis. Functional analysis by the Ingenuity® software grouped the genes by the processes they affected; these results are represented in Figure 2. We find significant differential regulation in genes that are related to cell death, the cell cycle, and cardiovascular system development and function. These broad functional categories help to identify the primary endothelial cell functions that are affected by physiological shear stress, and hence help us characterize the effect of such stress on EPCs.

Tabulated data from the microarray is included in Appendix B. While not an exhaustive list, it provided the basis for our investigation by grouping the differentially regulated genes by function and cell type.

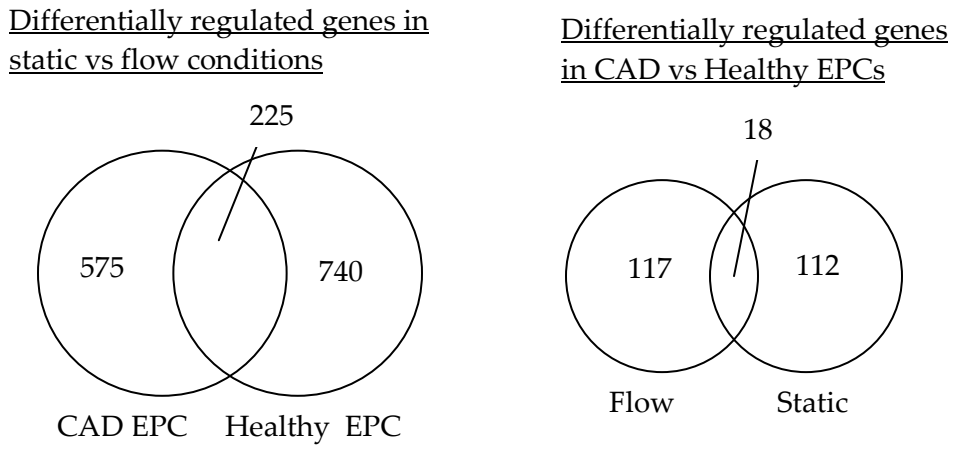

Figure 33: Venn diagram representation of gene overlap under different experimental conditions. The left hand diagram shows that while a large number of genes (575 for CAD and 740 for healthy) are differentially regulated in response to flow condition, 225 of those genes are shared between the two cell types. In contrast, while much fewer genes are differentially regulated between cell types for flow vs static culturing, only 18 genes are always differentially regulated in these two groups.

Response of late outgrowth EPCs to shear stress

Cell adhesion and the extracellular matrix (ECM). The adhesion molecules integrin α-V (ITGAV) and fibronectin-1 (FN1) are upregulated, indicating improved cell adhesion in response to flow. Collagen types Iα2, Vα1, and XV (COL1A2, COL5A1, COL15A1) are also upregulated, revealing increased production of both fibrillar (types I and V) and basement membrane-associated (XV) collagens (232). However, the tight junction-related proteins claudin 5 and claudin 11 are down regulated, indicating a reduction in cell-cell adhesion alongside an improvement in cell-matrix adhesion (233). Finally, the occurrence of matrix remodeling is evidenced by the upregulation of matrix metalloproteinase 2 (MMP2) (234).

Vasodilatory regulation. A number of genes involved in vascular function have altered expression levels with shear stress. Krüppel-like factor 2 is upregulated with flow, possibly mediating communication between ECs and vascular smooth muscle cells (235). Nitric oxide signaling is found to be significantly regulated as well: the expression of VEGF receptor 2 (KDR) is increased, which would induce the expression of eNOS, producing the vasodilatory agent nitric oxide (NO) and contributing to the flow-induced

dilation response (236). At the same time, the expression of caveolin-1 (CAV1) is suppressed, further contributing to increased eNOS levels and NO activity (237).

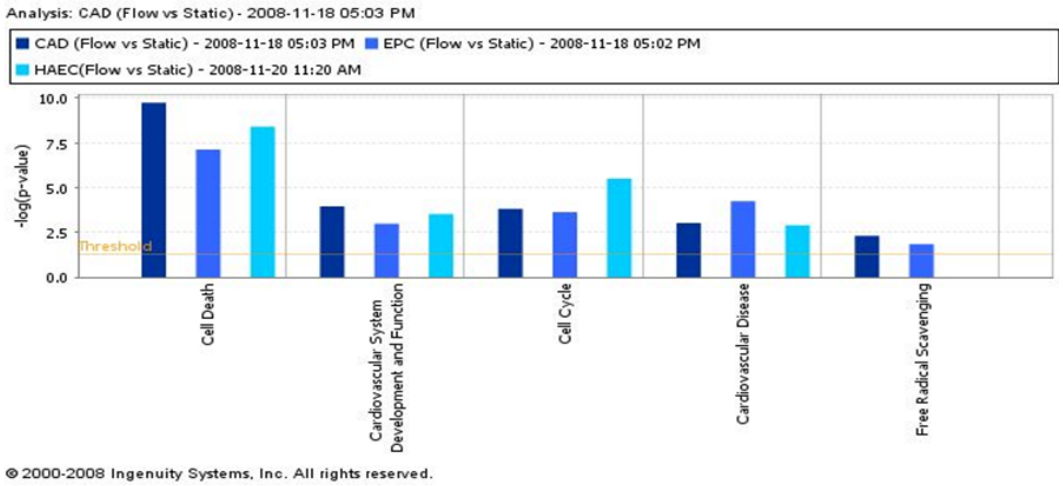

Figure 34: Functional analysis of differentially expressed genes.

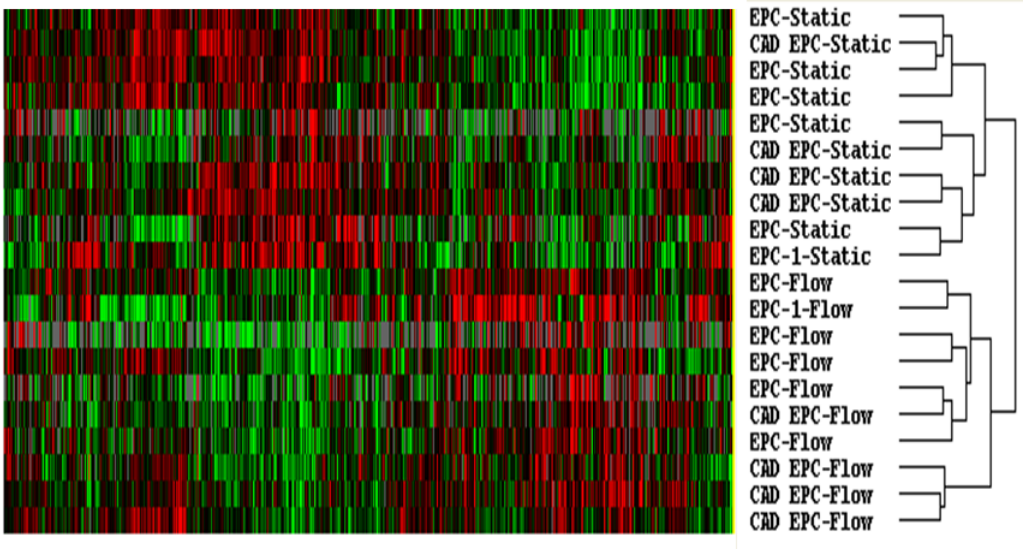

Figure 35: Gene expression patterns of EPCs isolated from healthy donors (designated "EPC") and EPCs isolated from patients with CAD (designated "CAD EPC"). Global gene expression patterns were sorted by hierarchical clustering. Red markers represent increased expression for a particular gene and green markers indicate reduced expression. Color intensity indicates the level of such regulation. While expression of individual genes vary, static and flow conditions induce a clear difference in expression patterns in both EPC and CAD EPC conditions while the difference between the EPC and CAD EPC groups is substantially less clear.

Regulation of cell growth. Physiological shear stress is known to be a regulator of the proliferation and survival of endothelial cells (238). Accordingly, we find that a number of genes related to cellular compromise and cell proliferation are affected. However, the genes show varying responses to shear stress: HMOX1 and SOD2, both of which function to protect the endothelium against oxidative stress (239, 240), are respectively upregulated and down regulated. A DNA repair gene, ERCC2, is down regulated. Inhibin A, which promotes cell proliferation (241), is upregulated in these

studies, but there are indications that both cell proliferation and apoptosis are reduced in a functional endothelium. The processes regulating cell proliferation and apoptosis need a closer look if we are to accurately determine the effect of shear stress therein.

RT-PCR

Regulation of key genes with flow. Genes of particular interest were further investigated using RT-PCR. The microarray data on its own was insufficient, since significant differences in gene expression were often obtained for either healthy or CAD EPCs, but not both cell types – hence, a meaningful comparison was rarely obtained. In addition, each spot on the microarray represents a different gene, so there is only a single data point per condition per gene and no representation of experimental variance. RT-PCR allowed for the further investigation of the mean and spread in expression of key genes identified through the microarray results, or through current literature.

Cell adhesion. EPCs from CAD and healthy subjects responded similarly in their expression of representative cell adhesion and ECM genes under physiological shear stress (Figure 4). Collagen IV (COL4A1) expression was sharply increased in both cell types, showing that EPCs increase production of basement membrane collagen in response to shear stress. ECs bind to Collagen IV via fibronectin-1 (FN1) (242), which saw an increase in expression level for both cell types, as in the microarray.

Interestingly, the production of laminin, a key cell adhesion protein in the ECM, does not seem to be regulated by shear stress, with both healthy and diseased EPCs producing the same amount of laminin as mature ECs (control cells).

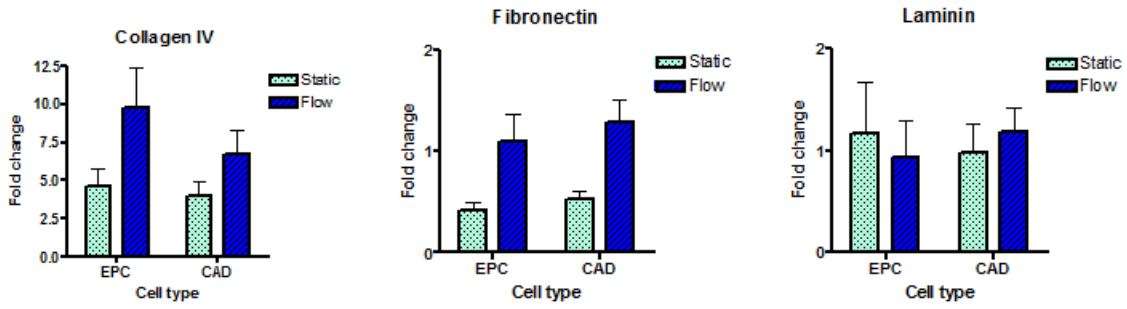

Figure 36: Response of cell adhesion genes to shear stress.

Previously, we found that CAD and healthy EPCs had excellent resistance to shear under short-term superphysiological flow. Both cell types adhered firmly to fibronectin-coated Teflon-AF™ after exposure to high shear stresses in a variable height flow chamber. Both cell types showed greater than 95% retention after exposure to a shear of 187 dynes/cm^2 (173). The increased production of fibronectin-1 and collagen IV contributes to such retention by increasing the adhesive forces between EPCs and Teflon-AF™.

As a final point of interest, we tested the expression levels of fibrillar collagen (Collagen I, COL1A2) with RT-PCR as well. EPCs generally produced much less collagen I than mature endothelia, and samples generally showed an increase in collagen I production after exposure to physiological shear stress. However, the base

levels of collagen varied very widely between the different cell types, up to differences of an order of magnitude in fold change values. This made it difficult to draw any kind of definitive conclusion from the collagen I data. It is unclear if the variation between samples was due to experimental variation or disease characteristics in different individuals.

Vasodilatory regulation. Both diseased and healthy cells showed increased expression of KLF2 and KDR, confirming results seen in the microarray (Figure 5). In addition, eNOS (NOS3) is confirmed to be upregulated, increasing the production of the vasodilatory gas nitric oxide (NO). NO causes the relaxation of vascular smooth muscle, and also maintains an antiproliferative and antiapoptotic environment in the vessel wall (243). COX-2 (PTGS2) is also upregulated in both cell types, showing that prostaglandins are involved in the vasodilatory response (244). While the expression levels of KDR and KLF2 did not vary significantly between healthy and diseased EPCs, those of eNOS and COX-2 did, with diseased EPCs having significantly greater expression of eNOS and COX-2 under physiological shear stress than healthy cells.

Thrombomodulin. Thrombomodulin levels were similar between healthy and diseased individuals. However, thrombomodulin was more highly expressed when cells were exposed to physiological shear stress.

Nitric oxide assay. As a means of assessing the functional effect of nitric oxide production by the EPCs, nitric oxide assays were conducted on the cell media after the

flow experiments were concluded. Although there is a significant difference in RNA levels of eNOS between CAD and healthy EPCs, the levels of nitric oxide products in the media remained largely the same for both static and flow conditions when compared between CAD and healthy EPCs, and even mature endothelia (Figure 6).

DISCUSSION

It is clear that the presence of shear stress is a much more significant regulator of endothelial gene expression than whether the cells were taken from healthy or diseased individuals. As identified in the microarray, hundreds of genes had their expression levels significantly altered by shear stress for both healthy and CAD EPCs. The 225 genes that were shared in those two groups accounted for about half and two-thirds of those two gene populations respectively. This indicates a great amount of similarity between healthy and CAD EPCs in their response to physiological shear stress, and this is also evident in our confirmatory RT-PCR studies. In contrast, only a hundred or so genes had their expression significantly changed by cell type in either static or flow conditions, and only 18 of those genes were shared under both static and flow conditions; in addition, the 18 genes that are significantly regulated in both cell types do so in the same manner, with only some differences in magnitude.

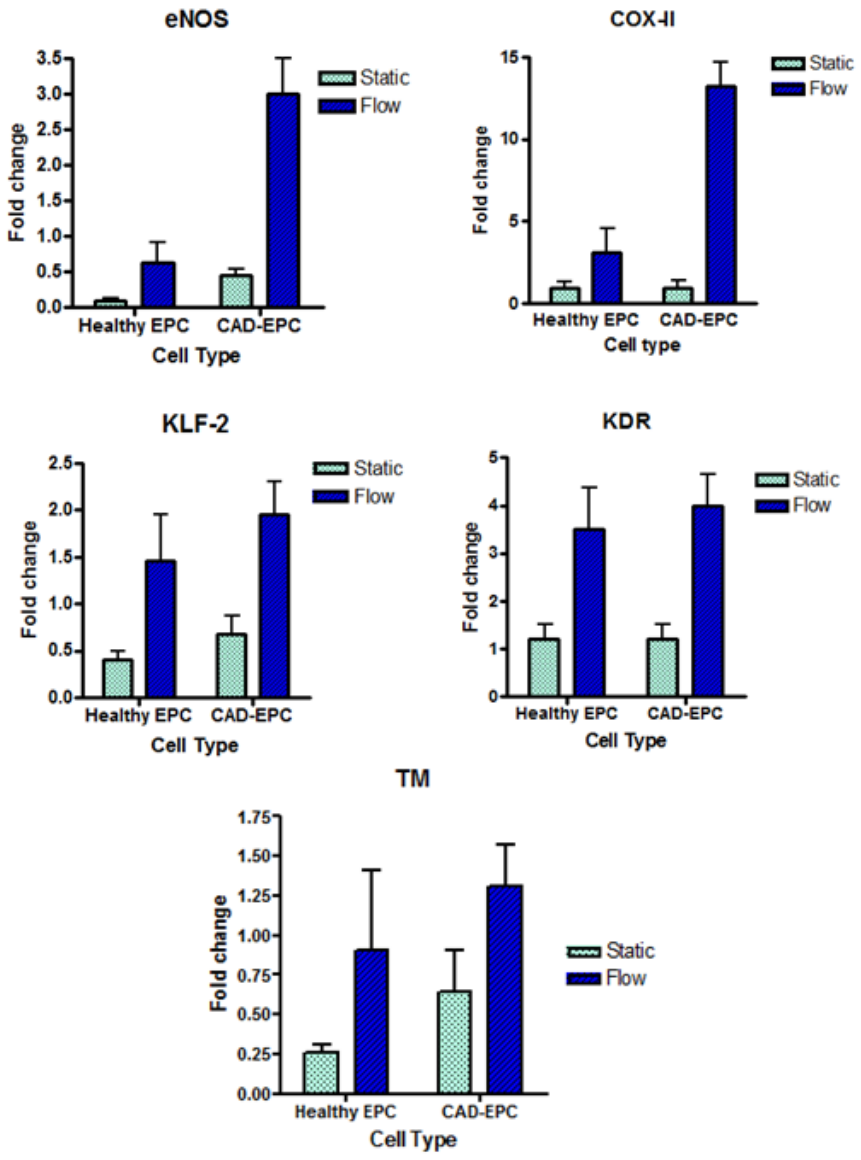

Figure 37: RNA expression levels determined by real time RT-PCR.

When healthy and CAD EPCs are exposed to prolonged physiological shear stress, their response in genes relating to cell adhesion are fairly similar. While the

microarray gives us evidence of increased cell anchorage through the upregulation of collagens, fibronectin, and integrin α-V, as well as evidence of matrix remodeling through MMP and claudin regulation, RT-PCR results show that the expression of key molecules involved in cell adhesion, namely fibronectin-1, laminin, and collagen IV, are very similar between healthy and CAD EPCs. In particular, the upregulation of fibronectin-1 and collagen IV indicate the enhancement of endothelial attachment to the basement membrane. This has been further supported by our previous findings of excellent cell retention for both healthy and CAD EPCs under superphysiological shear stress. These results are excellent indications that EPCs taken from CAD patients would have no trouble adhering to and retaining on synthetic bypass grafts in these patients.

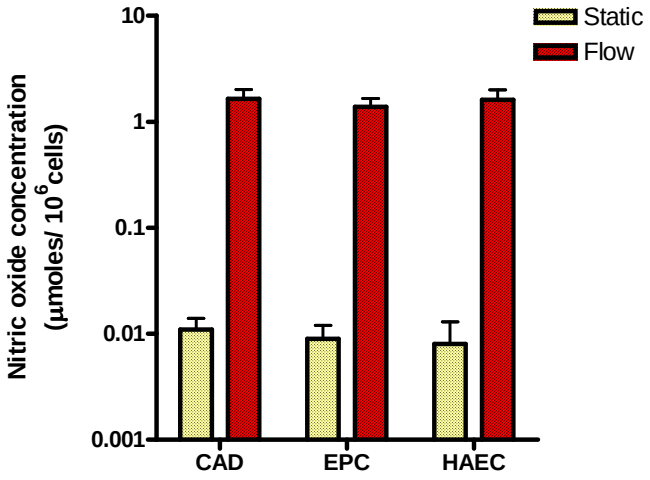

Figure 38: Levels of nitric oxide products in media after flow experiments

We also note the reduced expression of claudins, as well as the remodeling of the endothelium in the direction of flow after prolonged exposure to laminar shear stress. While such remodeling is clearly the result of shear stress, indicated by the lack of such behavior under static (control) conditions, the reduced expression of tight-junction specific claudins may allow the cells to alter their orientation in order to allow for such realignment. The improved anchorage accorded by increased collagen and fibronectin expression would help the cells to maintain a stable endothelium even while undergoing such remodeling.

Another important aspect of the endothelial response to shear stress is the vasodilatory response, which again is fairly similar between healthy and CAD EPCs. Vasodilation has long been recognized as a physiological response to increased blood flow *in vivo*; early canine studies compared vasodilation in vessels with healthy and damaged endothelia, and the importance of a functionally intact endothelium was established for this physiological response (245). The upregulation of KLF2, KDR, and eNOS indicate an increase in NO production (235, 236); the strong upregulation of COX-2 indicates the activation of a prostaglandin-assisted vasodilatory pathway, as supported by its established role in maintaining flow-induced dilation in eNOS-knockout mouse models (244).

It is particularly interesting that expression levels of eNOS and COX-2 are strongly elevated in patients with CAD as compared to healthy EPCs. This would then

indicate that both the NO-mediated and prostaglandin-mediated pathways for rapid arterial dilation are enhanced in patients with CAD; to our knowledge, there is no explanation for this phenomenon in the current literature. There appears to be no significant disadvantage for such an elevation of the vasodilatory pathways: this could in fact help relieve local shear stress around the graft site, and the activation of eNOS in particular could also induce regression of intimal hyperplasia via several mechanisms (246). However, functional nitric oxide assays show similar results between CAD and healthy EPCs, and mature endothelia as well. While this is an indication that the functional response will remain the same regardless of cell type, it also suggests that functional data will not always match trends seen in RNA or protein expression. We need to look at all the data that we have together before we can pass judgment on the effect of a particular applied condition on an area of endothelial function.

CONCLUSION

In our results so far, we have determined that CAD EPCs are fairly similar to healthy EPCs in terms of both adhesive properties and vasodilatory response. While the expanse of data generated by the microarray still needs to be worked through, especially in the areas of cell proliferation and cellular compromise, we have good indications that CAD EPCs respond to shear stress in very similar ways as compared to healthy EPCs and even mature endothelia. Although much work still has to be done, this study

provides a useful first step towards using EPCs from patients with CAD in synthetic vascular grafts.

Appendix B

RT-PCR Primers Sequences

Gene	*Primer*	*Sequence (5'-3')*	*T_m (^oC)*
β2 microglobulin*	fwd	GGC TAT CCA GCG TAC TCC AAA G	57.5
	rev	CAA CTT CAA TGT CGG ATG GAT	52.9
COS-II (PTGS2)	fwd	TGA GCA TGT ACG GTT TGC TG	55.7
	rev	TGC TTG TCT GGA ACA ACT GC	55.9
eNOS (NOS3)	fwd	ACC CTC ACC GCT ACA ACA TC	57.1
	rev	GCT CAT TCT CCA GGT GCT TC	55.9
VEGF-R2 (KDR)	fwd	GTG ACC AAC ATG GAG TCG TG	55.9
	rev	TGC TTC ACA GAA GAC CAT GC	55.5
KLF2	fwd	CCT CCC AAA CTG TGA CTG GT	57.1
	rev	ACT CGT CAA GGA GGA TCG TG	56.4
TM	fwd	TAC GGG AGA CAA CAA CAC CA	56.1
	rev	AAG TGG AAC TCG CAG AGG AA	56.2
Collagen I (COL1A2)	fwd	CTG CAA GAA CAG CAT TGC AT	54.3
	rev	GGC GTG ATG GCT TAT TTG TT	53.8
Collagen IV (COL4A2)	fwd	AAG GAA TCA TGG GCT TTC CT	54.2
	rev	CTC TGG CAC CTT TTG CTA GG	55.9
Fibronectin-1 (FN1)	fwd	ACC AAC CTA CGG ATG ACT CG	56.5
	rev	GCT CAT CAT CTG GCC ATT TT	53.4
Laminin α5 (LAMA5)	fwd	TGA CCT TTT CTG GCT CGT CT	56.2
	rev	GTT CAG CAC AAA GGG CTC TC	56.3

*Microglobulin is used as the housekeeping gene in the $2^{-\Delta\Delta CT}$ method.

Key Differentially Expressed Genes within Microarray Data Identified through Ingenuity Software (organized by function)

Cell Adhesion Genes

Gene ID	Gene Name	EPC: Flow / Static		CAD: Flow / Static		Static: CAD / EPC		Flow: CAD / EPC	
		Fold change	t-test p value	Fold change	t-test p value	Fold change	t-test p value	Fold change	t-test p value
ITGAV	integrin alpha V	2.584675	9.30E-05						
ITGB4	integrin beta 4			2.225248	5.94E-05				
NRCAM	neuronal cell adhesion molecule			1.813136	0.000589				
ICAM2	ICAM-2	0.38871	0.000134	0.486812	0.000122				
CLDN5	claudin-5 transcript variant 2	0.303092	0.000417	0.315096	5.42E-05				
CLDN11	claudin 11	0.300089	0.000536			0.035391	1.00E-07	0.155137	1.50E-06
Adhesion-related									
RAC2	ras-related C3 botulinum toxin substrate 2	0.267461	1.06E-05					3.809852	4.14E-05
KDR	KDR	1.848496	0.000673						
PVRL2	poliovirus receptor related 2	1.757438	0.000776						
CD44	CD44	3.094916	1.68E-05	1.774796	0.000609				
VEGFB	vascular endothelial growth factor B (VEGFB), mRNA.	0.589958	0.003175						
Matrix molecules									
FN1	fibronectin 1	1.965851	0.000738						
COL1A2	collagen I alpha 2	2.583161	0.000615						
COL5A1	collagen V alpha 1	2.375226	0.000386						
COL8A1	collagen VIII alpha 1							2.386794	0.003215
COL13A1	collagen XIII alpha 1					3.913741	0.000147		
COL15A1	collagen XV	6.453115	0.000742						

Cellular Compromise Genes

Gene ID	Gene Name	EPC: Flow / Static		CAD: Flow / Static		Static: CAD / EPC		Flow: CAD / EPC	
		Fold change	t-test p value	Fold change	t-test p value	Fold change	t-test p value	Fold change	t-test p value
Oxidative Stress Response									
ALDH3A2	aldehyde dehydrogenase 3 family, member A2 (ALDH3A2), transcript variant 2, mRNA.			1.944047	0.000745				
GMFB	glia maturation factor, beta (GMFB), mRNA.	0.211817	1.60E-06	0.18707	8.00E-07				
HMOX1	heme oxygenase (decycling) 1 (HMOX1), mRNA.			2.796571	0.000418				
MAPT	microtubule-associated protein tau (MAPT), transcript variant 4, mRNA.			1.579374	0.004198				
MT1E	metallothionein 1E (MT1E), mRNA.			0.247412	9.00E-06				
MYC	v-myc myelocytomatosis viral oncogene homolog (avian) (MYC), mRNA.	0.363016	0.000104	0.437828	0.000513				
NQO1	NAD(P)H dehydrogenase, quinone 1 (NQO1), transcript variant 3, mRNA.	3.59576	9.81E-05	3.364683	2.20E-06				
PON2	paraoxonase 2 (PON2), transcript variant 2, mRNA.			0.586624	0.003016				
PRDX1	peroxiredoxin 1 (PRDX1), transcript	2.051575	2.56E-05	1.880164	0.000311				

	variant 3								

Damage of cells

ERCC2	excision repair cross-complementing rodent repair deficiency, complementation group 2 (ERCC2), transcript variant 1, mRNA.			0.57502	0.004049				
HMOX1	heme oxygenase (decycling) 1 (HMOX1), mRNA.			2.796571	0.000418				
MT1E	metallothionein 1E (MT1E), mRNA.			0.247412	9.00E-06				
SOD2	superoxide dismutase 2, mitochondrial (SOD2)	0.213664	< 1e-07	0.39806	0.001608	0.544364	0.0046		
STAT3	signal transducer and activator of transcription 3 (acute-phase response factor) (STAT3), transcript variant 3, mRNA.			0.53484	0.002397				
TNFSF10	tumor necrosis factor (ligand) superfamily, member 10 (TNFSF10), mRNA.	0.489093	0.002562	0.483768	8.73E-05				

Fragmentation of nucleus

BCAR1	breast cancer anti-estrogen resistance 1 (BCAR1), mRNA.	0.273736	8.00E-07	0.524973	0.000926				

CLU	clusterin (CLU), transcript variant 1, mRNA.	0.496389	0.003258	0.279748	9.30E-06				
FST	follistatin (FST), transcript variant FST317, mRNA.								
INHBA	inhibin, beta A (INHBA), mRNA.			2.816351	0.000503				
MYC	v-myc myelocytomatosis viral oncogene homolog (avian) (MYC), mRNA.	0.363016	0.000104	0.437828	0.000513				

Cell Proliferation Genes

Gene ID	Gene Name	EPC: Flow / Static		CAD: Flow / Static		Static: CAD / EPC		Flow: CAD / EPC	
		Fold change	t-test p value	Fold change	t-test p value	Fold change	t-test p value	Fold change	t-test p value
FN1	fibronectin 1	1.9658505	0.0007384						
KDR	KDR	1.8484961	0.0006725						
ADM	adrenomedullin (ADM), mRNA.	0.3089166	2.77E-05						
MGP	matrix Gla protein (MGP), mRNA.	2.8723894	0.0005267			3.002324	0.00027		
VEGFB	vascular endothelial growth factor B (VEGFB), mRNA.	0.5899577	0.0031746						
CAV1	caveolin 1, caveolae protein, 22kDa (CAV1), mRNA.	0.343675	0.0001891	0.26996	1.94E-05				
ANGPT2	angiopoietin 2 (ANGPT2), transcript variant 3, mRNA.	0.1709631	0.0008575	0.206356	1.68E-05	0.242178	0.004719		
FOXO1	forkhead box O1 (FOXO1), mRNA.	0.4602323	0.0010724	0.584228	0.003508				
CD44	CD44	3.0949159	1.68E-05	1.774796	0.000609				
ENG	endoglin (Osler-Rendu-Weber syndrome 1) (ENG), transcript variant 2, mRNA.	1.9477882	0.0027933	1.778187	0.00147				
ADAMTS1	ADAM metallopeptidase with thrombospondin type 1 motif, 1 (ADAMTS1), mRNA.	2.3275249	0.0005526	2.38446	9.52E-05				

TNFSF 10	tumor necrosis factor (ligand) superfamily, member 10 (TNFSF10), mRNA.	0.4890925	0.0025619	0.483768	8.73E-05				
ANGPTL4	angiopoietin-like 4 (ANGPTL4), transcript variant 3, mRNA.			v	0.000128				
CEACAM1	carcinoembryonic antigen-related cell adhesion molecule 1 (biliary glycoprotein) (CEACAM1), transcript variant 2, mRNA.			0.602516	0.001593				
ERAP1	endoplasmic reticulum aminopeptidase 1 (ERAP1), transcript variant 1, mRNA.			0.593103	0.002991				
F11R	F11 receptor (F11R), mRNA.			0.548251	0.003189				
GBP1	guanylate binding protein 1, interferon-inducible, 67kDa (GBP1), mRNA.			0.482702	0.000126				
HMOX1	heme oxygenase (decycling) 1 (HMOX1), mRNA.	2.7965707	0.0004184						
INHBA	inhibin, beta A (INHBA), mRNA.			2.816351	0.000503				

Reduction-Oxidation Genes

Gene ID	Gene Name	EPC: Flow / Static		CAD: Flow / Static		Static: CAD / EPC		Flow: CAD / EPC	
		Fold change	t-test p value	Fold change	t-test p value	Fold change	t-test p value	Fold change	t-test p value
CYP1B1	cytochrome P450, family 1, subfamily B, polypeptide 1 (CYP1B1), mRNA.	17.42217	0.000144	24.15485	1.90E-06				
CYP1A1	cytochrome P450, family 1, subfamily A, polypeptide 1 (CYP1A1), mRNA.	9.5803995	2.50E-06	11.83562	8.00E-07				
HMOX1	heme oxygenase (decycling) 1 (HMOX1), mRNA.	2.7965707	0.000418						
PTGR1	prostaglandin reductase 1 (PTGR1), mRNA.	1.9421812	0.00284						
SOD2	superoxide dismutase 2, mitochondrial (SOD2)	0.2136643	< 1e-07	0.39806	0.001608	0.544364	0.0046		
NOX4	NADPH oxidase 4 (NOX4), mRNA.			3.173266	0.001663				
NQO1	NAD(P)H dehydrogenase, quinone 1 (NQO1), transcript variant 3, mRNA.	3.5957598	0.03125	1.797685	0.003694				
NQO2	NAD(P)H dehydrogenase, quinone 2 (NQO2), mRNA.	1.7779388	0.000132	1.725306	0.004885				
GSR	glutathione reductase (GSR), mRNA.	1.9572177	0.000962	2.518831	2.49E-05			1.779414	0.002565

References

1. Association AH. Heart Disease and Stroke Statistics-2009 Update. presented at the" AHA, Dallas, Year.

2. Kempczinski RF. In: Rutherford R, ed. Vascular Surgery. Denver: W.B. Saunders; 2000. pp. 527-32.

3. Roger VL, Go AS, Lloyd-Jones DM, Adams RJ, Berry JD, Brown TM, et al. Heart Disease and Stroke Statistics--2011 Update: A Report From the American Heart Association. Circulation.123:e18-209. 2011.

4. Davies MG, Hagen PO. Pathophysiology of vein graft failure: a review. Eur J Vasc Endovasc Surg.9:7-18. 1995.

5. Davids L, Dower T, Zilla P. The lack of healing in conventional vascular grafts. In: Zilla P, Greisler H, eds. Tissue Engineering of Prosthetic Vascular Grafts. Austin: RG Landes Company; 1999. pp. 3-44.

6. Stewart GJ, Essa N, Chang KH, Reichle FA. A scanning and transmission electron microscope study of the luminal coating on Dacron prostheses in the canine thoracic aorta. J Lab Clin Med.85:208-26. 1975.

7. Harrison JH. Synthetic materials as vascular prostheses. I. A comparative study in small vessels of nylon, dacron, orlon, ivalon sponge and teflon. Am J Surg.95:3-15. 1958.

8. Zilla P, Bezuidenhout D, Human P. Prosthetic vascular grafts: Wrong models, wrong questions and no healing. Biomaterials.28:5009-27. 2007.

9. Ombrellaro MP, Stevens SL, Kerstetter K, Freeman MB, Goldman MH. Healing characteristics of intraarterial stented grafts: effect of intraluminal position on prosthetic graft healing. Surgery.120:60-70. 1996.

10. Berger K, Sauvage LR, Rao AM, Wood SJ. Healing of arterial prostheses in man: its incompleteness. Ann Surg.175:118-27. 1972.

11. Clagett GP, Burkel WE, Sharefkin JB, Ford JW, Hufnagel H, Vinter DW, et al. Platelet reactivity in vivo in dogs with arterial prostheses seeded with endothelial cells. Circulation.69:632-9. 1984.

12. Kempczinski RF, Ramalanjaona GR, Douville C, Silberstein EB. Thrombogenicity of a fibronectin-coated, experimental polytetrafluoroethylene graft. Surgery.101:439-44. 1987.

13. Clowes AW, Gown AM, Hanson SR, Reidy MA. Mechanisms of arterial graft failure. 1. Role of cellular proliferation in early healing of PTFE prostheses. Am J Pathol.118:43-54. 1985.

14. Clowes AW, Kirkman TR, Clowes MM. Mechanisms of arterial graft failure. II. Chronic endothelial and smooth muscle cell proliferation in healing polytetrafluoroethylene prostheses. J Vasc Surg.3:877-84. 1986.

15. Lemson MS, Tordoir JH, Daemen MJ, Kitslaar PJ. Intimal hyperplasia in vascular grafts. Eur J Vasc Endovasc Surg.19:336-50. 2000.

16. Tai NR, Salacinski HJ, Edwards A, Hamilton G, Seifalian AM. Compliance properties of conduits used in vascular reconstruction. British Journal of Surgery.87:1516-24. 2000.

17. Cines DB, Pollak ES, Buck CA, Loscalzo J, Zimmerman GA, McEver RP, et al. Endothelial cells in physiology and in the pathophysiology of vascular disorders. Blood.91:3527-61. 1998.

18. Herring M, Gardner A, Glover J. A single-staged technique for seeding vascular grafts with autogenous endothelium. Surgery.84:498-504. 1978.

19. Zilla P, Deutsch M, Meinhart J, Puschmann R, Eberl T, Minar E, et al. Clinical in vitro endothelialization of femoropopliteal bypass grafts: an actuarial follow-up over three years. J Vasc Surg.19:540-8. 1994.

20. Herring M, Smith J, Dalsing M, Glover J, Compton R, Etchberger K, et al. Endothelial seeding of polytetrafluoroethylene femoral popliteal bypasses: the failure of low-density seeding to improve patency. J Vasc Surg.20:650-5. 1994.

21. Rosenman JE, Kempczinski RF, Pearce WH, Silberstein EB. Kinetics of endothelial cell seeding. J Vasc Surg.2:778-84. 1985.

22. Brown MA, Wallace CS, Anamelechi CC, Clermont E, Reichert WM, Truskey GA. The use of mild trypsinization conditions in the detachment of endothelial cells to promote subsequent endothelialization on synthetic surfaces. Biomaterials.28:3928-35. 2007.

23. Anamelechi CC, Truskey GA, Reichert WM. Mylar(TM) and Teflon-AF(TM) as cell culture substrates for studying endothelial cell adhesion. Biomaterials.26:6887-96. 2005.

24. Chan B, Liu W, Klitzman B, Reichert W, Truskey G. In vivo performance of dual ligand augmented endothelialized expanded polytetrafluoroethylene vascular grafts. Journal of Biomedical Materials Research.72B:52-63. 2005.

25. Kannan RY, Salacinski HJ, Butler PE, Hamilton G, Seifalian AM. Current status of prosthetic bypass grafts: a review. J Biomed Mater Res B Appl Biomater.74:570-81. 2005.

26. Zilla P, Fasol R, Preiss P, Kadletz M, Deutsch M, Schima H, et al. Use of fibrin glue as a substrate for in vitro endothelialization of PTFE vascular grafts. Surgery.105:515-22. 1989.

27. Laube H, Duwe J, Rutsch W, Konertz W. Clinical experience with autologous endothelial cell-seeded polytetrafluoroethylene coronary artery bypass grafts. Journal of Thoracic and Cardiovascular Surgery.120:134-41. 2000.

28. Leseche G, Bikfalvi A, Dupuy E, Tobelem G, Andreassian B, Caen J. Prelining of polytetrafluoroethylene grafts with cultured human endothelial cells isolated from varicose veins. Surgery.105:36-45. 1989.

29. Zilla P, Deutsch M, Meinhart J. Endothelial cell transplantation. Semin Vasc Surg.12:52-63. 1999.

30. Hehrlein FW, Schlepper M, Loskot F, Scheld HH, Walter P, Mulch J. The use of expanded polytetrafluoroethylene (PTFE) grafts for myocardial revascularization. J Cardiovasc Surg (Torino).25:549-53. 1984.

31. Faries PL, LoGerfo FW, Arora S, Hook S, Pulling MC, Akbari CM, et al. A comparative study of alternative conduits for lower extremity revascularization: All-autogenous conduit versus prosthetic grafts. Journal of Vascular Surgery.32:1080-90. 2000.

32. Gibson KD, Gillen DL, Caps MT, Kohler TR, Sherrard DJ, Stehman-Breen CO. Vascular access survival and incidence of revisions: A comparison of prosthetic grafts, simple autogenous fistulas, and venous transposition fistulas from the United States Renal Data System Dialysis Morbidity and Mortality Study. Journal of Vascular Surgery.34:694-700. 2001.

33. Stump MM, Jordan GL, Jr., Debakey ME, Halpert B. Endothelium Grown from Circulating Blood on Isolated Intravascular Dacron Hub. Am J Pathol.43:361-7. 1963.

34. Asahara T, Murohara T, Sullivan A, Silver M, van der Zee R, Li T, et al. Isolation of putative progenitor endothelial cells for angiogenesis. Science.275:964-7. 1997.

35. Avci-Adali M, Paul A, Ziemer G, Wendel HP. New strategies for in vivo tissue engineering by mimicry of homing factors for self-endothelialisation of blood contacting materials. Biomaterials.29:3936-45. 2008.

36. Blindt R, Vogt F, Astafieva I, Fach C, Hristov M, Krott N, et al. A novel drug-eluting stent coated with an integrin-binding cyclic Arg-Gly-Asp peptide inhibits

neointimal hyperplasia by recruiting endothelial progenitor cells. J Am Coll Cardiol.47:1786-95. 2006.

37. Rotmans JI, Heyligers JM, Verhagen HJ, Velema E, Nagtegaal MM, de Kleijn DP, et al. In vivo cell seeding with anti-CD34 antibodies successfully accelerates endothelialization but stimulates intimal hyperplasia in porcine arteriovenous expanded polytetrafluoroethylene grafts. Circulation.112:12-8. 2005.

38. Civin C, Handgretinger R, Urbano-Ispizua A. Use of purified stem and progenitor cells for transplantation. In: Atkinson K, Champlin R, Ritz J, Fibbe W, Ljungman P, Brenner M, eds. Clinical Bone Marrow and Blood Stem Cell Transplantation. Cambridge, UK: Cambridge University Press; 2004. pp. 426.

39. Hoffmann J, Paul A, Harwardt M, Groll J, Reeswinkel T, Klee D, et al. Immobilized DNA aptamers used as potent attractors for porcine endothelial precursor cells. Journal of Biomedical Materials Research Part A.84A:614-21. 2008.

40. Shi Q, Bhattacharya V, Hong-De Wu M, Sauvage LR. Utilizing granulocyte colony-stimulating factor to enhance vascular graft endothelialization from circulating blood cells. Ann Vasc Surg.16:314-20. 2002.

41. Cho SW, Lim JE, Chu HS, Hyun HJ, Choi CY, Hwang KC, et al. Enhancement of in vivo endothelialization of tissue-engineered vascular grafts by granulocyte colony-stimulating factor. J Biomed Mater Res A.76:252-63. 2006.

42. Gott VL, Whiffen JD, Dutton RC. Heparin Bonding on Colloidal Graphite Surfaces. Science.142:1297-8. 1963.

43. Devine C, McCollum C. Heparin-bonded Dacron or polytetrafluorethylene for femoropopliteal bypass: five-year results of a prospective randomized multicenter clinical trial. J Vasc Surg.40:924-31. 2004.

44. Lin PH, Chen C, Bush RL, Yao Q, Lumsden AB, Hanson SR. Small-caliber heparin-coated ePTFE grafts reduce platelet deposition and neointimal hyperplasia in a baboon model. J Vasc Surg.39:1322-8. 2004.

45. Peeters P, Verbist J, Deloose K, Bosiers M. Results with heparin bonded polytetrafluoroethylene grafts for femorodistal bypasses. J Cardiovasc Surg (Torino).47:407-13. 2006.

46. Bosiers M, Deloose K, Verbist J, Schroe H, Lauwers G, Lansink W, et al. Heparin-bonded expanded polytetrafluoroethylene vascular graft for femoropopliteal and femorocrural bypass grafting: 1-year results. J Vasc Surg.43:313-8; discussion 8-9. 2006.

47. Wyers MC, Phaneuf MD, Rzucidlo EM, Contreras MA, LoGerfo FW, Quist WC. In Vivo Assessment of a Novel Dacron Surface with Covalently Bound Recombinant Hirudin. Cardiovascular Pathology.8:153-9. 1999.

48. Heise M, Schmidmaier G, Husmann I, Heidenhain C, Schmidt J, Neuhaus P, et al. PEG-hirudin/iloprost Coating of Small Diameter ePTFE Grafts Effectively Prevents Pseudointima and Intimal Hyperplasia Development. European Journal of Vascular and Endovascular Surgery.32:418-24. 2006.

49. Sperling C, Salchert K, Streller U, Werner C. Covalently immobilized thrombomodulin inhibits coagulation and complement activation of artificial surfaces in vitro. Biomaterials.25:5101-13. 2004.

50. Fleser PS, Nuthakki VK, Malinzak LE, Callahan RE, Seymour ML, Reynolds MM, et al. Nitric oxide-releasing biopolymers inhibit thrombus formation in a sheep model of arteriovenous bridge grafts. J Vasc Surg.40:803-11. 2004.

51. Yoon JH, Wu CJ, Homme J, Tuch RJ, Wolff RG, Topol EJ, et al. Local Delivery of Nitric Oxide from an Eluting Stent to Inhibit Neointimal Thickening in a Porcine Coronary Injury Model. Yonsei Med J.43:242-51. 2002.

52. Buergler JM, Tio FO, Schulz DG, Khan MM, Mazur W, French BA, et al. Use of nitric-oxide-eluting polymer-coated coronary stents for prevention of restenosis in pigs. Coronary Artery Disease.11:351-7. 2000.

53. Oh BK, Meyerhoff ME. Spontaneous Catalytic Generation of Nitric Oxide from S-Nitrosothiols at the Surface of Polymer Films Doped with Lipophilic Copper(II) Complex. Journal of the American Chemical Society.125:9552-3. 2003.

54. Crombez M, Chevallier P, Gaudreault RC, Petitclerc E, Mantovani D, Laroche G. Improving arterial prosthesis neo-endothelialization: Application of a proactive VEGF construct onto PTFE surfaces. Biomaterials.26:7402-9. 2005.

55. Masuda S, Doi K, Satoh S, Oka T, Matsuda T. Vascular endothelial growth factor enhances vascularization in microporous small caliber polyurethane grafts. ASAIO J.43:M530-4. 1997.

56. Randone B, Cavallaro G, Polistena A, Cucina A, Coluccia P, Graziano P, et al. Dual Role of VEGF in Pretreated Experimental ePTFE Arterial Grafts. Journal of Surgical Research.127:70-9. 2005.

57. Lahtinen M, Blomberg P, Baliulis G, Carlsson F, Khamis H, Zemgulis V. In vivo h-VEGF165 gene transfer improves early endothelialisation and patency in synthetic vascular grafts. Eur J Cardiothorac Surg.31:383-90. 2007.

58. Seifalian AM, Giudiceandrea A, Schmitz-Rixen T, Hamilton G. Noncompliance: The Silent Acceptance of a Villain. In: Zilla P, Greisler H, eds. Tissue Engineering of Prosthetic Vascular Grafts. Georgetown, TX: R.G. Landes Co; 1999. pp. 45-58.

59. Greenwald SE, Berry CL. Improving vascular grafts: the importance of mechanical and haemodynamic properties. J Pathol.190:292-9. 2000.

60. Ballyk PD, Walsh C, Butany J, Ojha M. Compliance mismatch may promote graft-artery intimal hyperplasia by altering suture-line stresses. J Biomech.31:229-37. 1998.

61. van der Lei B, Wildevuur CR, Dijk F, Blaauw EH, Molenaar I, Nieuwenhuis P. Sequential studies of arterial wall regeneration in microporous, compliant, biodegradable small-caliber vascular grafts in rats. J Thorac Cardiovasc Surg.93:695-707. 1987.

62. Jeschke MG, Hermanutz V, Wolf SE, Koveker GB. Polyurethane vascular prostheses decreases neointimal formation compared with expanded polytetrafluoroethylene. J Vasc Surg.29:168-76. 1999.

63. Zhang Z, Marois Y, Guidoin RG, Bull P, Marois M, How T, et al. Vascugraft polyurethane arterial prosthesis as femoro-popliteal and femoro-peroneal bypasses in humans: pathological, structural and chemical analyses of four excised grafts. Biomaterials.18:113-24. 1997.

64. Hong Y, Ye S-H, Nieponice A, Soletti L, Vorp DA, Wagner WR. A small diameter, fibrous vascular conduit generated from a poly(ester urethane)urea and phospholipid polymer blend. Biomaterials.30:2457-67. 2009.

65. Nemcova S, Noel AA, Jost CJ, Gloviczki P, Miller VM, Brockbank KG. Evaluation of a xenogeneic acellular collagen matrix as a small-diameter vascular graft in dogs--preliminary observations. J Invest Surg.14:321-30. 2001.

66. Roeder RA, Lantz GC, Geddes LA. Mechanical remodeling of small-intestine submucosa small-diameter vascular grafts--a preliminary report. Biomed Instrum Technol.35:110-20. 2001.

67. Conklin BS, Richter ER, Kreutziger KL, Zhong DS, Chen C. Development and evaluation of a novel decellularized vascular xenograft. Med Eng Phys.24:173-83. 2002.

68. Schaner PJ, Martin ND, Tulenko TN, Shapiro IM, Tarola NA, Leichter RF, et al. Decellularized vein as a potential scaffold for vascular tissue engineering. J Vasc Surg.40:146-53. 2004.

69. Gui L, Muto A, Chan SA, Breuer CK, Niklason LE. Development of Decellularized Human Umbilical Arteries as Small-Diameter Vascular Grafts. Tissue Engineering Part A.0.

70. Schmidt CE, Baier JM. Acellular vascular tissues: natural biomaterials for tissue repair and tissue engineering. Biomaterials.21:2215-31. 2000.

71. Kakisis JD, Liapis CD, Breuer C, Sumpio BE. Artificial blood vessel: the Holy Grail of peripheral vascular surgery. J Vasc Surg.41:349-54. 2005.

72. Isenberg BC, Williams C, Tranquillo RT. Small-diameter artificial arteries engineered in vitro. Circ Res.98:25-35. 2006.

73. L'Heureux N, Dusserre N, Marini A, Garrido S, de la Fuente L, McAllister T. Technology Insight: the evolution of tissue-engineered vascular grafts[mdash]from research to clinical practice. Nat Clin Pract Cardiovasc Med.4:389-95. 2007.

74. Dahl SLM, Kypson AP, Lawson JH, Blum JL, Strader JT, Li Y, et al. Readily Available Tissue-Engineered Vascular Grafts. Science Translational Medicine.3:68ra9. 2011.

75. Shin'oka T, Matsumura G, Hibino N, Naito Y, Watanabe M, Konuma T, et al. Midterm clinical result of tissue-engineered vascular autografts seeded with autologous bone marrow cells. J Thorac Cardiovasc Surg.129:1330-8. 2005.

76. McAllister TN, Maruszewski M, Garrido SA, Wystrychowski W, Dusserre N, Marini A, et al. Effectiveness of haemodialysis access with an autologous tissue-engineered vascular graft: a multicentre cohort study. Lancet.373:1440-6. 2009.

77. Konig G, McAllister TN, Dusserre N, Garrido SA, Iyican C, Marini A, et al. Mechanical properties of completely autologous human tissue engineered blood vessels compared to human saphenous vein and mammary artery. Biomaterials.30:1542-50. 2009.

78. Tiwari A, Salacinski HJ, Hamilton G, Seifalian AM. Tissue engineering of vascular bypass grafts: role of endothelial cell extraction. Eur J Vasc Endovasc Surg.21:193-201. 2001.

79. Jarrell BE, Williams SK, Stokes G, Hubbard FA, Carabasi RA, Koolpe E, et al. Use of freshly isolated capillary endothelial cells for the immediate establishment of a monolayer on a vascular graft at surgery. Surgery.100:392-9. 1986.

80. Arts CH, Hedeman Joosten PP, Blankensteijn JD, Staal FJ, Ng PY, Heijnen-Snyder GJ, et al. Contaminants from the transplant contribute to intimal hyperplasia associated with microvascular endothelial cell seeding. Eur J Vasc Endovasc Surg.23:29-38. 2002.

81. Lin Y, Weisdorf DJ, Solovey A, Hebbel RP. Origins of circulating endothelial cells and endothelial outgrowth from blood. J Clin Invest.105:71-7. 2000.

82. Gulati R, Jevremovic D, Peterson TE, Chatterjee S, Shah V, Vile RG, et al. Diverse origin and function of cells with endothelial phenotype obtained from adult human blood. Circ Res.93:1023-5. 2003.

83. Hur J, Yoon CH, Kim HS, Choi JH, Kang HJ, Hwang KK, et al. Characterization of two types of endothelial progenitor cells and their different contributions to neovasculogenesis. Arterioscler Thromb Vasc Biol.24:288-93. 2004.

84. Ingram DA, Mead LE, Tanaka H, Meade V, Fenoglio A, Mortell K, et al. Identification of a novel hierarchy of endothelial progenitor cells using human peripheral and umbilical cord blood. Blood.104:2752-60. 2004.

85. Shi Q, Rafii S, Wu MH-D, Wijelath ES, Yu C, Ishida A, et al. Evidence for Circulating Bone Marrow-Derived Endothelial Cells. Blood.92:362-7. 1998.

86. Sieveking DP, Buckle A, Celermajer DS, Ng MKC. Strikingly Different Angiogenic Properties of Endothelial Progenitor Cell Subpopulations: Insights From a Novel Human Angiogenesis Assay. Journal of the American College of Cardiology.51:660-8. 2008.

87. Urbich C, Aicher A, Heeschen C, Dernbach E, Hofmann WK, Zeiher AM, et al. Soluble factors released by endothelial progenitor cells promote migration of endothelial cells and cardiac resident progenitor cells. Journal of Molecular and Cellular Cardiology.39:733-42. 2005.

88. Rehman J, Li J, Orschell CM, March KL. Peripheral blood "endothelial progenitor cells" are derived from monocyte/macrophages and secrete angiogenic growth factors. Circulation.107:1164-9. 2003.

89. Yoder MC, Mead LE, Prater D, Krier TR, Mroueh KN, Li F, et al. Redefining endothelial progenitor cells via clonal analysis and hematopoietic stem/progenitor cell principals. Blood.109:1801-9. 2007.

90. Timmermans F, Van Hauwermeiren F, De Smedt M, Raedt R, Plasschaert F, De Buyzere ML, et al. Endothelial outgrowth cells are not derived from CD133+ cells or CD45+ hematopoietic precursors. Arterioscler Thromb Vasc Biol.27:1572-9. 2007.

91. Gulati R, Jevremovic D, Witt TA, Kleppe LS, Vile RG, Lerman A, et al. Modulation of the vascular response to injury by autologous blood-derived outgrowth endothelial cells. Am J Physiol Heart Circ Physiol.287:H512-7. 2004.

92. Timmermans F, Plum J, Yoder M, Ingram D, Vandekerckhove B, Case J. Endothelial progenitor cells: identity defined? Journal of Cellular and Molecular Medicine.13:87-102. 2009.

93. Ingram DA, Mead LE, Moore DB, Woodard W, Fenoglio A, Yoder MC. Vessel wall-derived endothelial cells rapidly proliferate because they contain a complete hierarchy of endothelial progenitor cells. Blood.105:2783-6. 2005.

94. Fuchs S, Hermanns MI, Kirkpatrick CJ. Retention of a differentiated endothelial phenotype by outgrowth endothelial cells isolated from human peripheral blood and expanded in long-term cultures. Cell Tissue Res.326:79-92. 2006.

95. Allen J, Khan S, Serrano M, Ameer G. Characterization of porcine circulating progenitor cells: toward a functional endothelium. Tissue Eng Part A.14:183-94. 2008.

96. Griese DP, Ehsan A, Melo LG, Kong D, Zhang L, Mann MJ, et al. Isolation and Transplantation of Autologous Circulating Endothelial Cells Into Denuded Vessels and Prosthetic Grafts: Implications for Cell-Based Vascular Therapy. Circulation.108:2710-5. 2003.

97. Kaushal S, Amiel GE, Guleserian KJ, Shapira OM, Perry T, Sutherland FW, et al. Functional small-diameter neovessels created using endothelial progenitor cells expanded ex vivo. Nat Med.7:1035-40. 2001.

98. Shirota T, He H, Yasui H, Matsuda T. Human Endothelial Progenitor Cell-Seeded Hybrid Graft: Proliferative and Antithrombogenic Potentials in Vitro and Fabrication Processing. Tissue Engineering.9:127-36. 2003.

99. Shirota T, Yasui H, Matsuda T. Intralumenal Tissue-Engineered Therapeutic Stent Using Endothelial Progenitor Cell-Inoculated Hybrid Tissue and in Vitro Performance. Tissue Engineering.9:473-85. 2003.

100. Guven H, Shepherd RM, Bach RG, Capoccia BJ, Link DC. The Number of Endothelial Progenitor Cell Colonies in the Blood Is Increased in Patients With Angiographically Significant Coronary Artery Disease. Journal of the American College of Cardiology.48:1579-87. 2006.

101. Thill M, Strunnikova NV, Berna MJ, Gordiyenko N, Schmid K, Cousins SW, et al. Late Outgrowth Endothelial Progenitor Cells in Patients with Age-Related Macular Degeneration. Invest Ophthalmol Vis Sci.49:2696-708. 2008.

102. Chandiwal A, Balasubramanian V, Baldwin ZK, Conte MS, Schwartz LB. Gene therapy for the extension of vein graft patency: a review. Vasc Endovascular Surg.39:1-14. 2005.

103. Conte MS. Molecular engineering of vein bypass grafts. J Vasc Surg.45 Suppl A:A74-81. 2007.

104. Wilson JM, Birinyi LK, Salomon RN, Libby P, Callow AD, Mulligan RC. Implantation of vascular grafts lined with genetically modified endothelial cells. Science.244:1344-6. 1989.

105. Jankowski RJ, Severyn DA, Vorp DA, Wagner WR. Effect of retroviral transduction on human endothelial cell phenotype and adhesion to Dacron vascular grafts. J Vasc Surg.26:676-84. 1997.

106. Baer RP, Whitehill TE, Sarkar R, Sarkar M, Messina LM, Komorowski TA, et al. Retroviral-mediated transduction of endothelial cells with the lac Z gene impairs cellular proliferation in vitro and graft endothelialization in vivo. J Vasc Surg.24:892-9. 1996.

107. Dunn PF, Newman KD, Jones M, Yamada I, Shayani V, Virmani R, et al. Seeding of vascular grafts with genetically modified endothelial cells. Secretion of recombinant TPA results in decreased seeded cell retention in vitro and in vivo. Circulation.93:1439-46. 1996.

108. Dichek DA, Anderson J, Kelly AB, Hanson SR, Harker LA. Enhanced in vivo antithrombotic effects of endothelial cells expressing recombinant plasminogen activators transduced with retroviral vectors. Circulation.93:301-9. 1996.

109. Scott-Burden T, Tock CL, Bosely JP, Clubb FJ, Jr., Parnis SM, Schwarz JJ, et al. Nonthrombogenic, adhesive cellular lining for left ventricular assist devices. Circulation.98:II339-45. 1998.

110. Griese DP, Achatz S, Batzlsperger CA, Strauch UG, Grumbeck B, Weil J, et al. Vascular gene delivery of anticoagulants by transplantation of retrovirally-transduced endothelial progenitor cells. Cardiovasc Res.58:469-77. 2003.

111. Choi J-H, Hur J, Yoon C-H, Kim J-H, Lee C-S, Youn S-W, et al. Augmentation of Therapeutic Angiogenesis Using Genetically Modified Human Endothelial Progenitor Cells with Altered Glycogen Synthase Kinase-3{beta} Activity. J Biol Chem.279:49430-8. 2004.

112. Nagaya N, Kangawa K, Kanda M, Uematsu M, Horio T, Fukuyama N, et al. Hybrid Cell-Gene Therapy for Pulmonary Hypertension Based on Phagocytosing Action of Endothelial Progenitor Cells. Circulation.108:889-95. 2003.

113. Kong D, Melo LG, Mangi AA, Zhang L, Lopez-Ilasaca M, Perrella MA, et al. Enhanced Inhibition of Neointimal Hyperplasia by Genetically Engineered Endothelial Progenitor Cells. Circulation.109:1769-75. 2004.

114. Herder C, Tonn T, Oostendorp R, Becker S, Keller U, Peschel C, et al. Sustained Expansion and Transgene Expression of Coagulation Factor VIII-Transduced Cord Blood-Derived Endothelial Progenitor Cells. Arterioscler Thromb Vasc Biol.23:2266-72. 2003.

115. Newman KD, Dunn PF, Owens JW, Schulick AH, Virmani R, Sukhova G, et al. Adenovirus-mediated gene transfer into normal rabbit arteries results in prolonged vascular cell activation, inflammation, and neointimal hyperplasia. J Clin Invest.96:2955-65. 1995.

116. Wu K, Thiagarajan P. Role of endothelium in thrombosis and hemostasis. Annual Review of Medicine.47:315-31. 1996.

117. Lin M-C, Almus-Jacobs F, Chen H-H, Parry GCN, Mackman N, Shyy JYJ, et al. Shear Stress Induction of the Tissue Factor Gene. J Clin Invest.99:737-44. 1997.

118. Allen S, Khan S, Al-Mohanna F, Batten P, Yacoub M. Native Low Density Lipoprotein-induced Calcium Transients Trigger VCAM-1 and E-selectin Expression in Cultured Human Vascular Endothelial Cells. J Clin Invest.101:1064-75. 1998.

119. Dimmeler S, Leri A. Aging and Disease as Modifiers of Efficacy of Cell Therapy. Circ Res.102:1319-30. 2008.

120. Conboy IM, Conboy MJ, Wagers AJ, Girma ER, Weissman IL, Rando TA. Rejuvenation of aged progenitor cells by exposure to a young systemic environment. Nature.433:760-4. 2005.

121. Zhang Y, Herbert B-S, Rajashekhar G, Ingram DA, Yoder MC, Clauss M, et al. Premature senescence of highly proliferative endothelial progenitor cells is induced by tumor necrosis factor-{alpha} via the p38 mitogen-activated protein kinase pathway. FASEB J.fj.08-110296. 2009.

122. Esmon CT. The roles of protein C and thrombomodulin in the regulation of blood coagulation. J Biol Chem.264:4743-6. 1989.

123. Esmon CT. The Protein C Pathway. Chest.124:26S-32. 2003.

124. Coughlin S. Thrombin signalling and protease-activated receptors. Nature.407:258. 2000.

125. Murakami K, Okajima K, Uchiba M, Johno M, Nakagaki T, Okabe H, et al. Activated protein C attenuates endotoxin-induced pulmonary vascular injury by inhibiting activated leukocytes in rats. Blood.87:642-7. 1996.

126. Hirose K, Okajima K, Taoka Y, Uchiba M, Tagami H, Nakano K, et al. Activated protein C reduces the ischemia/reperfusion-induced spinal cord injury in rats by inhibiting neutrophil activation. Ann Surg.232:272-80. 2000.

127. Grey ST, Tsuchida A, Hau H, Orthner CL, Salem HH, Hancock WW. Selective inhibitory effects of the anticoagulant activated protein C on the responses of human mononuclear phagocytes to LPS, IFN-gamma, or phorbol ester. J Immunol.153:3664-72. 1994.

128. Grinnell BW, Hermann RB, Yan SB. Human Protein C inhibits selectin-mediated cell adhesion: role of unique fucosylated oligosaccharide. Glycobiology.4:221-5. 1994.

129. Mosnier LO, Griffin JH. Inhibition of staurosporine-induced apoptosis of endothelial cells by activated protein C requires protease-activated receptor-1 and endothelial cell protein C receptor. Biochem J.373:65-70. 2003.

130. Conway EM, Van de Wouwer M, Pollefeyt S, Jurk K, Van Aken H, De Vriese A, et al. The Lectin-like Domain of Thrombomodulin Confers Protection from Neutrophil-mediated Tissue Damage by Suppressing Adhesion Molecule Expression via Nuclear Factor {kappa}B and Mitogen-activated Protein Kinase Pathways. J Exp Med.196:565-77. 2002.

131. Conway EM, Rosenberg RD. Tumor necrosis factor suppresses transcription of the thrombomodulin gene in endothelial cells. Mol Cell Biol.8:5588-92. 1988.

132. Moore KL, Esmon CT, Esmon NL. Tumor necrosis factor leads to the internalization and degradation of thrombomodulin from the surface of bovine aortic endothelial cells in culture. Blood.73:159-65. 1989.

133. Sperry JL, Deming CB, Bian C, Walinsky PL, Kass DA, Kolodgie FD, et al. Wall tension is a potent negative regulator of in vivo thrombomodulin expression. Circ Res.92:41-7. 2003.

134. Kim AY, Walinsky PL, Kolodgie FD, Bian C, Sperry JL, Deming CB, et al. Early loss of thrombomodulin expression impairs vein graft thromboresistance: implications for vein graft failure. Circ Res.90:205-12. 2002.

135. Waugh JM, Li-Hawkins J, Yuksel E, Kuo MD, Cifra PN, Hilfiker PR, et al. Thrombomodulin overexpression to limit neointima formation. Circulation.102:332-7. 2000.

136. Waugh JM, Yuksel E, Li J, Kuo MD, Kattash M, Saxena R, et al. Local overexpression of thrombomodulin for in vivo prevention of arterial thrombosis in a rabbit model. Circ Res.84:84-92. 1999.

137. Wong G, Li J-m, Hendricks G, Eslami MH, Rohrer MJ, Cutler BS. Inhibition of experimental neointimal hyperplasia by recombinant human thrombomodulin coated ePTFE stent grafts. Journal of Vascular Surgery.47:608-15. 2008.

138. Li JM, Singh MJ, Itani M, Vasiliu C, Hendricks G, Baker SP, et al. Recombinant human thrombomodulin inhibits arterial neointimal hyperplasia after balloon injury. J Vasc Surg.39:1074-83. 2004.

139. Tabuchi N, Shichiri M, Shibamiya A, Koyama T, Nakazawa F, Chung J, et al. Non-viral in vivo thrombomodulin gene transfer prevents early loss of thromboresistance of grafted veins. Eur J Cardiothorac Surg.26:995-1001. 2004.

140. Scheubel RJ, Zorn H, Silber RE, Kuss O, Morawietz H, Holtz J, et al. Age-dependent depression in circulating endothelial progenitor cells in patients undergoing coronary artery bypass grafting. J Am Coll Cardiol.42:2073-80. 2003.

141. Schmidt-Lucke C, Rossig L, Fichtlscherer S, Vasa M, Britten M, Kamper U, et al. Reduced Number of Circulating Endothelial Progenitor Cells Predicts Future

Cardiovascular Events: Proof of Concept for the Clinical Importance of Endogenous Vascular Repair. Circulation.111:2981-7. 2005.

142. Werner N, Kosiol S, Schiegl T, Ahlers P, Walenta K, Link A, et al. Circulating Endothelial Progenitor Cells and Cardiovascular Outcomes. N Engl J Med.353:999-1007. 2005.

143. Massa M, Rosti V, Ferrario M, Campanelli R, Ramajoli I, Rosso R, et al. Increased circulating hematopoietic and endothelial progenitor cells in the early phase of acute myocardial infarction. Blood.105:199-206. 2005.

144. Lambiase PD, Edwards RJ, Anthopoulos P, Rahman S, Meng YG, Bucknall CA, et al. Circulating Humoral Factors and Endothelial Progenitor Cells in Patients With Differing Coronary Collateral Support. Circulation.109:2986-92. 2004.

145. Hirschi KK, Ingram DA, Yoder MC. Assessing Identity, Phenotype, and Fate of Endothelial Progenitor Cells. Arterioscler Thromb Vasc Biol.28
1584-95. 2008.

146. Broxmeyer HE, Srour E, Orschell C, Ingram DA, Cooper S, Plett PA, et al. Cord Blood Stem and Progenitor Cells. Methods in Enzymology: Academic Press; 2006. pp. 439-73.

147. Truskey GA, Proulx TL. Relationship between 3T3 cell spreading and the strength of adhesion on glass and silane surfaces. Biomaterials.14:243-54. 1993.

148. Lusska A, Wu L, Whitlock JP, Jr. Superinduction of CYP1A1 transcription by cycloheximide. Role of the DNA binding site for the liganded Ah receptor. J Biol Chem.267:15146-51. 1992.

149. Rozen S, Skaletsky H. Primer3 on the WWW for general users and for biologist programmers. In: Krawetz S, Misener S, eds. Bioinformatics Methods and Protocols: Methods in Molecular Biology. Totowa, NJ: Humana Press; 2000. pp. 365-86.

150. van der Loo B, Fenton MJ, Erusalimsky JD. Cytochemical Detection of a Senescence-Associated [beta]-Galactosidase in Endothelial and Smooth Muscle Cells from Human and Rabbit Blood Vessels. Experimental Cell Research.241:309-15. 1998.

151. Magometschnigg H, Kadletz M, Vodrazka M, Grabenwöger M, Moritz A, Grimm M, et al. Changes following in vitro endothelial cell lining of ePTFE prostheses: Late morphologic evaluation of six failed grafts. European Journal of Vascular Surgery.8:502-7. 1994.

152. Melero-Martin JM, Khan ZA, Picard A, Wu X, Paruchuri S, Bischoff J. In vivo vasculogenic potential of human blood-derived endothelial progenitor cells. Blood.109:4761-8. 2007.

153. Walter DH, Rittig K, Bahlmann FH, Kirchmair R, Silver M, Murayama T, et al. Statin Therapy Accelerates Reendothelialization: A Novel Effect Involving Mobilization and Incorporation of Bone Marrow-Derived Endothelial Progenitor Cells. Circulation.105:3017-24. 2002.

154. Brooks PC, Clark RA, Cheresh DA. Requirement of vascular integrin alpha v beta 3 for angiogenesis. Science.264:569-71. 1994.

155. Ingram DA, Krier TR, Mead LE, McGuire C, Prater DN, Bhavsar J, et al. Clonogenic Endothelial Progenitor Cells Are Sensitive to Oxidative Stress. Stem Cells.25:297-304. 2007.

156. Sieveking DP, Buckle A, Celermajer DS, Ng MK. Strikingly different angiogenic properties of endothelial progenitor cell subpopulations: insights from a novel human angiogenesis assay. J Am Coll Cardiol.51:660-8. 2008.

157. Naseem KM. The role of nitric oxide in cardiovascular diseases. Molecular Aspects of Medicine.26:33-65. 2005.

158. Dekker RJ, Boon RA, Rondaij MG, Kragt A, Volger OL, Elderkamp YW, et al. KLF2 provokes a gene expression pattern that establishes functional quiescent differentiation of the endothelium. Blood.107:4354-63. 2006.

159. Lin Z, Kumar A, SenBanerjee S, Staniszewski K, Parmar K, Vaughan DE, et al. Kruppel-Like Factor 2 (KLF2) Regulates Endothelial Thrombotic Function. Circ Res.96:e48-57. 2005.

160. Case J, Mead LE, Bessler WK, Prater D, White HA, Saadatzadeh MR, et al. Human CD34+AC133+VEGFR-2+ cells are not endothelial progenitor cells but distinct, primitive hematopoietic progenitors. Experimental Hematology.35:1109-18. 2007.

161. Veleva A, Cooper S, Patterson C. Selection and initial characterization of novel peptide ligands that bind specifically to human blood outgrowth endothelial cells. Biotechnology and Bioengineering.98:306-12. 2007.

162. Massa M, Campanelli R, Bonetti E, Ferrario M, Marinoni B, Rosti V. Rapid and large increase of the frequency of circulating endothelial colony-forming cells (ECFCs) generating late outgrowth endothelial cells in patients with acute myocardial infarction. Exp Hematol.37:8-9. 2009.

163. Huang L, Hou D, Thompson MA, Baysden SE, Shelley WC, Ingram DA, et al. Acute myocardial infarction in swine rapidly and selectively releases highly proliferative endothelial colony forming cells (ECFCs) into circulation. Cell Transplant.16:887-97. 2007.

164. Deschaseaux F, Selmani Z, Falcoz P-E, Mersin N, Meneveau N, Penfornis A, et al. Two types of circulating endothelial progenitor cells in patients receiving long term therapy by HMG-CoA reductase inhibitors. European Journal of Pharmacology.562:111-8. 2007.

165. Xing Z, Ryan MA, Daria D, Nattamai KJ, Van Zant G, Wang L, et al. Increased hematopoietic stem cell mobilization in aged mice. Blood.108:2190-7. 2006.

166. Aranguren XL, Verfaillie CM, Luttun A. Emerging hurdles in stem cell therapy for peripheral vascular disease. J Mol Med.87:3-16. 2009.

167. Reyes M, Dudek A, Jahagirdar B, Koodie L, Marker PH, Verfaillie CM. Origin of endothelial progenitors in human postnatal bone marrow. J Clin Invest.109:337-46. 2002.

168. Ross JJ, Hong Z, Willenbring B, Zeng L, Isenberg B, Lee EH, et al. Cytokine-induced differentiation of multipotent adult progenitor cells into functional smooth muscle cells. J Clin Invest.116:3139-49. 2006.

169. Amatschek S, Kriehuber E, Bauer W, Reininger B, Meraner P, Wolpl A, et al. Blood and lymphatic endothelial cell-specific differentiation programs are stringently controlled by the tissue environment. Blood.109:4777-85. 2007.

170. Meinhart JG, Deutsch M, Fischlein T, Howanietz N, Fröschl A, Zilla P. Clinical autologous in vitro endothelialization of 153 infrainguinal ePTFE grafts. The Annals of Thoracic Surgery.71:S327-S31. 2001.

171. Schmidt D, Mol A, Breymann C, Achermann J, Odermatt B, Gossi M, et al. Living Autologous Heart Valves Engineered From Human Prenatally Harvested Progenitors. Circulation.114:I-125-31. 2006.

172. McGuigan AP, Sefton MV. The influence of biomaterials on endothelial cell thrombogenicity. Biomaterials.28:2547-71. 2007.

173. Stroncek JD, Grant BS, Brown MA, Povsic TJ, Truskey GA, Reichert WM. Comparison of endothelial cell phenotypic markers of late-outgrowth endothelial progenitor cells isolated from patients with coronary artery disease and healthy volunteers. Tissue Eng Part A.15:3473-86. 2009.

174. Abou-Saleh H, Yacoub D, Theoret J-F, Gillis M-A, Neagoe P-E, Labarthe B, et al. Endothelial Progenitor Cells Bind and Inhibit Platelet Function and Thrombus Formation. Circulation.120:2230-9. 2009.

175. Allen JB, Khan S, Lapidos KA, Ameer GA. Toward Engineering a Human Neoendothelium with Circulating Progenitor Cells. STEM CELLS.28:318-28. 2010.

176. He H, Shirota T, Yasui H, Matsuda T. Canine endothelial progenitor cell-lined hybrid vascular graft with nonthrombogenic potential. J Thorac Cardiovasc Surg.126:455-64. 2003.

177. Fujiwara Y, Tagami S, Kawakami Y. Circulating thrombomodulin and hematological alterations in type 2 diabetic patients with retinopathy. J Atheroscler Thromb.5:21-8. 1998.

178. Laszik ZG, Zhou XJ, Ferrell GL, Silva FG, Esmon CT. Down-Regulation of Endothelial Expression of Endothelial Cell Protein C Receptor and Thrombomodulin in Coronary Atherosclerosis. Am J Pathol.159:797-802. 2001.

179. Wagner DD, Burger PC. Platelets in Inflammation and Thrombosis. Arterioscler Thromb Vasc Biol.23:2131-7. 2003.

180. Gawaz M, Langer H, May AE. Platelets in inflammation and atherogenesis. J Clin Invest.115:3378-84. 2005.

181. Broxmeyer HE, Srour E, Orschell C, Ingram DA, Cooper S, Plett PA, et al. Cord blood stem and progenitor cells. Methods Enzymol.419:439-73. 2006.

182. Cheng C, Helderman F, Tempel D, Segers D, Hierck B, Poelmann R, et al. Large variations in absolute wall shear stress levels within one species and between species. Atherosclerosis.195:225-35. 2007.

183. Cohn L, Edmunds L. Cardiac surgery in the adult: McGraw-Hill; 2003.

184. Yang JJ, Chen YM, Kurokawa T, Gong JP, Onodera S, Yasuda K. Gene expression, glycocalyx assay, and surface properties of human endothelial cells cultured on hydrogel matrix with sulfonic moiety: Effect of elasticity of hydrogel. Journal of Biomedical Materials Research Part A.95A:531-42.

185. Kishida A, Ueno Y, Fukudome N, Yashima E, Maruyama I, Akashi M. Immobilization of human thrombomodulin onto poly(ether urethane urea) for developing antithrombogenic blood-contacting materials. Biomaterials.15:848-52. 1994.

186. Grunkemeier JM, Tsai WB, Horbett TA. Hemocompatibility of treated polystyrene substrates: Contact activation, platelet adhesion, and procoagulant activity of adherent platelets. Journal of Biomedical Materials Research.41:657-70. 1998.

187. McGuigan AP, Sefton MV. The thrombogenicity of human umbilical vein endothelial cell seeded collagen modules. Biomaterials.29:2453-63. 2008.

188. Streller U, Sperling C, Hübner J, Hanke R, Werner C. Design and evaluation of novel blood incubation systems for in vitro hemocompatibility assessment of planar solid surfaces. Journal of Biomedical Materials Research Part B: Applied Biomaterials.66B:379-90. 2003.

189. Liao D, Wang X, Lin PH, Yao Q, Chen CJ. Covalent linkage of heparin provides a stable anti-coagulation surface of decellularized porcine arteries. J Cell Mol Med.13:2736-43. 2009.

190. Amiji M, Park K. Surface modification of polymeric biomaterials with poly(ethylene oxide), albumin, and heparin for reduced thrombogenicity. Journal of Biomaterials Science, Polymer Edition.4:217-34. 1993.

191. Tsai C-C, Chang Y, Sung H-W, Hsu J-C, Chen C-N. Effects of heparin immobilization on the surface characteristics of a biological tissue fixed with a naturally occurring crosslinking agent (genipin): an in vitro study. Biomaterials.22:523-33. 2001.

192. Lin J-C, Tseng S-M. Surface characterization and platelet adhesion studies on polyethylene surface with hirudin immobilization. Journal of Materials Science: Materials in Medicine.12:827-32. 2001.

193. Seifert B, Romaniuk P, Groth T. Covalent immobilization of hirudin improves the haemocompatibility of polylactide-polyglycolide in vitro. Biomaterials.18:1495-502. 1997.

194. Oltrona L, Eisenberg PR, Abendschein DR, Rubin BG. Efficacy of local inhibition of procoagulant activity associated with small-diameter prosthetic vascular grafts. J Vasc Surg.24:624-31. 1996.

195. Lahann J, Plüster W, Klee D, Gattner H-G, Höcker H. Immobilization of the thrombin inhibitor r-hirudin conserving its biological activity. Journal of Materials Science: Materials in Medicine.12:807-10. 2001.

196. Kang IK, Kwon OH, Kim MK, Lee YM, Sung YK. In vitro blood compatibility of functional group-grafted and heparin-immobilized polyurethanes prepared by plasma glow discharge. Biomaterials.18:1099-107. 1997.

197. Li J-m, Singh MJ, Nelson PR, Hendricks GM, Itani M, Rohrer MJ, et al. Immobilization of Human Thrombomodulin to Expanded Polytetrafluoroethylene. Journal of Surgical Research.105:200-8. 2002.

198. Kealy B, Liew A, McMahon JM, Ritter T, O'Doherty A, Hoare M, et al. Comparison of Viral and Nonviral Vectors for Gene Transfer to Human Endothelial Progenitor Cells. Tissue Engineering Part C: Methods.15:223-31. 2009.

199. Murasawa S, Llevadot J, Silver M, Isner JM, Losordo DW, Asahara T. Constitutive Human Telomerase Reverse Transcriptase Expression Enhances Regenerative Properties of Endothelial Progenitor Cells. Circulation.106:1133-9. 2002.

200. van den Biggelaar M, Bouwens EAM, Kootstra NA, Hebbel RP, Voorberg J, Mertens K. Storage and regulated secretion of factor VIII in blood outgrowth endothelial cells. Haematologica.94:670-8. 2009.

201. Zaiss AK, Machado HB, Herschman HR. The influence of innate and pre-existing immunity on adenovirus therapy. Journal of Cellular Biochemistry.108:778-90. 2009.

202. Sumida SM, Truitt DM, Lemckert AAC, Vogels R, Custers JHHV, Addo MM, et al. Neutralizing Antibodies to Adenovirus Serotype 5 Vaccine Vectors Are Directed Primarily against the Adenovirus Hexon Protein. The Journal of Immunology.174:7179-85. 2005.

203. Parker AL, Waddington SN, Buckley SMK, Custers J, Havenga MJE, van Rooijen N, et al. Effect of Neutralizing Sera on Factor X-Mediated Adenovirus Serotype 5 Gene Transfer. J Virol.83:479-83. 2009.

204. Kidd KR, Patula VB, Williams SK. Accelerated endothelialization of interpositional 1-mm vascular grafts. Journal of Surgical Research.113:234-42. 2003.

205. Bensen C, Vann R, Koger K, Klitzman B. Quantification of gas denucleation and thrombogenicity of vascular grafts. Journal of Biomedical Materials Research.25:373-86. 1991.

206. Wigod MD, Klitzman B. Quantification of in vitro endothelial cell adhesion to vascular graft material. J Biomed Mater Res.27:1057-62. 1993.

207. Rickard RF, Meyer C, Hudson DA. Computational modeling of microarterial anastomoses with size discrepancy (small-to-large). J Surg Res.153:1-11. 2009.

208. Ahlswede K, Williams S. Microvascular endothelial cell sodding of 1-mm expanded polytetrafluoroethylene vascular grafts Arterioscler Thromb Vasc 14:25-31. 1994.

209. Pektok E, Cikirikcioglu M, Tille JC, Kalangos A, Walpoth BH. Alcohol pretreatment of small-diameter expanded polytetrafluoroethylene grafts: quantitative analysis of graft healing characteristics in the rat abdominal aorta interposition model. Artif Organs.33:532-7. 2009.

210. Hagensen MK, Shim J, Thim T, Falk E, Bentzon JF. Circulating Endothelial Progenitor Cells Do Not Contribute to Plaque Endothelium in Murine Atherosclerosis. Circulation.121:898-905. 2010.

211. Roussel JC, Moran CJ, Salvaris EJ, Nandurkar HH, d'Apice AJ, Cowan PJ. Pig thrombomodulin binds human thrombin but is a poor cofactor for activation of human protein C and TAFI. Am J Transplant.8:1101-12. 2008.

212. Takahashi Y, Hosaka Y, Imada K, Adachi T, Niina H, Mochizuki H. Species Specificity of the Anticoagulant Activity of Human Urinary Soluble Thrombomodulin. Thrombosis Research.89:187-97. 1998.

213. Chiu J-J, Chien S. Effects of Disturbed Flow on Vascular Endothelium: Pathophysiological Basis and Clinical Perspectives. Physiological Reviews.91:327-87. 2011.

214. Wang N, Miao H, Li Y-S, Zhang P, Haga JH, Hu Y, et al. Shear stress regulation of Krüppel-like factor 2 expression is flow pattern-specific. Biochemical and Biophysical Research Communications.341:1244-51. 2006.

215. Cheng C, van Haperen R, de Waard M, van Damme LCA, Tempel D, Hanemaaijer L, et al. Shear stress affects the intracellular distribution of eNOS: direct demonstration by a novel in vivo technique. Blood.106:3691-8. 2005.

216. Cheng C, Tempel D, van Haperen R, van der Baan A, Grosveld F, Daemen MJAP, et al. Atherosclerotic Lesion Size and Vulnerability Are Determined by Patterns of Fluid Shear Stress. Circulation.113:2744-53. 2006.

217. Lee HB, Blaufox MD. Blood volume in the rat. J Nucl Med.26:72-6. 1985.

218. Nicklin SA, Reynolds PN, Brosnan MJ, White SJ, Curiel DT, Dominiczak AF, et al. Analysis of cell-specific promoters for viral gene therapy targeted at the vascular endothelium. Hypertension.38:65-70. 2001.

219. Goverdhana S, Puntel M, Xiong W, Zirger JM, Barcia C, Curtin JF, et al. Regulatable gene expression systems for gene therapy applications: progress and future challenges. Mol Ther.12:189-211. 2005.

220. Jun H-W, Taite LJ, West JL. Nitric Oxide-Producing Polyurethanes. Biomacromolecules.6:838-44. 2005.

221. Yan Y, Hong Wang X, Yin D, Zhang R. A New Polyurethane/Heparin Vascular Graft for Small-Caliber Vein Repair. Journal of Bioactive and Compatible Polymers.22:323-41. 2007.

222. Ladhoff J, Fleischer B, Hara Y, Volk H-D, Seifert M. Immune privilege of endothelial cells differentiated from endothelial progenitor cells. Cardiovascular Research.88:121-9. 2010.

223. Yu J, Vodyanik MA, Smuga-Otto K, Antosiewicz-Bourget J, Frane JL, Tian S, et al. Induced pluripotent stem cell lines derived from human somatic cells. Science.318:1917-20. 2007.

224. Takahashi K, Tanabe K, Ohnuki M, Narita M, Ichisaka T, Tomoda K, et al. Induction of Pluripotent Stem Cells from Adult Human Fibroblasts by Defined Factors. Cell.131:861-72. 2007.

225. Kaji K, Norrby K, Paca A, Mileikovsky M, Mohseni P, Woltjen K. Virus-free induction of pluripotency and subsequent excision of reprogramming factors. Nature.458:771-5. 2009.

226. Zhang J, Wilson GF, Soerens AG, Koonce CH, Yu J, Palecek SP, et al. Functional Cardiomyocytes Derived From Human Induced Pluripotent Stem Cells. Circ Res.104:e30-41. 2009.

227. Li Z, Hu S, Ghosh Z, Han Z, Wu JC. Functional Characterization and Expression Profiling of Human Induced Pluripotent Stem Cell- and Embryonic Stem Cell-Derived Endothelial Cells. Stem Cells and Development.Ahead of print. 2011.

228. Belmonte JCI, Ellis J, Hochedlinger K, Yamanaka S. Induced pluripotent stem cells and reprogramming: seeing the science through the hype. Nat Rev Genet.10:878-83. 2009.

229. Mosquera DA, Goldman M. Endothelial cell seeding. Br J Surg.78:656-60. 1991.

230. Deutsch M, Meinhart J, Vesely M, Fischlein T, Groscurth P, von Oppell U, et al. In vitro endothelialization of expanded polytetrafluoroethylene grafts: a clinical case report after 41 months of implantation. J Vasc Surg.25:757-63. 1997.

231. Wang E, Miller LD, Ohnmacht GA, Liu ET, Marincola FM. High-fidelity mRNA amplification for gene profiling. Nat Biotechnol.18:457-9. 2000.

232. Ricard-Blum S, Ruggiero F. The collagen superfamily: from the extracellular matrix to the cell membrane. Pathologie Biologie.53:430-42. 2005.

233. Morita K, Furuse M, Fujimoto K, Tsukita S. Claudin multigene family encoding four-transmembrane domain protein components of tight junction strands. Proc Natl Acad Sci U S A.96:511-6. 1999.

234. Visse R, Nagase H. Matrix metalloproteinases and tissue inhibitors of metalloproteinases: structure, function, and biochemistry. Circ Res.92:827-39. 2003.

235. Suzuki T, Aizawa K, Matsumura T, Nagai R. Vascular implications of the Kruppel-like family of transcription factors. Arterioscler Thromb Vasc Biol.25:1135-41. 2005.

236. Kroll J, Waltenberger J. A novel function of VEGF receptor-2 (KDR): rapid release of nitric oxide in response to VEGF-A stimulation in endothelial cells. Biochem Biophys Res Commun.265:636-9. 1999.

237. Minshall RD, Sessa WC, Stan RV, Anderson RG, Malik AB. Caveolin regulation of endothelial function. Am J Physiol Lung Cell Mol Physiol.285:L1179-83. 2003.

238. Kadohama T, Nishimura K, Hoshino Y, Sasajima T, Sumpio BE. Effects of different types of fluid shear stress on endothelial cell proliferation and survival. J Cell Physiol.212:244-51. 2007.

239. True AL, Olive M, Boehm M, San H, Westrick RJ, Raghavachari N, et al. Heme oxygenase-1 deficiency accelerates formation of arterial thrombosis through oxidative damage to the endothelium, which is rescued by inhaled carbon monoxide. Circ Res.101:893-901. 2007.

240. Tsan MF, White JE, Caska B, Epstein CJ, Lee CY. Susceptibility of heterozygous MnSOD gene-knockout mice to oxygen toxicity. Am J Respir Cell Mol Biol.19:114-20. 1998.

241. Seder CW, Hartojo W, Lin L, Silvers AL, Wang Z, Thomas DG, et al. Upregulated INHBA expression may promote cell proliferation and is associated with poor survival in lung adenocarcinoma. Neoplasia.11:388-96. 2009.

242. van Wachem PB, Beugeling T, Mallens BW, Dekker A, Feijen J, Bantjes A, et al. Deposition of endothelial fibronectin on polymeric surfaces. Biomaterials.9:121-3. 1988.

243. Sessa WC. eNOS at a glance. J Cell Sci.117:2427-9. 2004.

244. Sun D, Liu H, Yan C, Jacobson A, Ojaimi C, Huang A, et al. COX-2 contributes to the maintenance of flow-induced dilation in arterioles of eNOS-knockout mice. Am J Physiol Heart Circ Physiol.291:H1429-35. 2006.

245. Pohl U, Holtz J, Busse R, Bassenge E. Crucial role of endothelium in the vasodilator response to increased flow in vivo. Hypertension.8:37-44. 1986.

246. Allaire E, Clowes AW. Endothelial cell injury in cardiovascular surgery: the intimal hyperplastic response. Ann Thorac Surg.63:582-91. 1997.

Biography

John David Stroncek

Birth Date April 4th, 1983
Edina, Minnesota

Education **Duke University**, Durham, NC
Ph.D., Biomedical Engineering, March 2011

University of Maryland, College Park, MD
B.S., Mechanical Engineering, May 2005

Publications **Stroncek JD**, Ren L, Klitzman B, Reichert WM. *In Vivo* Testing of Small Diameter Vascular Grafts Lined with Endothelial Progenitor Cells that Overexpress Thrombomodulin. *In preparation*.

Stroncek JD, Haque N, Xue Y, Lawson JH, Reichert WM. *In Vitro* Functional Testing of Endothelial Progenitor Cells that Overexpress Thrombomodulin, Tissue Engineering Part A, *Accepted.*

Stroncek JD, Grant BS, Brown MA, Povsic TJ, Truskey GA, Reichert WM. Comparison of Endothelial Cell Phenotypic Markers of Late-Outgrowth Endothelial Progenitor Cells Isolated from Patients with Coronary Artery Disease and Healthy Volunteers, Tissue Engineering Part A, 2009, 15(11): 3473-3486.

Stroncek JD, and Reichert WM. Overview of Wound Healing in Different Tissue Types, *Indwelling Neural Implants: Strategies for Contending with the in vivo Environment,* CRC Press: Boca Raton, 2008.

Stroncek JD, Bell N, Reichert WM. Instructional PowerPoint Presentations for Cutaneous Wound Healing and the Tissue Response to Sutures, Journal of Biomedical Materials Research Part A, 2008 [Epub].

Awards **Tissue Engineering & Regenerative Medicine Conf.**, 50 Best Abstracts; **Duke University, CBTE,** Translational Achievement Award ; **Southeast BIO BIO/Plan competition**, Grand Prize Winner; **Duke Univ. Start-Up Challenge**, Overall Grand Prize Winner; **Univ. of Maryland Business Plan Competition**, 1st place ; **Center for Biomolecular and Tissue Engineering at Duke Univ.**, Pre-doctoral Fellowship (2006-2008)